The morphology of the Late Pleistocene hominin remains from the site of La Cotte de St Brelade, Jersey (Channel Islands)

ABSTRACT

Thirteen permanent fully-erupted teeth were excavated at the Paleolithic site of La Cotte de St Brelade in Jersey in 1910 and 1911. These were all found in the same location, on a ledge behind a hearth in a Mousterian occupation level. They were originally identified as being Neanderthal. A fragment of occipital bone was found in a separate locality in a later season. Recent dating of adjacent sediments gives a probable age of <48 ka. The purpose of this paper is to provide an updated description of the morphology of this material, and consider its likely taxonomic assignment from comparison with Neanderthal and *Homo sapiens* samples. One of the original teeth has been lost, and we identify one as non-hominin. At least two adult individuals are represented. Cervix shape and the absence of common Neanderthal traits in several teeth suggest affinities with *H. sapiens* in both individuals, while crown and root dimensions and root morphology of all the teeth are entirely consistent with a Neanderthal attribution, pointing towards a possible shared Neanderthal and *H. sapiens* ancestry (the likely date of this material corresponds with the time in which both Neanderthals and *H. sapiens* were present in Europe). The occipital fragment is stratigraphically more recent and does not exhibit any diagnostic Neanderthal features.

Keywords: Hominin teeth; Late Pleistocene; Neanderthal; European Pleistocene *Homo sapiens*; La Cotte de St. Brelade; Hominin morphology.

1. Introduction

The timing and duration of overlaps between *Homo sapiens* and Neanderthals in Europe, and the nature of their interaction, have long been debated by archaeologists and anthropologists (e.g., Stringer, 2006; Hoffecker, 2009). Recent evidence points towards contemporaneity or alternation of occupation of the two populations (Benazzi et al., 2011; Harvati et al., 2019). The application of improved radiocarbon dating methods has shown that the Mousterian ended by ~41–39 ka cal BP across much of Europe (Higham et al., 2014). Furthermore, new data from Bulgaria suggest that *H. sapiens* were already in Eastern Europe by ~45 ka, several millennia before the physical disappearance of the Neanderthals from the region. Hominin fossils from Bacho Kiro were identified as *H. sapiens* from morphology and mtDNA analysis, and directly dated to ~46.8–42.8 ka cal BP (Fewlass et al., 2020; Hublin et al., 2020). Radiocarbon dating shows a clear overlap of the initial Upper Paleolithic at Bacho Kiro with the late Mousterian and Châtelperronian attributed to late Neanderthal populations (Fewlass et al., 2020). In central and northwestern Europe, the Châtelperronian (~44–40 ka) overlaps with both the Early Aurignacian, starting at ~43–42 ka, and the Proto-Aurignacian, starting at ~42 ka (Hublin, 2015). In Western Europe, there is direct fossil evidence for the presence of both *H. sapiens* and Neanderthals at ~41–40.4 ka. A tooth discovered in a Proto-Aurignacian context at the site of Grotta di Fumane in northern Italy and dated to ~41–38.5 ka cal BP was found to have *H. sapiens* DNA (Benazzi et al., 2015), while a Neanderthal tibia from Saint-Césaire in western France was directly dated to ~42–40.6 ka cal BP (Hublin et al., 2012) and Neanderthal fossils from Spy in Belgium have been directly dated to ~42.2–40.4 ka cal BP (Semal et al., 2013). The Oase 1 *H. sapiens* from Romania, dated to ~42.5–40.5 ka cal BP (Zilhão et al., 2007), had a Neanderthal ancestor within the previous six generations (Fu et al., 2015), which demonstrates that these populations probably did overlap in Europe before 40 ka. In support of this, Peter (2019) has determined that, while the majority of Neanderthal ancestry entered *H. sapiens* populations between ~55 and ~48 ka,

there was a lesser amount of gene flow within Europe, ending at ~40 ka. Interestingly, Hajdinjak et al. (2018) found no evidence of recent gene flow from *H. sapiens* in four very late Neanderthals, dated to <45 ka cal BP, from Goyet, Spy, Les Cottes and Mezmaiskaya.

The hominin remains from La Cotte de St Brelade on Jersey (Fig. 1) probably fall within this key time period when both Neanderthals and *H. sapiens* were present in Western Europe. Their taxonomic status is therefore of considerable interest. The hominin remains ~~from La Cotte de St Brelade~~ originate from an area of complex sedimentation close to where the North and West Ravines meet (Fig. 2). Members of the Société Jersiaise undertook excavation in this area in 1910–1911 after the cave entrance had been cleared of clay and granite rubble deposits. The investigators located a series of fine-grained deposits, some of which were rich in ash and carbonized wood, which they described as hearths (Nicolle and Sinel, 1910). The excavations of these deposits continued until 1920 and produced at least 20,000 stone artifacts (Callow, 1986a), but it appears that smaller debitage elements were largely discarded during the initial seasons. These artifacts were described at the time as Mousterian in character (Marett, 1916), and more recent analysis has confirmed that all the stone artifacts are consistent with Late Middle Paleolithic technological practices (Callow, 1986a). The assemblage contains both Levallois and discoidal production elements, as well as formal tools, including side scrapers and two bifaces. No artifacts consistent with Upper Paleolithic technology have been identified among the artifact collections of La Cotte de St Brelade.

It is not possible to determine what fauna were found within deposits directly associated with the hominin remains from the surviving archive of the excavations carried out between 1910 and 1920. However, the faunal material recovered from ‘Weichselian’ units as a whole includes *Mammuthus primigenius*, *Coelodonta antiquitatis*, *Equus* sp., *Rangifer tarandus*, *Crocuta crocuta*, and *Vulpes vulpes* (see Callow, 1986b), species which would be consistent

with a Marine Isotope Stage (MIS) 3 attribution in northern France (Auguste, 2009). Mammoth, woolly rhinoceros and horse are specifically mentioned as coming from the same general area as the hominin teeth (Nicolle and Sinel, 1910; Keith and Knowles, 1911).

The hominin teeth were discovered over two seasons. In 1910, nine teeth were found in a mass of poorly preserved bone (for which no identifications are recorded) on a rock ledge above the layer identified as a hearth (Fig. 3; Nicolle and Sinel, 1910). They were described as lying side by side in original position, but with no trace of once supporting bone apparent. A further four teeth were found in clay adhering to the rock at the same location in 1911 (Nicolle and Sinel, 1912). An occipital fragment, together with two other bone fragments, were discovered in a ravine 6 ft (1.8 m) beyond the entrance of the cave and 18 ft (5.4 m) above the Mousterian cave floor level by Ernest Daghorn in 1915 (Marett, 1916).

Analysis of the surviving archive and a modern survey of the site have allowed us to broadly identify the location and position in the stratigraphic succession from which the hominin teeth were recovered and, more generally, the position and context of the hominin occipital fragment (Table 1). Although the deposits from this part of the site were removed during the early 20th century, their stratigraphic equivalents appear to extend into areas of remaining sediment within the main West Ravine (Bates et al., 2013). Optically stimulated luminescence (OSL) dating undertaken in 2011 within the middle parts of this sequence, approximately 4 m below the location where the teeth were discovered, suggests that the deposits containing the teeth and the occipital fragment both postdate ~48 ka (Bates et al., 2013). In view of the vertical extent of sediments between the lower dated horizon and the location from which we understand the teeth to have been discovered, a date that is clearly younger than 48 ka for the teeth is the only tenable proposition. It is plausible that these deposits span a period in which both late Neanderthal populations and those of *H. sapiens* were present in Western Europe, and during which sea levels were low enough for Jersey to

be part of a continuous landmass with France (Fig. 1B; Scott et al., 2014; Shaw et al., 2016). Consequently, understanding the exact date and taxonomic affinity of these hominin fossils is important for understanding Pleistocene population replacement at a regional scale.

The teeth were originally described by Keith and Knowles (1911, 1912). The 1912 paper is a reprint of the 1911 paper, with additional details of the four teeth found in 1911. Keith (1913) further addressed the considerable level of taurodontism in the molar teeth. The teeth were briefly described in Marett (1911) and Oakley et al. (1975), and more recently were studied by Stringer and Currant (1986), who noted that by this date two of the teeth were only represented by casts and one other tooth was missing. The missing tooth was a left I^1, represented only by the root. The crown of this tooth had disintegrated before it was seen by Arthur Keith, as the result of an accident during conservation (letter from J. Sinel to Keith dated 1st September 1911, in the archives of the Royal College of Surgeons). In 1929 Tom Watson, an amateur paleontologist/archaeologist on Jersey, sent a hominin lower canine that he had found at La Cotte to Arthur Keith for identification (letter dated 17th January 1929, in the archives of the Royal College of Surgeons). Although Tom Watson left all his finds to the Jersey Museum, this tooth has not come to light. This letter also states that Tom Watson had previously sent teeth and bones that he had discovered at La Cotte to Arthur Keith for identification, but no record of these has been found. The three bone fragments recovered in 1915 were initially identified as parts of an occipital, malar and mandible from a single juvenile skull (Marett, 1916). Angel and Coon (1954) reanalyzed the material and concluded that only the occipital fragment was human, and that it belonged to a child about 5 years old. This opinion was supported by Stringer and Currant (1986), who agreed that the other two fragments did not represent any part of the human skeleton.

The purpose of this paper is to provide an updated description of the morphology of the La Cotte teeth and the occipital fragment, and present data relevant to their taxonomic attribution.

2. Materials and methods

2.1. Described material from La Cotte

The material available for study consists of ten isolated permanent fully erupted teeth (Table 2), and a fragment of occipital. These are held by the Jersey Museum, and were temporarily loaned to the Natural History Museum, London, in 2015. Two other teeth, SJMJ2462 (right I_1) and SJMJ2467 (left M^3), are represented by casts. The casts made in 1911 and now held by the Natural History Museum, London, were used in this study because, of several casts available, they are the most similar to the teeth described and illustrated by Keith and Knowles (1912). The right I_1 (SJMJ2462) is thought to be non-hominin and is not included in the analysis (see Supplementary Online Material [SOM] S1). With permission of Jersey Heritage, the microtomographic scans of the La Cotte de St Brelade specimens published in this paper are publically available (under a CC BY-NC 4.0 license) through the Human Fossil Record online archive (https://human-fossil-record.org/).

2.2. Comparative material

Comparative samples for morphological traits scored at the outer enamel surface (OES) principally come from Bailey (2006a) and, where the trait is not scored by Bailey (2006a), from Martinón-Torres et al. (2012)—see SOM Tables S1 and S2. These samples consist of Neanderthals and fossil (primarily European Late Pleistocene) *H. sapiens*. Comparative CT-scan samples employed for geometric morphometrics, and occurrence of Tomes' root (Arizona State University dental anthropology system [ASUDAS] grades 4–5: Turner et al.,

1991) and taurodontism in P_3 and P_4, consist of Neanderthals, fossil (Pleistocene) *H. sapiens* and recent (Holocene) *H. sapiens* (SOM Tables S1, S3, S4). Comparative metrics data for the early Neanderthal site of Krapina, late Neanderthals and fossil (European Late Pleistocene) *H. sapiens* were taken from the literature and the NESPOS database (2013), identified in table legends and in SOM Tables S1–S3, S5, S6. For crown dimensions, the site of Krapina was separated from late Neanderthals because of the distorting effect caused by the relatively large size of the Krapina tooth crowns, and in some cases their different shape, together with the fact that the Krapina teeth make up approximately one third of the total Neanderthal sample.

2.3. Methods

Definitions We use the terms pre-Neanderthal (e.g., Atapuerca-SH, Pontnewydd), early Neanderthal (e.g., Krapina, Bourgeois-Delaunay), and classic/late Neanderthal, as proposed by Dean et al. (1998). Although this assumed a linear and almost certainly oversimplified model of Neanderthal evolution (Hublin and Roebroeks, 2009), Compton and Stringer (2015) found it useful in classifying morphological differences observed in Neanderthal dentitions.

Dental morphological traits Most of the morphological traits were assessed using the Arizona State University Dental Anthropology System (ASUDAS), and associated reference plaques (Turner et al., 1991; Scott and Turner, 1997; Scott et al., 2018). Additional traits described by other authors and not included in the ASUDAS were also utilized (see SOM S2 for descriptions of the traits studied). Wherever possible, traits were scored at the OES but, due to wear, some traits could only be scored at the enamel dentine junction (EDJ). There are few comparative data available for the frequency of traits at the EDJ, and they are only provided here for P^4. In other cases, traits scored at the EDJ were compared to frequencies of traits at the OES. Several authors have found a strong positive correlation between the EDJ and the

OES in the expression of morphological traits in hominins (Krenn et al., 2019 for lower premolars; Guy et al., 2015 for upper molars; Skinner et al., 2008, 2010 for lower molars) but we recognize that wear obscures the OES and can lead to misidentification of trait expression. For each trait, 95% confidence limits were calculated for trait frequency in each taxon, and for the difference in frequencies between the two taxa (SOM S3). Traits that are of potential use in making inferences about taxonomic affiliation are those where the confidence intervals for the two comparative samples do not overlap, or where the confidence limits for the difference in frequencies between the two comparative samples are both either above or below zero (i.e., do not include zero; Altman et al., 2000).

Relative cusp areas and occlusal polygon Relative cusp areas, and the angles and relative size of the occlusal polygon, on SJMJ2456 (right M^1) were measured from a high definition photograph of the occlusal surface taken perpendicular to the plane of the cervix, using ImageJ software (Rasband, 2008), according to the methodology described by Bailey (2004). The original positions of the cusp tips were estimated by determining the point of intersection of the principal ridges of each cusp visible at the EDJ,

Taurodontism The degree of taurodontism of the molars was determined using the method of Shifman and Chananel (1978). Shifman and Chananel's (1978) method was employed (SOM S2) because it provides an absolute measurement, rather than a relative measurement that requires complete roots. The distance between the bicervical line and the highest point on the floor of the pulp cavity of the molar teeth was measured from the CT scans (Table 2: pulp chamber height). This is preferable to taking the measurement from the roof of the pulp chamber, where secondary dentine may form as the tooth wears. The method presented by Keene (1966; see SOM S2) was used to measure the degree of taurodontism in SJMJ2461 (right M_2), because the original root length could be estimated. The original length of the root

of this tooth~~SJMJ2461 (right M_2)~~, where the broken sides of the tooth's root are converging, was estimated by extending these on a scaled photograph, and assuming a rounded tip.

Geometric morphometrics of cervix shape Microtomography was used to examine the internal structures of the teeth. Specimens were scanned at the Natural History Museum using an XTekCT scanner (180 kV, 205 µA, 0.25mm copper filter, 3000 projections) with a resultant isometric voxel size of ~30 µm. To facilitate segmentation, each image stack was filtered using a mean-of-least-variance filter (kernel size one) or a median and mean-of least variance filter (each with kernel size three; Wollny et al., 2013). Each tooth was segmented into its enamel and dentine components in Avizo 6.3 (ThermoFisher Scientific, Waltham). Surface models of the EDJ were produced using the surface generation module (unconstrained smoothing) and saved as PLY files.

Geometric morphometric analysis of cervix shape (in almost all cases the dentine horns, and the ridges between, were too worn for landmark-based measurement) was conducted in Mathematica 10 (Wolfram, Long Hanborough) following protocols outlined in previous publications (Skinner and Gunz, 2010; Martin et al., 2017). Thirty semilandmarks were placed around the cervix of each tooth. For the mandibular molars, the initial cervix landmark was placed on the mesiobuccal corner of the crown (beneath the protoconid) and continued mesially. In the maxillary molars, the initial landmark was placed on the middle part of the buccal face of the crown (between the paracone and metacone) and continued mesially. For mandibular and maxillary premolars the initial landmark was placed at the mid-point of the buccal face and continued mesially. Estimations of missing portions of the cervix were made for SJMJ 2457 (left P^4), 2456 (right M^1) and 2461 (right M_2; SOM Fig. S1), and subjected to Procrustes superimposition and then slid (Gunz and Mitteroecker, 2013) to create a geometrically homologous set of shape variables. Principal components analysis (PCA) was conducted to assess variation in cervix shape. Canonical variate analysis (CVA) was

conducted to assess taxonomic affinity using inclusive sets of principal component scores (i.e., first set using 1–5 PCs, second set using 1–6 PCs, etc.) that represented ~95% of overall shape variation. PCA was conducted in both shape space and form space; the latter including the log of centroid size as a variable. CVA was only conducted in shape space and attempted to assign La Cotte teeth to either Neanderthals or *H. sapiens*.

Crown and root measurements Measurements of the La Cotte teeth were taken with sliding calipers to the nearest 0.1 mm. The crown dimensions and root lengths were measured using the method of Moorrees (1957): crown = maximum dimensions parallel to and at right angles to the buccal surface; root = maximum vertical dimension from the cervix of the mesiobuccal root on the buccal aspect. In multirooted teeth, the term ‘trunk’ is used to describe the portion of the root between the cervix and the point at which the individual roots furcate, and root trunk length was measured as the distance between the cervix and the root furcation on the aspect of the tooth on which this was at a minimum. The dimensions of the root at the cervix were measured as the maximum dimensions at right angles to the mesial and buccal surfaces. This definition was also used to measure cervical dimensions from CT scans of comparative samples. Where the measurements for both left and right antimeres are available, the average was used. Mesiodistal crown dimensions of the La Cotte teeth were adjusted for wear using the method of Wood and Abbott (1983), in which the estimated original margins of the tooth are drawn on a scaled photograph of the occlusal surface and the difference between these and the actual margins measured. The adjusted measurements were used for comparisons with other teeth. Where the length of the La Cotte teeth could not be estimated, only the buccolingual dimension is used for comparison with other teeth. The level of occlusal wear was quantified using Murphy's method, as summarized by Smith (1984; Table 2).

An adjusted z-score method, using Student's t inverse distribution (Maureille et al., 2001), was employed to compare each of the La Cotte measurements with the means and standard deviations of comparative groups. The formula applied was:

$$\frac{\text{La Cotte dimension} - X}{\text{Invt}_{0.975;\, n\text{-}1} * SD}$$

where X, SD and *n* represent the mean, sample standard deviation and sample size respectively of the comparative sample. The interval between -1 and +1 comprises 95% of the variation in the comparative sample. A value of zero denotes that the La Cotte dimension equals the mean of the comparative sample. A positive adjusted Z score indicates a La Cotte dimension above the mean value and vice versa. All measurements and observations on the La Cotte teeth were repeated by the same observer after an interval of one month.

3. Results

3.1. Descriptions

The tooth crown and roots appear to not have undergone any erosive taphonomic processes. However, cracking and areas of taphonomic reworking of the dentine are evident in the CT scans. Layers of cementum are apparent on the apical half of the root surfaces, with the exception of SJMJ2459 (right M^3), but hypercementosis is not present. The pulp chambers of the teeth exhibit what appears to be demineralisation and subsequent desiccation ~~taphonomic alteration~~ of the circumpulpal primary dentine, leading to it having a 'feathered' appearance (C. Dean, pers. comm.). There are deposits of secondary dentine in the molar pulp chambers. All the teeth show some wear and this is generally flat and near horizontal. Most tooth crowns have dentine exposed on individual cusps, and the surface morphology has largely been obliterated.

Our identifications of tooth type are in agreement with those given by Keith and Knowles (1912). Traits are described using the ASUDAS grades (Turner et al., 1991) unless otherwise

stated. X-ray photographs of the teeth are shown in SOM Figures S2 and S3. Discrete morphological traits of the teeth, along with comparative data, are reported in Tables 3–7.

Lower left permanent canine (SJMJ2463) See Figure 4. The crown is complete, but the apex of the root is missing. Severe cracking is evident on the buccal surface of the root below the cervix and running down the distal surface from this point to the apex. This is also evident in the buccolingual CT slice (Fig. 4h).

There is moderate (grade 2) shoveling (Fig. 4a), trace (grade 1) double shoveling (Fig. 4a), a grade 4 distal accessory ridge (Fig. 4g), and a mesiobuccal bulge viewed occlusally. Lingually, a tuberculum dentale is present as a mild medially placed bulge without a free apex and there is a faint, wide but low, lingual medial ridge (Fig. 4g). The root is labiolingually wide, with deep mesial and distal longitudinal grooves. The mesial groove is particularly marked. The pulp canal is single and ovoid throughout the root, wide viewed distally, and mesiodistally flattened (Fig. 4h, i). There is distinct vertical convex curvature of the buccal aspect of the root, particularly towards the apex, and vertical convexity of the lingual aspect.

Upper left fourth premolar (SJMJ2457) See Figure 5. The preserved morphology (narrow and ovoid, rather than a more triangular crown shape) is consistent with a P^4. The tooth has matching occlusion (facets, wear shape and level of wear) with the left P_4 (SJMJ2465). The crown has a postmortem chip on the distolingual corner of the occlusal rim, at the edge of a large double fracture, and the root apices are missing. The distal aspect of the crown must have broken off in life, since there is rounding and vertical striations on the occlusal edge of the fracture.

The buccal surface of the crown is swollen, viewed mesially. The sagittal sulcus is visible at the OES, curved lingually at the distal end (Fig. 5d) and, from the EDJ, it can be seen that it terminates at the mesial margin (Fig. 5g). The EDJ reveals a small mesial accessory crest

(Fig. 5g), that likely delineated a small mesial fovea in the unworn tooth. A small pit is still visible in this location on the worn occlusal surface (Fig. 5d). There are two robust roots, with separate root canals, linked mesially by a radicular plate, creating a deep groove on the distal root surface (cross-section in Fig. 5i). The buccal root is vertically convex. The pulp chamber is taurodont, extending to the root furcation. It is mildly ovoid in distal and buccal views (Fig. 5h; SOM Fig. S4).

Lower left third premolar (SJMJ2464) See Figure 6. The large size of the buccal cusp, and its more lingual placement than in SJMJ2465 (left P_4), and our analysis of cervix shape (SOM Fig. S5) indicate a P_3. Additionally, a buccal cingulum is present at the EDJ, which occurs only on the P_3 in the comparative samples. The crown is complete, but the root apices are missing.

The occlusal crown outline is buccolingually oblong, with slight mesiolingual truncation (insufficient to score tooth as asymmetric) and the mesiodistal dimension greatest buccally. Viewed mesially, the upper part of the buccal surface is curved sharply lingually and the lingual surface is swollen. The bulbous metaconid is mesially placed, and there are two smaller distolingual cusps observable at the OES (Fig. 6a). The Y-shaped mesiobuccally slanted sagittal sulcus is not interrupted (Fig. 6a). It is narrow and the two foveae are insignificant, the distal being the deepest. Traces of mesial and distal accessory ridges can be seen on the buccal cusp at the OES, and are clearly visible at the EDJ (Fig. 6d, g). A faint distolingual groove is present at the OES (Fig. 6a, d), but the lingual margin is uninterrupted at the EDJ (Fig. 6g; Davies et al., 2019). The mesial and distal margins also both appear to have been uninterrupted (there is no evidence of interruption at the EDJ). Examination of the EDJ (Fig. 6g) indicates no evidence of a transverse crest. Small dentine horns underlie the two accessory cusps distal to the metaconid (Fig 6g). Although not visible at the enamel

surface, there is a faint buccal cingulum at the EDJ, consisting of a mesially placed horizontal ridge continuing from a slight mesial vertical groove/ridge (not shown).

There is a grade 4 Tomes' root (cross-section in Fig. 6i), with partial division into two roots, each with a single root canal. In the mesiobuccal root there is a vertical mesial groove and a prominent buccal groove. The buccal aspect of this root is vertically convex. The taurodont pulp chamber extends to the root furcation and is mildly ovoid in lingual view (SOM Fig. S6). In distal view it is convex lingually on the lingual side at the cervix, and is hourglass shaped below this. The root canal in the buccal root is enlarged buccolingually (Fig. 6h, i).

Lower left fourth premolar (SJMJ2465) See Figure 7. Morphological identification as a P_4 is confirmed by analysis of cervix shape (SOM Fig. S5). The tooth cannot be a metamere of SJMJ2464 (left P_3) because the interproximal facets do not match. The tooth is complete apart from the apex of the root, which is chipped. Severe cracking can be seen on the lingual side of the root in the buccolingual CT slice (Fig. 7h).

The occlusal outline is oblong, with very slight mesiolingual truncation. The worn down buccal surface of the crown lacks the convexity and lingual inclination observed in SJMJ2464 (left P_3), and the lingual face is less swollen. The narrow sagittal sulcus has a small bridge of enamel centrally (Fig 7d). However, examination of the EDJ reveals no evidence of a transverse crest (Fig. 7g). As with SJMJ2464 (left P_3), the mesial and distal foveae (distal deepest) do not appear to have been large. The sagittal sulcus does not interrupt either margin at the OES at this level of wear (Fig. 7d); and neither margin is interrupted at the EDJ. The EDJ reveals a distolingual cusp, in addition to the metaconid, as well as a small dentine horn on the mesial marginal ridge, and confirms the presence of a distal accessory ridge on the buccal cusp (Fig. 7g).

There is a single straight-sided root, mesially convex viewed apically, with a longitudinal groove in the apical half of the distal surface. The root is taurodont, with the pulp chamber extending to the apex (SOM Fig. S6). In distal view it can be seen that there has been considerable taphonomic alteration of the dentine towards the centre of the root, so that it is difficult to determine the original shape of the pulp chamber but, as with the left P_3 (SJMJ2464), the lingual side appears to be convex at the cervix (Fig. 7h; SOM Fig. S6).

Molars The molar buccal and lingual faces are mildly convex viewed mesially. The buccal surface grooves on upper molars are weak, and they are absent on lower molars. The loss of occlusal surface morphology on the molars, despite a relatively low level of wear, suggests that the unworn cusps were low. All the molar roots exhibit supraradicular taurodontism (Kallay, 1970), where the pulp chamber is enlarged before the furcation of the roots.

Upper right permanent first molar (SJMJ2456) See Figure 8. The low crown index value (equal mesiodistal and buccolingual measurements), particularly in relation to the other upper molars in the comparative samples, and our analysis of cervix shape among Neanderthal and *H. sapiens* M^1–M^3, indicate an M^1 (SOM Fig. S7). Additionally, the oblique ridge at the EDJ is type 1, running from the metacone dentine horn tip to the lingual marginal ridge distal to the protocone. Type 1 is typical of M^1, but not of M^2 and M^3 (Martin et al., 2017). The crown is complete, but the roots are missing above the trunk. Part of the distal margin of the crown broke off antemortem, as indicated by the presence of regular minor chipping along the occlusal edge of the fracture.

The occlusal shape is a rounded and slightly skewed rhomboid, with a metacone that is mesiolingually placed, resulting in distobuccal truncation, and a buccally protruding paracone (Fig. 8a). Taking into account corrections for the missing fractured areas, the metacone and hypocone are of similar size. Although worn, there appears to be a grade 2 metaconule (Fig. 8a; mesial and distal enamel protrusions from the uninterrupted oblique ridge: Reid and Van

Reenen, 1995). Examination of the EDJ (Fig. 8g) indicates no cusp 5 (hypoconule), two small accessory dentine horns on the mesial marginal ridge, and a grade 3 post-paracone tubercle (Ortiz et al., 2017) that cannot be detected at the enamel surface due to wear. The root is hypertaurodont. The lingual aspect of the root trunk is flared lingually, and there is a vertical groove reaching the cervix. At the broken root surface there is no evidence of separated roots buccally or mesially, but the base of the trunk is visible distally. Due to taphonomic alteration of the dentine it is difficult to determine the original shape of the pulp chamber.

Upper left permanent second molar (SJMJ2458) See Figure 9. The distal reduction in the crown and presence of a distal interproximal facet indicate an M^2. This tooth occludes with the left M_2 (SJMJ2455; Keith and Knowles, 1912). The tooth is complete apart from the root apices.

The occlusal outline is near triangular, convex mesially and distally, and flattened buccally. The tooth has a deep central fossa and no oblique ridge (Fig. 9a). No hypocone is visible on the worn OES. There is a hypocone dentine horn at the EDJ (Fig. 9g), which is likely to have been below grade 3 (reduced) on the original enamel surface due to its small size. The presence of a cusp 5 is indicated by dentine exposure on the distal margin of the OES (Fig. 9a). ~~There is~~ A~~a~~ grade 2 post-paracone tubercle (Ortiz et al., 2017)~~ visible at the EDJ (Fig. 9g),~~ and a mesial marginal ridge accessory tubercle are visible at the EDJ (Fig. 9g). The root is hypertaurodont. The individual roots are furcated mesially at the level at which they are preserved, but with both buccal and distal radicular plates (cross-section in Fig. 9i). Three individual root canals are evident. The roots curve inwards in the apical half viewed distally (Fig. 9b), and both root trunk and individual roots have a pronounced distal inclination. Though taphonomically altered buccally, the pulp chamber appears to have been hour glass shaped in distal view (Fig. 9h).

Upper right third molar (SJMJ2459) See Figure 10. The diminutive distal portion of the crown, and the lack of a distal interproximal facet despite the presence of substantial occlusal wear, indicate an M^3. The crown is complete, but the lingual root has been broken off at the trunk, and the buccal roots are missing above the trunk.

Viewed occlusally, the mesial aspect of the tooth, including the root trunk, is markedly concave, and the remainder of the tooth is near circular (Fig. 10a). Most surface morphology has been obliterated due to wear. It is unclear which cusps were present in the large distal area of dentine exposure, even at the EDJ (Fig. 10g). There are two dentine horns evident at the EDJ between this area and the protocone (Fig 10g). If one of these is the hypocone, it is most likely to be the more distally placed of the two, both from its position and its larger size. If this is the case, it implies the presence of multiple lingual cusps along the distal rim of the unworn tooth in addition to metacone, hypocone and cusp 5. No oblique ridge is evident at the EDJ. There is a faint horizontal ridge on the buccal OES of the paracone (Fig. 10a), not seen at the EDJ. The root is mesotaurodont. The lingual root is separated from the buccal root mesially and distally just below the fragmented root surface. The buccal root is not bifurcated at this level, though separate root canals are apparent.

Upper left third molar (SJMJ2467, cast) See Figure 11. The description is based on the 1911 Natural History Museum cast, and published details (Keith and Knowles, 1912; see SOM Fig. S8B). The crown appears to have been complete. Only part of the root trunk is present in the cast, but the root appears to have been complete in the original tooth according to the photograph in Keith and Knowles (1912; Fig. 11e).

Viewed occlusally, the crown is strongly tapered distally, and flattened mesially. Details of morphology are not clear due to the poor quality of the cast. There is a deep central fossa and no oblique ridge (Fig. 11a). Keith and Knowles (1912) described the tooth as three-cusped, lacking the hypocone. There is no evidence of a cusp 5 (Fig. 11e). The roots were

described as more compressed together than in the left M^2, but otherwise similar in form to those of the molars found previously (Keith and Knowles, 1911, 1912). The roots appear to have been hypertaurodont, with a greater degree of taurodontism than the other La Cotte molars (Fig. 11e).

Lower right permanent second molar (SJMJ2461) See Figure 12. This tooth is identified as an antimere of SJMJ2455 (left M_2). It has a distal interproximal facet, which is located lingually, implying lingual displacement of the adjacent tooth. Displacement of this nature is more likely to occur in an M_3 than in an M_2. The tooth is complete apart from the root apices.

The occlusal shape is rectangular, wider distally than mesially. It has rounded buccal and distal aspects (mesial worn), and partial flattening lingually. There is a 'Y' groove pattern, and a large (grade 5) distally oriented hypoconulid (cusp 5) visible at the OES (Fig. 12a). A small dentine horn at the EDJ indicates that a cusp 6 (entoconulid) was present (Fig. 12g). The sagittal sulcus is uninterrupted at the OES and no mid-trigonid crest is evident. It is absent also at the EDJ, with only a weak crest on the protoconid (grade 0: Bailey et al., 2011). Traces of a wide mesial fovea (trait referred to as an anterior fovea in the ASUDAS: Turner et al., 1991; Scott and Turner, 1997; Scott and Irish, 2017; Scott et al., 2018) can be identified at the OES and it is present as a linear depression at the EDJ. The entoconid dentine horn tip is positioned on the margin of the tooth (Martin et al., 2017; Fig. 12g). There is a pit (grade 1) protostylid at the OES (Fig. 12a), with a corresponding horizontal cingular crest at the EDJ (Fig. 12g).

The mesial root is rectangular in shape and bifurcated at the apex, but fused to the distal root buccally. The lingual furcation of the mesial root is convex mesially. The buccal sides of both roots curve lingually. Marginal ridges are present mesially and distally on the mesial root, and mesially on the distal root. The root is classed as hypertaurodont using Shifman and Chananel's (1978) method but, with an estimated root length of 14.9 mm, Keene's (1966)

method gives a figure of 37%, which is classed as hypotaurodont (25−49.9%). The pulp chamber is barrel shaped, viewed lingually, and widening of the mesial root canals is evident in the mesiodistal CT slices (Fig. 12h; SOM Fig. S9).

Lower left permanent second molar (SJMJ2455) See Figure 13. This tooth occludes with the left M^2 (SJMJ2458; Fig. 13i). It has mesial and distal interproximal wear facets, and, as with SJMJ2461 (right M_2), the distal interproximal facet is located lingually. Based on a similar degree of wear, similar dimensions and crown morphology, and the description of the original root morphology (Keith and Knowles, 1912), this is likely to be the antimere to SJMJ2461 (right M_2). The crown is complete, but Keith and Knowles (1912) sectioned the root just below, and parallel to, the cervix (line visible in Fig. 13b). Part of the root has been restored with filler. Only 9 mm of the trunk remains and the apical part of the root has been lost. The tooth was described by Keith and Knowles (1912) as having roots of the same form as the right M_2, fused buccally but not lingually, inclined distally and lingually, and having a trunk length of 7 mm.

The occlusal shape is rectangular, with rounded margins (mesial worn), and partially flattened lingually. As with the right M_2, there is a 'Y' groove pattern, and a large (grade 5) distally placed hypoconulid is present (Fig. 13a, d). Unlike the right M_2 there is no cusp 6 dentine horn and no protostylid crest at the EDJ, though a trace protostylid is present on the hypoconid (Fig. 13g). However, as with the right M_2, there is no mid-trigonid crest at the EDJ (site worn at the OES; grade 0: Bailey et al., 2011) and only a weak crest evident on the protoconid. The entoconid dentine horn tip is positioned on the margin of the tooth (Martin et al., 2017).

Lower right third molar (SJMJ2460) See Figure 14. This tooth lacks a distal interproximal facet despite the presence of dentine exposure. This, together with its shape and the presence of a large number of accessory crests, indicates an M_3. The interproximal wear facet matches

with that of the right M_2 (SJMJ2461) (Fig. 14i) and it is likely the teeth are metameres. Only the crown and less than one-quarter of the root are present. A portion of the mesial margin of the crown has broken off postmortem. A lingual crack can be seen in the CT slice (Fig. 14h).

The overall occlusal shape of the crown is near circular. The unworn lingual half of the tooth is very wrinkled, with multiple cusps present at the OES (Fig. 14a, d). There is an 'X' groove pattern (Fig. 14a). There are three crests running from the mesial margin into, and filling, the mesial (anterior) fovea at the OES, but the presence of any associated mesial marginal ridge tubercles cannot be assessed because the mesial face of the tooth is missing (Fig. 14a). There is no mid-trigonid crest (grade 0 at the EDJ: Bailey et al., 2011). There is a single mesiodistal groove at the OES on the buccal slope of the hypoconid, and lingual to the dentine exposure, that delineates the large protostylid cingular crest seen at the EDJ (Fig. 14d, g). Examination of the EDJ (Fig. 14g) reveals the presence of numerous primary and accessory dentine horns. Some of these can be reasonably identified as cusps, while others reflect repeated enamel knot initiation (Martin et al., 2017). Moving distally from the metaconid dentine horn, there is a small (grade 3) cusp 7, the entoconid, an undulating ridge that potentially exhibits incipient dentine horns, a cusp 6, and then one additional dentine horn lingual to the grade 4 hypoconulid. Additionally, there is a small dentine horn on the protostylid ridge on the buccal aspect of the hypoconulid. The degree of internal placement of the hypoconid relative to the protostylid cingulum is uncommon (not seen in any of the CT-scan comparative samples), and may further reflect a general perturbation of the development of this tooth. The metaconid and entoconid dentine horn tips are positioned on the margin of the tooth (Martin et al., 2017).

<u>Occipital fragment (SJMJ2452)</u> See Figure 15. The occipital fragment comprises a small part of a left squamous, measuring 53 mm between the broken anterior and posterior edges, and 37 mm from the asterion to the broken medial edge. The endocranial and exocranial surfaces

are weathered and marked by superficial cracks and abraded areas. One edge of the piece is defined by the lambdoid suture, which extends 45 mm from the asterion. All the other edges are defined by natural breaks. The thickness of the bone, and weak markings on the external surface, are consistent with an immature age at death. The lambdoid suture has several abraded patches but appears to be mostly open. An area of interdigitated bone, visible on the external surface located 35 mm from the asterion, may represent an early stage of fusion at the lambdoid suture. A finger of bone projecting inwards from the lambdoid suture, situated 6 mm from the asterion, and measuring 6.2 by 2.6 mm, appears to be a small wormian bone. The endocranial surface has a well demarcated transverse sulcus that extends 35 mm from just below the asterion to the broken medial edge along the lower border, and 32 mm from the lambdoid suture to the broken medial edge along the upper border. The transverse sulcus passes directly across the asterion and would have crossed the posteroinferior (mastoid) corner of the parietal bone before reaching the temporal bone, instead of crossing directly onto the temporal bone (Fig. 15B, indicated by dotted lines). Taken together, the size and morphology of the occipital fragment are consistent with an immature individual who died in late childhood or adolescence.

3.2. Qualitative morphological comparisons

Trait frequencies for the tooth types found in the La Cotte material, and in comparative samples of Late Pleistocene hominins, are reported in Tables 3–7. Traits that show a significant difference between Neanderthal and fossil *H. sapiens* are identified: (1) where the 95% confidence interval for the difference between the proportions for the two samples is entirely above or below zero, i.e., does not include 0% difference; (2) where the 95% confidence intervals for the two sample proportions do not overlap (SOM S3). These are the traits principally discussed.

Lower canine (SJMJ2463) The characteristics of this tooth support a Neanderthal affinity. Shoveling is present in the entire Neanderthal comparative sample and most (88%) of the fossil *H. sapiens* sample (Table 3). The distal accessory ridge is more common in Neanderthals (78%) than fossil *H. sapiens* (42%; Table 3). It tends to be more strongly expressed in Neanderthals, as it is at La Cotte, than in fossil *H. sapiens* (50% compared to 8% at their grade 2 in Martinón-Torres et al.'s [2012: Table 17] samples). The mild expressions of the tuberculum dentale and lingual medial ridge in SJMJ2463 (C_1) are the forms frequently found in both comparative samples (Martinón-Torres et al., 2012).

The buccal curvature of the root is typical of Neanderthals, but not of *H. sapiens* (Bilsborough and Thompson, 2005; Le Cabec et al., 2013), as is the convex buccal contour of crown and root together, known as 'cyrtodonty' (Patte, 1962; Brabant and Sahly, 1964). The wide root canal, as viewed distally, is unlike the narrow straight sided canals found in recent human teeth (van Beek, 1983).

Upper fourth premolar (SJMJ2457) The morphological traits of this tooth support a Neanderthal affinity. The swollen buccal surface, viewed mesially, and sharp lingual inclination from the point of maximum curvature, is typical of Neanderthals, and more pronounced than is generally found in *H. sapiens* (TC, personal observation). The absence of a buccal mesial accessory ridge is also typical of Neanderthals (83%) and less common in fossil *H. sapiens* (40%; Table 4).

The roots are robust compared to *H. sapiens*. The two-rooted form present is the most common type in Neanderthals (Maureille et al., 2008). The taurodontism, and a relatively longer root trunk before furcation of the roots than in recent humans, are also seen in some Neanderthal P^4 (Kallay, 1963).

Lower third (SJMJ2464) and fourth (SJMJ2465) premolars The characteristics of both premolars give an ambiguous picture. For the P_3 (SJMJ2464) the Neanderthal features are the

large lingually placed buccal cusp (Gómez-Robles et al., 2008), and the presence of a buccal cingulum at the EDJ, which occurs frequently in the Neanderthal sample but is not seen in the recent human sample. For the P_4 (SJMJ2465) the Neanderthal features are the presence of multiple lingual cusps (94%), a mesially placed metaconid (97%), and a buccal distal accessory ridge (88%; Table 4). The corresponding figures for fossil *H. sapiens* are significantly lower (Table 4). The cusp on the mesial margin, represented by a dentine horn at the EDJ, found on SJMJ2465 (left P_4), also occurs on three Krapina P_4 (Compton and Stringer, 2012). Three or more lingual cusps on P_4 (three at La Cotte) are present in 89% of Neanderthals but only 20% of fossil *H. sapiens* (Martinón-Torres et al 2012: Table 19).

In contrast, the absence of a transverse crest, and a symmetrical shape, found on both premolars, are rare in Neanderthal P_3 (3% and 6% respectively) and P_4 (both at 6%; Table 4). Additionally, Davies et al. (2019) recorded the presence of a transverse crest in their entire Neanderthal P_3 sample. Martinón-Torres et al. (2012: Tables 18 and 19), however, reported absence of a transverse crest in 15% of P_3 and 19% of P_4 in their Neanderthal sample. The absence of a transverse crest, and a symmetrical shape, are more frequently observed for P_3 and P_4 in fossil *H. sapiens* (Table 4). Bailey (2002) looked at the combination of three characteristics (well-developed metaconid, transverse crest and asymmetry) in P_4 and found that 98% of modern humans had only one of these traits, as at La Cotte, compared to only 6% of Neanderthals.

The robust roots of SJMJ2464 (left P_3) are more typical of Neanderthals than of *H. sapiens*. Interestingly, grade 4–5 Tomes' root, present on the P_3, occurs less frequently in the P_3 (12%) than in the P_4 (25%) in Neanderthals, the reverse of that found in fossil *H. sapiens* (38% and 23% respectively; Table 4) and recent humans. Tomes' root occurs less frequently in recent humans than in fossil *H. sapiens* (12.5% and 2.5% respectively for P_3 and P_4 in a large mixed sample; Shields, 2005). The wide root canal observed in SJMJ2465 (left P_4) is

typical of Neanderthal P_4 but uncommon in recent humans (Prado-Simón et al., 2012). The extended taurodont pulp chambers in SJMJ2464 (left P_3) and SJMJ2465 (left P_4) are apparent as widening in both buccolingual and mesiodistal directions (SOM Fig. S6). In some teeth, in both comparative samples (Table 4), extension of the pulp chamber into the root is only apparent as widening in a buccolingual direction. Considering the small samples involved (Table 4), the frequency of taurodontism is similar between P_3 and P_4 and between Neanderthals and fossil *H. sapiens*. Taken overall, widening in a buccolingual direction, with or without mesiodistal widening, occurs at approximately twice the frequency as widening in both directions together (51% against 23%; Table 4).

Molars The upper molar cusps are internally placed, as is often observed in Neanderthals. Carabelli's trait is absent in the upper molars. This was previously thought to be unusual in Neanderthals (McCown and Keith, 1939; Smith, 1989). More recently Martinón-Torres et al. (2012) reported 20% absence for M^1, 42% for M^2 and 80% for M^3, in their Neanderthal sample. The post-paracone dentine horn, which is present at the EDJ in SJMJ2456 (right M^1) and SJMJ2458 (left M^2) and could not be scored in SJMJ2459 (right M^3), was ubiquitous in a sample of Neanderthal maxillary molars and present in 86% of a recent human sample (Martin et al., 2017: Table 10). In contrast, Ortiz at al. (2017: Table 4) reported the presence of post-paracone dentine horns in 98% of a Neanderthal sample but only 25% of a recent human sample. Taurodontism is particularly associated with Neanderthals, but it is also found in fossil *H. sapiens* from Skhūl and Qafzeh (McCown and Keith, 1939; Vandermeersch, 1981) and in Aterians (Kupczik and Hublin, 2010). Kupczik et al. (2019: Table S1) found taurodontism (grades III and IV of their bifurcation index) in 88% (14 of 16) of their sample of Neanderthal M_2. Studies of recent Europeans have shown taurodontism is present in less than 10% of molars (Jafarzadeh et al., 2008: Table 3). The absence of enamel extensions

above trace level on any of the molars is also typical of Neanderthals, and most *H. sapiens* outside Asia (Bailey, 2006b).

Upper first molar (SJMJ2456) The Neanderthal M^1 crown has a distinct shape (Bailey, 2004; Gómez-Robles et al., 2007; Martinón-Torres et al., 2013): The main cusp tips are more internally placed, leading to a relatively smaller occlusal polygon (formed by linking the tips of the four principal cusps) compared to the total occlusal area (Table 5). There is a statistically significant difference at $p \leq 0.01$ between Neanderthal and *H. sapiens* for this percentage figure (Martinón-Torres et al., 2013). The occlusal shape is skewed and there is a large distally projected and swollen hypocone, leading to a narrow hypocone angle (Table 5; Fig. 16). The metacone is relatively smaller than the hypocone and mesiolingually oriented, leading to distobuccal truncation of the occlusal outline and a wide metacone angle (Table 5; Fig. 16). The hypocone is larger than the metacone in 14/16 molars in Bailey's (2004) Neanderthal sample. The occlusal polygon is narrower distally than mesially (Fig. 16).

The M^1 (SJMJ2456) shows clear Neanderthal affinities (see Table 5; Fig. 16). It has a relatively small occlusal polygon (24%), a mesiolingually placed metacone, along with a large metacone angle (116°), and an occlusal polygon that is narrower distally than mesially.

However, in contrast, the crown has only a mildly skewed appearance, with a small protocone angle (100°) compared to the means of both the comparative samples (106°). The relative size of the hypocone compared to total occlusal area (19%) is small in comparison to the Neanderthal sample mean (23.7%) and smaller than the metacone (21%), and the hypocone angle (76°) is large. While being within the Neanderthal range of variation, both of these features are more similar to the fossil *H. sapiens* sample. Additionally, the protocone is relatively large (33%) compared to Neanderthal (29.9%).

Upper second molar (SJMJ2458) The presence of a cusp 5 is common in Neanderthals (68%), and the presence of a mesial accessory cusp is ubiquitous. Both are less frequent in

fossil *H. sapiens* (39% and 13% respectively; Table 6). The reduced hypocone is unusual, though, in both Neanderthals and fossil *H. sapiens*, occurring at frequencies of only 6% and 15% respectively (Table 6). It is, however, common in the pre-Neanderthal Atapuerca-SH sample (Martinón-Torres et al., 2012).

Upper third molars (SJMJ2459 and SJMJ2467) The concave mesial aspect, viewed occlusally, of SJMJ2459 (right M^3) is distinctly unusual. The presence of multiple cusps along the distal rim (i.e., in excess of metacone, hypocone and a single cusp 5), as inferred for SJMJ2459 (right M^3), has been reported in Krapina M^3 (Compton and Stringer, 2012); and Martin et al. (2017) found considerable variation in distal cusp pattern in Neanderthal M^3. Multiple distal cusps and split hypocones occur in Aterian teeth (Bailey et al., 2017), and split hypocones have been reported in recent humans (Greene et al., 1967; Bermúdez de Castro and Martínez, 1986), but mention of multiple distal cusps in recent humans is rare in the literature. Ortiz et al. (2017: Table S3) found multiple cusp 5 at the EDJ in ~20% of Neanderthals but only in ~1% of recent humans.

Lower molars (SJMJ2455 and SJMJ2461 M_2; SJMJ2460 M_3) We did not observe the protostylid forms seen at the EDJ on SJMJ2461 (right M_2) and SJMJ2460 (right M_3) in our comparative samples. The hypoconulid expression in the M_2 (SJMJ2455 and SJMJ2461) is particularly large. Martinón-Torres et al. (2012: Table 21) found only 16.6% of Neanderthal and 4% of fossil *H. sapiens* M_2 with grade 5 hypoconulids. The characteristics of the La Cotte lower molars give an ambiguous picture. Neanderthal characteristics include the presence of a hypoconulid (found in the entire Neanderthal sample), a wide mesial (anterior) fovea (89% of M_2 and 93% of M_3), and a 'Y' groove pattern in M_2 (75%; Table 7). The corresponding figures for fossil *H. sapiens* are significantly lower (Table 7). Additionally, the multiple cusps and accessory crests found on SJMJ2460 (right M_3) have been observed in

Neanderthals (McCown and Keith, 1939; Radovčić et al., 1988; Bailey and Hublin, 2006), as has the repeated enamel knot initiation seen at the EDJ (Martin et al., 2017).

In contrast, the absence of a mid-trigonid crest at the OES, observed in SJMJ2461 (right M_2) and SJMJ2460 (right M_3), is rare in Neanderthal M_2 and M_3 (4% and 7% respectively), but almost ubiquitous in the fossil *H. sapiens* sample, at 96% and 100% respectively (Table 7). At the EDJ, Bailey et al. (2011: Table 3) recorded the presence of a continuous mid-trigonid crest in their entire Neanderthal M_2 and M_3 sample (absent at La Cotte), but only 35.5% and 14.3% respectively of a recent European sample. Furthermore, the position of the metaconid dentine horn tip on the occlusal margin of SJMJ2460 (right M_3) is rare in Neanderthals. The metaconid dentine horn was centrally placed in 95% of a late Neanderthal sample but only 36% of a recent human sample (Martin et al., 2017: Table 9).

The non-tapering shape and bifurcation of the mesial root, and the presence of longitudinal marginal ridges on mesial and distal roots, observed in SJMJ2461 (right M_2), are typical of Neanderthal M_2 (Compton and Stringer, 2015).

Occipital fragment (SJMJ2452) The occipital lacks any diagnostic Neanderthal anatomical features. The transverse sulcus pathway is typical of recent humans, and differs from the pathway observed in some Neanderthals, in which the transverse sulcus passes directly from the occipital to the temporal without crossing the parietal bone (Arsuaga et al., 2002).

3.3. Geometric morphometric analysis of cervix shape

Figures 17–23 illustrate PCAs of cervix morphology in shape and form (form including the log of centroid size as a variable) space for upper and lower molars and premolars.

The P^4 (SJMJ2457) falls closer to the *H. sapiens* samples (fossil and recent humans) in shape space but with the Neanderthals in form space, reflecting its large size (Fig. 17a, b). It differs from the mean Neanderthal cervix shape in being somewhat compressed

mesiolingually and distobuccally (Fig. 17c, d). Using 11 shape PCs, attribution accuracy of the comparative P^4 sample is ~65% (i.e., the proportion of specimens of known taxonomic affiliation that are attributed correctly using cross-validated canonical variate analysis) and posterior probabilities of discriminant analysis consistently assign SJMJ2457 (P^4) to *H. sapiens* rather than Neanderthal.

The identification of SJMJ2464 as a P_3 and SJMJ2465 as a P_4 is supported by their cervix shape that groups them with the *H. sapiens* (fossil and recent humans) P_3 and P_4 samples (SOM Fig. S5). The P_3 falls with the *H. sapiens* samples in shape space but closer to the Neanderthal sample in form space due to its large size (Fig 18a, b). Wireframe models indicate Neanderthals have a distally expanded cervix compared to the *H. sapiens* samples and SJMJ2464 (P_3; Fig. 18c, d). Using 11 shape PCs, attribution accuracy of the comparative P_3 sample is ~70% (with cross-validation), and posterior probabilities consistently assign SJMJ2464 (P_3) to *H. sapiens*. The P_4 falls with the *H. sapiens* samples in both shape and form space (Fig. 19a, b), sharing a buccolingually expanded cervix with both *H. sapiens* samples (Fig. 19c, d) but being more similar in size to the earlier sample. Using 9 shape PCs, attribution accuracy of the P_4 sample is ~90% (with cross-validation) and posterior probabilities consistently assign SJMJ2465 (P_4) to *H. sapiens*.

The SJMJ2456 M^1 plots with Neanderthals in both shape space and form space (Fig. 20a, b). It shares a distolingual expansion of the cervix with Neanderthals although it is not as marked as the average Neanderthal M^1 wireframe (Fig. 20c, d). Using 11 shape PCs, attribution accuracy of the comparative M^1 sample is ~90% (with cross-validation) and posterior probabilities consistently assign SJMJ2456 (M^1) to Neanderthals.

The SJMJ2458 M^2 falls on the margin of the overlapping distributions of the *H. sapiens* and Neanderthal samples in shape space, and the form analysis demonstrates it is larger than most of the *H. sapiens* comparative sample and of average size for a Neanderthal (Fig. 21a,

b). The wireframe model highlights the unusually small hypocone of SJMJ2458 (M^2) compared to the mean *H. sapiens* and Neanderthal cervix shapes (Fig. 21c, d). Using 13 shape PCs, attribution accuracy of the comparative M^2 sample is ~70% (with cross-validation) and SJMJ2458 (M^2) assigns with near equal frequency as either a Neanderthal or *H. sapiens* (i.e., its taxonomic attribution cannot be determined based on cervix shape).

The SJMJ2459 M^3 falls well outside of both Neanderthal and *H. sapiens* ranges and it is considerably larger than the largest Neanderthals in this analysis (Fig 22a, b). As with the SJMJ2458 M^2, the wireframe comparisons of mean shape illustrate the particularly strange contour of the SJMJ2459 M^3 (Fig. 22c, d). Using 9 shape PCs, attribution accuracy of the comparative M^3 sample is ~70% (with cross-validation) and SJMJ2459 (M^3) is consistently assigned to Neanderthals.

The two M_2 (SJMJ2455 and SJMJ2461) fall in an intermediate position between the Neanderthals and *H. sapiens* in shape space but fall closer to the fossil *H. sapiens* and Neanderthal samples when size is included (Fig. 23a, b). The M_2s are similar to the Neanderthal sample in having a buccally expanded cervix without the buccal pinching distal to the protoconid present in the *H. sapiens* samples (Fig. 23c, d). Using 14 shape PCs, attribution accuracy of the comparative sample is ~85% (with cross-validation) and posterior probabilities consistently assign both SJMJ2455 and SJMJ2461 (M_2) to Neanderthals.

Cervix shape alone tends to perform less well at taxonomic discrimination than analyzes that also incorporate the EDJ marginal ridge (Martin et al., 2017) and, at a number of tooth positions, attribution accuracy of the comparative sample (in which taxonomic affiliation is known) ranges between 60–90%. In summary, the P_3, P_4 and P^4 are consistently assigned as *H. sapiens*, while the two M_2, the M^1 and the M^3 are consistently assigned as Neanderthals. Attribution of the M^2 is less consistent and cervix shape cannot contribute strongly to its taxonomic assessment.

3.4. Metrical comparisons

Comparative data for crown dimensions are presented in SOM Tables S7 and S8, and adjusted Z scores for crown dimensions are illustrated in Figures 24 and 25.

Crown area See Figure 24. The crown areas of the La Cotte teeth are all close to or above the late Neanderthal comparative sample means, with associated adjusted Z scores under ±0.5, except for SJMJ2463 (left C_1) and SJMJ2464 (left P_3), which are particularly large. The C_1 crown area is above the range of the late Neanderthal comparative sample, and its buccolingual dimension is only exceeded by Kebara 2 (10.2 mm). The buccolingual dimension of the P_3 is only exceeded by La Quina 9 (11.0 mm), and this is the only tooth in the late Neanderthal comparative sample with a larger crown area (99 sq mm). With the exception of these two teeth, the crown areas of the La Cotte teeth are all within the ranges of the other comparative samples, with associated adjusted Z scores up to ±0.7 (-0.8 for the Krapina P_4). In contrast, the adjusted Z scores for SJMJ2463 (left C_1) and SJMJ2464 (left P_3) are 0.8 and 0.7 respectively in relation to late Neanderthals, and 1.0 and 1.4 in relation to fossil *H. sapiens*.

Crown index See Figure 25. The crown indices of the La Cotte teeth all have adjusted Z scores under ±0.5 in relation to the late Neanderthal comparative sample except for the left M^3 SJMJ2467 (-0.7). The La Cotte M^1, M^2 and M^3 have crown indices below the means of all the comparative samples (SOM Table S7; with the lone exception of the right M^3 SJMJ2459 in relation to Krapina), indicating that they are squarer; and C_1, P_3 and P_4 have crown indices above the means of the comparative samples (SOM Table S8), indicating that they are relatively buccolingually expanded. Two large differences in the comparative samples stand out. The fossil *H. sapiens* M^1 has an adjusted Z score of -1.3, reflecting the more rectangular shape of these teeth compared to Neanderthals. The Krapina P_3 has an adjusted Z score of 2.2

due to the lower crown indices of these teeth and this is also apparent in the Krapina lower molars.

Cervical dimensions See Table 8. In all but one case (SJMJ2461, right M_2) the La Cotte dimensions are above the Neanderthal comparative sample means. The mesiodistal dimensions of SJMJ2463 (left C_1) and SJMJ2464 (left P_3), and the buccolingual dimension of SJMJ2457 (left P^4), at the cervix are either above or at the upper end of the Neanderthal ranges. SJMJ2464 (left P_3) has adjusted Z scores for Neanderthal of 1.5 for the mesiodistal dimension and 1.0 for the buccolingual dimension. Keith and Knowles (1912) noted the large cervical dimensions; and the particularly high cervical dimensions of the La Cotte canine and premolars, other than SJMJ2465 (left P_4), is very distinctive. Fossil *H. sapiens* have smaller cervical dimensions than Neanderthals, and this difference is most pronounced in the P_4, M^2 and M_2. The fossil *H. sapiens* adjusted Z scores for SJMJ2463 (left C_1) and SJMJ2464 (left P_3) in both mesiodistal and buccolingual dimensions, and for SJMJ2458 (left M^2) in the mesiodistal dimension, are all at 1.0 or above.

Root length The only La Cotte tooth with a complete root is SJMJ2467 (LM^3), for which only a cast is now available (Keith and Knowles, 1912: preface). It has a length of 16.0 mm, which is within the Neanderthal range (13.5–16.7 mm, mean 15.2 mm; Bailey, 2005), and above the ranges for Předmostí (11.0–14.0 mm; Matiegka, 1934) and contemporary humans (8.0–15.0 mm; Black, 1902).

3.5. Number of individuals

Since all the teeth from La Cotte were found in one place, and are broadly similar in their degree of development and wear, the ‘null hypothesis’ would be that they all come from the same individual (Keith and Knowles, 1912). Our observations demonstrate that the eleven

teeth from La Cotte represent a maximum of six individuals, made up of three groups of teeth that can be confidently associated with one another and three isolated teeth:

i) The largest group of unambiguously associated teeth comprises four molars, SJMJ 2455, 2458, 2460 and 2461 (referred to hereafter as individual A-1). SJMJ2455 (left M_2) and SJMJ2458 (left M^2) occlude (Fig. 13i). SJMJ2455 (left M_2) and SJMJ2461 (right M_2) are likely to be antimeres, due to the similarities of morphology and size, and the shared presence of lingually placed distal interproximal facets, a highly unusual pattern of distal wear (Fig. 12a, marked 'a') and unusually lingually inclined roots. SJMJ2461 (right M_2) and SJMJ2460 (right M_3) are likely metameres. The lingual placement of the interproximal facet on SJMJ2461 suggests lingual displacement of the adjacent M_3, and the form of wear on SJMJ2460 is consistent with this (Fig. 14i). SJMJ2460 (right M_3) also has a prominent form of the protostylid, similar to, although larger than, that seen on SJMJ2461.

ii) The matching interproximal wear between SJMJ2463 (left C_1) and SJMJ2464 (left P_3), and their unusually large size, demonstrates that they are metameres (A-2)

iii) SJMJ2456, right M^1 (A-3)

iv) SJMJ2467, left M^3 (A-4)

v) SJMJ2457 (left P^4) and SJMJ2465 (left P_4) occlude (B-1)

vi) SJMJ2459, right M^3 (B-2).

The minimum number of individuals (MNI) represented by these eleven teeth is two, referred to as Individuals A and B. This can be confidently inferred from the fact that some of the groupings identified above cannot belong to the same dentition. Firstly, SJMJ2459 (right M^3; B-2) does not occlude with either the right M_2 or the right M_3 from A-1. Secondly, premolars SJMJ2464 (left P_3; A-2) and SJMJ2465 (left P_4; B-1) are not metameres, since the

interproximal facets do not match, and their large difference in size is inconsistent with a single dentition.

Teeth from individual B (SJMJ2457 [left P^4; B-1] and SJMJ2465 [left P_4; B-1] and SJMJ2459 [right M^3; B-2]) exhibit a similar degree of wear that is proportionally greater than that of the other teeth and consistent with a single individual. The remaining four teeth, SJMJ 2456, 2467, 2463 and 2464, cannot with complete confidence be associated with either Individual A or B, but are tentatively included with Individual A on the basis of dental metrics. SJMJ2456 (right M^1; A-3), SJMJ2467 (left M^3; A-4) and SJMJ2458 (left M^2; A-1) have similar crown area and crown index values in relation to the Neanderthal means. Likewise, the relationship of crown area to the Neanderthal mean in SJMJ2463 (left C_1) and SJMJ2464 (left P_3; A-2) is similar to that in M_2 SJMJ2461 and SJMJ2455 (A-1).

In summary, Individual A is represented by four teeth that are unambiguously associated and another four teeth that could belong to this individual, and Individual B is represented by three teeth. Based on the level of wear and the fact that there is dentine exposure on third molars in both individuals, it is likely that Individuals A and B were (young) adults. Trinkaus (1995) found a uniform pattern of wear in a sample of Neanderthals and noted that there was slight dentine exposure on first molars, as at La Cotte, in the third decade of life. However, the accumulation of cementum on the apical two thirds of the roots and the amount of secondary dentine in the pulp chambers of the molars, from both individuals, could indicate a greater age at death, as these are age related processes (Hillson, 1996; Guatelli-Steinberg and Huffman, 2012). The teeth found in the first season (1910) clearly did not all come from a right mandible as stated by Nicolle and Sinel (1910), but the fact that the teeth were in a row suggests that those from Individual A, at least, might have been originally deposited in anatomical association.

The occipital fragment came from an individual who died in late childhood or adolescence. It can therefore be concluded, from the degree of root development and wear on the teeth, that this fragment is not associated with the dental remains and therefore comes from a third individual.

4. Discussion

Individually, all of the La Cotte teeth have diagnostically Neanderthal characteristics and seven teeth also have *H. sapiens* characteristics. The teeth that lack *H. sapiens* characteristics are SJMJ2463 (left C_1), SJMJ2458 (left M^2), and the upper third molars, SJMJ2459 (right M^3) and SJMJ2467 (left M^3). Table 9 summarizes the mix of Neanderthal and *H. sapiens* characteristics within the individual teeth, grouped according to the maximum number of six individuals (A-1, A-2, A-3, A-4, B-1 and B-2) and minimum number of two individuals (A and B).

Within A-1 (SJMJ2458, left M^2; SJMJ2461, right M_2; SJMJ2455, left M_2; SJMJ2460, right M_3), the M^2 has no *H. sapiens* characteristics and the other three molars have a mixture of characteristics. Within A-2 (SJMJ2463, left C_1; SJMJ2464, left P_3), the canine has entirely Neanderthal diagnostic characteristics but those of the premolar are mixed. A-3 (SJMJ2456, right M^1) has mixed characteristics. A-4 (SJMJ2467, left M^3) only has Neanderthal characteristics. Within B1, both premolars (SJMJ2457, left P^4; SJMJ2465, left P_4) have a mixture of characteristics. B-2 (SJMJ2459, right M^3) only has Neanderthal characteristics.

Traits that are specific to one of these six groups include absence of mid-trigonid crest in lower molars (A-1), and particularly large teeth compared to Neanderthal and *H. sapiens* (A-2). Traits that occur in more than one group include absence of transverse crest and mesiolingual truncation in lower premolars, and cervix shape of *H. sapiens* form (A-2 and B-1). It is notable that for teeth with multiple crown traits that show a significant difference in

prevalence between Neanderthals and fossil *H. sapiens* (P_4, M_2, M_3) there is an ambiguous picture.

Four of the maximum of six individuals have a mixture of diagnostic Neanderthal, and *H. sapiens*, characteristics. Three of these sets of teeth could belong to the same dentition (Individual A) but the fourth belongs to a second dentition (Individual B). This suggests that the occurrence of mixed characteristics relates to a group of individuals, rather than being specific to one individual. The *H. sapiens* characteristics occur principally in the lower premolars, are less common in the P^4, M^1 and lower molars, and are reflected in cervix shape and crown morphological traits. The analysis of cervix shape gives a varied picture. The molars (other than M^2) are assigned to Neanderthals, while the premolars are assigned to *H. sapiens*. The root forms and the tooth dimensions are entirely compatible with Neanderthals. Several traits that are considered to be particularly typical of Neanderthals (Bailey, 2002, 2004, 2006a; Martin et al., 2017) are absent in the La Cotte teeth. These are the presence of a transverse crest, and mesiolingual truncation in lower premolars; the presence of a mid-trigonid crest, and metaconid central dentine horn tip placement in lower molars; and peculiarities of the occlusal shape of M^1. The first four of these traits are not diagnostic of either Neanderthals or *H. sapiens*, but they are consistently present in Neanderthals and less common in *H. sapiens*. The small occlusal polygon of the M^1 from La Cotte is diagnostically Neanderthal, but other aspects of the M^1 morphology are more ambiguous.

Three aspects of the morphology of the La Cotte teeth are unusual in both Neanderthals and fossil *H. sapiens*. These are the reduced hypocone on SJMJ2458 (left M^2); the concave mesial surface and unusual cervical shape of SJMJ2459 (right M^3); and the protostylid form on SJMJ2461 (right M_2) and SJMJ2460 (right M_3). The protostylid form of SJMJ2461 (right M_2) is superficially similar to that observed in *Paranthropus robustus* (Skinner et al., 2009), although not identical. We consider the SJMJ2460 (right M_3) protostylid form to reflect

abnormal development of the distal part of the crown and thus not useful for its taxonomic assessment.

With the exception of the possibly early form of the protostylid, there are no traits relating to earlier hominins in the La Cotte teeth. Traits that are only seen in *Homo heidelbergensis*, pre-Neanderthals or early Neanderthals (Compton and Stringer, 2015) are absent. These include a buccal cingulum at the enamel surface on P_3 (*H. heidelbergensis*); a distal occlusolingual cleft on P_3 (*H. heidelbergensis* and pre-Neanderthal); mesiobuccal swelling (viewed occlusally) of P_4 (*H. heidelbergensis*, pre-Neanderthal and early Neanderthal); and grade 2 buccal vertical grooves/cingula on lower molars (*H. heidelbergensis*, pre-Neanderthal and early Neanderthal). Multiple lingual cusps on the P_3 (present at La Cotte) are not found in *H. heidelbergensis* (Compton and Stringer, 2015; M. Bermúdez de Castro, pers. comm. regarding Arago),

The dental morphology of at least two dental individuals from La Cotte therefore displays a mixture of Neanderthal and *H. sapiens* characteristics, with Neanderthal features more strongly represented, and is clearly distinct from earlier hominins. Since there is more than one individual involved, abnormality of development can be dismissed as a likely cause. This mix of features could suggest shared ancestry or, alternatively, a need to extend the phenotype of one or other species to accommodate this variation. If this combination of features is not the result of introgression, it could be due to genetic drift as a consequence of isolation, but this does not seem probable since, at the likely date of these fossils (<48 ka), sea levels were lower and Jersey was connected to mainland Europe. Another possibility is short term evolutionary pressures, although it is difficult to see what advantage would be conveyed by these minor morphological differences. The small sample of teeth from La Cotte does not enable us to determine which of these scenarios is more likely. Attempts to extract DNA and resolve the issue through genetic analysis have thus far proved unsuccessful.

The site of Palomas in southern Spain has hominin dental material from secure stratigraphic contexts dated to ~45–38 ka cal BP (Walker et al., 2017), which shows a comparable mix of dental features to those found at La Cotte. The traits of the Palomas teeth are primarily Neanderthal, but not all the P_4 exhibit asymmetry and a transverse crest (present in 50% and 75% respectively); only one of the eight lower molars has a mid-trigonid crest at the OES, and fewer than half (43%) have a mesial (anterior) fovea of grade >1 (Zapata et al., 2017). However, unlike La Cotte, the crown breadths of some of the anterior teeth, and crown areas of some of the lower molars, are more than two standard deviations below the Neanderthal mean (Pinilla and Trinkaus, 2017). Trinkaus (2017) concluded that the Palomas remains were Neanderthals, but acknowledged that the Neanderthal range of variation would need to be extended to accommodate this group within Neanderthals because of differences in dental traits, their small size, and other aspects of their skeletal morphology. DNA analysis might help resolve the taxonomic ambiguity, but to date none has been reported.

Trinkaus (2007) identified distinct Neanderthal dental characteristics that appear in European Late Pleistocene *H. sapiens* dated earlier than 33 ka, and considered these to be due to the assimilation of Neanderthals into these populations. The characteristics listed involve: (1) morphological traits in I^1, C^1 and P_4 (multiple lingual cusps, mesially placed metaconid, and asymmetry for P_4) that are present in the earlier material and generally absent in later, post 33 ka, material; (2) relatively large anterior teeth; and (3) megadont distal molars. The only *H. sapiens* specimen known to have~~with~~ a high level of Neanderthal ancestry is the Oase 1 mandible and, by association, the Oase 2 cranium (Fu et al., 2015). Between 6 and 9% of its genome was derived from Neanderthals and it was concluded that there had been a Neanderthal ancestor 4–6 generations back (Fu et al., 2015). However, the Oase teeth (molars) do not exhibit any Neanderthal features. The lower molar mesial (anterior) foveae are small and there are no mid-trigonid crests; the M^1 is of *H. sapiens* form; and the teeth are

non-taurodont. The complex crown morphology of the M^3 was considered unique (Trinkaus et al., 2012). The teeth, however, are very large, particularly the second and third molars. A discriminant function analysis of the lower molar crown dimensions plotted them with Neanderthals (Trinkaus et al., 2003).

There is no evidence of transitional or Upper Paleolithic characteristics in the stone artifacts retained from the excavations at La Cotte. However, the degree of association between the teeth and the Mousterian artifacts in the occupation level is uncertain because the teeth were found on a ledge above the occupation level (though clearly accessible). The stone artifacts recovered at Palomas are similarly described as Mousterian (Walker et al., 2017).

The supraradicular taurodontism found in the La Cotte molars is the type generally found in Neanderthals. The more extreme radicular or total taurodontism, where the pulp chamber extends to the tip of a single root, is only found at a few sites, e.g., Krapina (Smith, 1976); Fondo Cattíe (Tarli, 1983); Palomas (Walker et al., 2008). Pyramidal roots, defined by Kupczik and Hublin (2010) as fused roots that can have apical root canal branches in addition to radicular or total taurodontism, are found at Regourdou, Kebara and La Quina (Kupczik and Hublin, 2010) and Aubesier (Lebel et al., 2001). The description of SJMJ2461 (M_2), where both Shifman and Chananel's (1978) and Keene's (1966) methods are used to measure the degree of taurodontism, demonstrates that different methods can give very different results. The degree of taurodontism in the La Cotte premolars is particularly notable. The extent of taurodontism in molars can be identified by the type, the height of the pulp chamber, and its shape—hourglass or barrel. In the comparative samples of Neanderthal P_3 and P_4 there is considerably greater variation of form than is found in molars. There is variation in the degrees of buccolingual and mesiodistal widening, and in the overall shape and the degree of tapering, in addition to the extent to which the pulp chamber expands towards the root apex. Consideration is needed as to how this should be measured. A point of

interest is that P_3 and P_4 show a similar degree and shape of the taurodontism when both teeth are present in a specimen in the comparative samples in six of nine cases, and the P_4 has a slightly greater level of taurodontism in the remainder. This contrasts with the situation in molars, where the degree of taurodontism frequently increases from first to third (Dumančić et al., 2001).

5. Conclusions

The crown and root dimensions for the La Cotte teeth fit well with the Neanderthal comparative samples, and the morphology of the crowns and roots are, in most aspects, typical of Neanderthals. However, there are also *H. sapiens* characteristics, specifically the lack of asymmetry and absence of transverse crests in the lower premolars; the mixture of characteristics in the M^1; and the absence of mid-trigonid crests, and the marginal position of the metaconid dentine horn tip, in the lower molars. Furthermore, the cervix shape of molars and premolars gives a mixed picture, Neanderthal for molars and *H. sapiens* for premolars. The taxonomic attribution of the teeth is therefore ambiguous. Neanderthal characteristics are present in all eleven teeth, but seven of the teeth also have *H. sapiens* characteristics. *Homo sapiens* characteristics occur in teeth from both the minimum of two adult individuals identified, suggesting a group or kin with these characteristics. Also of note is the unusual form of the protostylids found at the EDJ on lower molars, which has not previously been observed in Neanderthal or *H. sapiens* teeth.

The occipital fragment, which was found in a stratigraphically higher archaeological horizon, is likely to be from an immature individual who died in late childhood or adolescence. Its taxonomic status cannot be determined with certainty, but there are no anatomical features preserved in the bone that clearly indicate a Neanderthal affinity.

Of the various scenarios that can be considered to explain the mix of features in the La Cotte teeth, we favor shared Neanderthal and *H. sapiens* ancestry. The likely dating of the fossils during a period of temporal overlap between these groups is consistent with this interpretation.

References

Altman, D.G., Machin, D., Bryant, T.N., Gardner, M.J., 2000. Statistics with Confidence: Confidence Intervals and Statistical Guidelines, 2nd ed. BMJ Books, London.

Angel, J.L., Coon, C.S., 1954. La Cotte de St. Brelade II: Present status. Man 54, 53–55.

Arsuaga, J.L., Villaverde, V., Quam, R., Gracia, A., Lorenzo, C., Martínez, I., Carretero, J.M., 2002. The Gravettian occipital bone from the site of Malladetes (Barx, Valencia, Spain). Journal of Human Evolution 43, 381–393.

Auguste, P., 2009. Évolution des peuplements mammaliens en Europe du Nord-Ouest durant le Pléistocène moyen et supérieur. Le cas de la France septentrionale. Quaternaire. Revue de l'Association Française pour l'étude du Quaternaire 20, 527–550.

Bailey, S.E., 2002. A closer look at Neanderthal postcanine dental morphology. I. The mandibular dentition. Anatomical Record 269, 148–156.

Bailey, S.E., 2004. A morphometric analysis of maxillary molar crowns of Middle–Late Pleistocene hominins. Journal of Human Evolution 47, 183–198.

Bailey, S.E., 2005. Diagnostic dental differences between Neandertals and Upper Paleolithic modern humans: Getting to the root of the matter. In: Zadzinska, E. (Ed.), Current Trends in Dental Morphology Research. University of Lodz Press, Lodz, pp. 201–210.

Bailey, S.E., 2006a. Beyond shovel-shaped incisors: Neandertal dental morphology in a comparative context. Periodicum Biologorum 108, 253–267.

Bailey, S.E., 2006b. The evolution of non-metric dental variation in Europe. Mitteilungen der Gesellschaft für Urgeschichte 15, 9–30.

Bailey, S.E., Hublin, J.J., 2006. Dental remains from the Grotte du Renne at Arcy-sur-Cure (Yonne). Journal of Human Evolution 50, 485–508.

Bailey, S.E., Glantz, M., Weaver, T.D., Viola, B., 2008. The affinity of the dental remains from Obi-Rakhmat Grotto, Uzbekistan. Journal of Human Evolution 55, 238–248.

Bailey, S.E., Skinner, M.M., Hublin, J.J., 2011. What lies beneath? An evaluation of lower molar trigonid crest patterns based on both dentine and enamel expression. American Journal of Physical Anthropology 145, 505–518.

Bailey, S.E., Weaver, T.D., Hublin, J.J., 2017. The dentition of the earliest modern humans: How 'modern' are they? In: Marom, A., Hovers, E. (Eds), Human Paleontology and Prehistory. Springer, Cham, pp. 215–232.

Bates, M., Pope, M., Shaw, A., Scott, B., Schwenninger, J.L., 2013. Late Neanderthal occupation in North-West Europe: rediscovery, investigation and dating of a last glacial sediment sequence at the site of La Cotte de Saint Brelade, Jersey. Journal of Quaternary Science 28, 647–652.

Becam, G., Verna, C., Gómez-Robles, A., Gómez-Olivencia, A., Albessard, L., Arnaud, J., Frelat, M.A., Madelaine, S., Schwab, C., Souday, C., Turq, A., 2019. Isolated teeth from La Ferrassie: Reassessment of the old collections, new remains, and their implications. American Journal of Physical Anthropology 169, 132–142.

Benazzi, S., Douka, K., Fornai, C., Bauer, C.C., Kullmer, O., Svoboda, J., Pap, I., Mallegni, F., Bayle, P., Coquerelle, M., Condemi, S., 2011. Early dispersal of modern humans in Europe and implications for Neanderthal behaviour. Nature 479, 525–528.

Benazzi, S., Slon, V., Talamo, S., Negrino, F., Peresani, M., Bailey, S.E., Sawyer, S., Panetta, D., Vicino, G., Starnini, E., Mannino, M.A., 2015. The makers of the Protoaurignacian and implications for Neandertal extinction. Science 348, 793–796.

Bermúdez de Castro, J.M., Martínez, I., 1986. Hypocone and metaconule: identification and variability on human molars. International Journal of Anthropology 1, 165–168.

Bilsborough, A., Thompson, J.L., 2005. The dentition of the Le Moustier 1 Neandertal. In: Ullrich, H. (Ed.), The Neandertal Adolescent Le Moustier 1 – New Aspects, New Results. Staatliche Museum, Berlin, pp. 157–186.

Black, G.V., 1902. Descriptive Anatomy of the Human Teeth, 4th ed. S White Dental Manufacturing Co., Philadelphia.

Brabant, H., Sahly, A., 1964. Étude des dents Néandertaliennes découvertes dans la Grotte du Portel, en Ariège (France). Bulletin du Groupement International pour la Recherche Scientifique en Stomatologie & Odontologie 7, 237–254.

Burdo, C., 1960. La Cotte-de-Saint-Brelade, Jersey, British Channel Islands: Excavation of a Pre-Mousterian Horizon, 1950-1958. Société Jersiaise, St. Helier.

Callow, P., 1986a. Appendix B: Artefacts from the Weichselian deposits. In: Callow, P., Cornford, J.M. (Eds.), La Cotte de St. Brelade 1961–1978. Excavations by C.B.M. McBurney. Geobooks, Norwich, pp. 397–408.

Callow, P., 1986b. Appendix F: Fauna from deposits of the last cold stage at La Cotte de St Brelade. In: Callow, P., Cornford, J.M. (Eds.), La Cotte de St. Brelade 1961–1978. Excavations by C.B.M. McBurney. Geobooks, Norwich, microfiche bound with book.

Callow, P., 1986c. Interpreting the La Cotte sequence. In: Callow, P., Cornford, J.M. (Eds.), La Cotte de St. Brelade 1961–1978. Excavations by C.B.M. McBurney. Geobooks, Norwich, pp. 73–82.

Compton, T., Stringer, C.B., 2012. The human remains. In: Aldhouse-Green, S., Peterson, R., Walker, E.A. (Eds.), Neanderthals in Wales: Pontnewydd and the Elwy Valley Caves. Oxbow Books, Oxford, pp. 118–230.

Compton, T., Stringer, C., 2015. The morphological affinities of the Middle Pleistocene hominin teeth from Pontnewydd Cave, Wales. Journal of Quaternary Science 30, 713–730.

Davies, T.W., Delezene, L.K., Gunz, P., Hublin, J.J., Skinner, M.M., 2019. Endostructural morphology in hominoid mandibular third premolars: Discrete traits at the enamel-dentine junction. Journal of Human Evolution 136, 102670.

Dean, D., Hublin, J.-J., Holloway, R., Ziegler, R., 1998. On the phylogenetic position of the pre-Neandertal specimen from Reilingen, Germany. Journal of Human Evolution 34, 485–508.

Dumančić, J., Kaić, Z., Petrovečki, M., 2001. Evaluation of taurodontism in Krapina Neanderthals. In: Brook, A. (Ed.), Dental Morphology 2001. Sheffield Academic Press, Sheffield, pp. 111–121.

Fewlass, H., Talamo, S., Wacker, L., Kromer, B., Tuna, T., Fagault, Y., Bard, E., McPherron, S.P., Aldeias, V., Maria, R., Martisius, N.L., 2020. A ^{14}C chronology for the Middle to Upper Palaeolithic transition at Bacho Kiro Cave, Bulgaria. Nature Ecology & Evolution 4, 794–801.

Fu, Q., Hajdinjak, M., Moldovan, O.T., Constantin, S., Mallick, S., Skoglund, P., Patterson, N., Rohland, N., Lazaridis, I., Nickel, B., Viola, B., Prüfer, K., Meyer, M., Kelso, J., Reich, D., Pääbo, S., 2015. An early modern human from Romania with a recent Neanderthal ancestor. Nature 524, 216–219.

Gómez-Robles, A., Martinón-Torres, M., Bermúdez de Castro, J.M., Margvelashvili, A., Bastir, M., Arsuaga, J.L., Pérez-Pérez, A., Estebaranz, F., Martínez, L.M., 2007. A

geometric morphometric analysis of hominin upper first molar shape. Journal of Human Evolution 53, 272–285.

Gómez-Robles, A., Martinón-Torres, M., de Castro, J.M.B., Prado, L., Sarmiento, S., Arsuaga, J.L., 2008. Geometric morphometric analysis of the crown morphology of the lower first premolar of hominins, with special attention to Pleistocene *Homo*. Journal of Human Evolution 55, 627–638.

Greene, D.L., Ewing, G.H., Armelagos, G.J., 1967. Dentition of a Mesolithic population from Wadi Halfa, Sudan. American Journal of Physical Anthropology 27, 41–55.

Guatelli-Steinberg, D., Huffman, M., 2012. Histological features of dental hard tissues and their utility in forensic anthropology. In: Crowder, C., Stout, S.D. (Eds.), Bone Histology. An Anthropological Perspective. CRC Press, Boca Raton, pp. 91–107.

Gunz, P., Mitteroecker, P., 2013. Semilandmarks: a method for quantifying curves and surfaces. Hystrix 24, 103–109.

Guy, F., Lazzari, V., Gilissen, E., Thiery, G., 2015. To what extent is primate second molar enamel occlusal morphology shaped by the enamel-dentine junction? PLoS One 10, e0138802.

Hajdinjak, M., Fu, Q., Hübner, A., Petr, M., Mafessoni, F., Grote, S., Skoglund, P., Narasimham, V., Rougier, H., Crevecoeur, I., Semal, P., 2018. Reconstructing the genetic history of late Neanderthals. Nature 555, 652–656.

Harvati, K., Röding, C., Bosman, A.M., Karakostis, F.A., Grün, R., Stringer, C., Karkanas, P., Thompson, N.C., Koutoulidis, V., Moulopoulos, L.A., Gorgoulis, V.G., 2019. Apidima Cave fossils provide earliest evidence of *Homo sapiens* in Eurasia. Nature 571, 500–504.

Higham, T., Douka, K., Wood, R., Ramsey, C.B., Brock, F., Basell, L., Camps, M., Arrizabalaga, A., Baena, J., Barroso-Ruíz, C., Bergman, C., 2014. The timing and spatiotemporal patterning of Neanderthal disappearance. Nature 512, 306–309.

Hillson, S., 1996. Dental Anthropology. Cambridge University Press, Cambridge.

Hoffecker, J.F., 2009. The spread of modern humans in Europe**.** Proceedings of the National Academy of Sciences USA 106, 16040–16045.

Hublin, J.J., 2015. The modern human colonization of western Eurasia: when and where? Quaternary Science Reviews 118, 194–210.

Hublin, J-J., Roebroeks, W., 2009. Ebb and flow or regional extinctions? On the character of Neandertal occupation of northern environments. Comptes Rendus Palevol 8, 503–509.

Hublin, J.J., Talamo, S., Julien, M., David, F., Connet, N., Bodu, P., Vandermeersch, B., Richards, M.P., 2012. Radiocarbon dates from the Grotte du Renne and Saint-Césaire support a Neandertal origin for the Châtelperronian. Proceedings of the National Academy of Sciences USA 109, 18743–18748.

Hublin, J.J., Sirakov, N., Aldeias, V., Bailey, S., Bard, E., Delvigne, V., Endarova, E., Fagault, Y., Fewlass, H., Hajdinjak, M., Kromer, B., 2020. Initial Upper Palaeolithic *Homo sapiens* from Bacho Kiro Cave, Bulgaria. Nature 581, 299–302.

Jafarzadeh, H., Azarpazhooh, A., Mayhall, J.T., 2008. Taurodontism: a review of the condition and endodontic treatment challenges. International Endodontic Journal 41, 375–388.

Kallay, J., 1963. A radiographic study of the Neanderthal teeth from Krapina, Croatia. In: Brothwell, D.R. (Ed.), Dental Anthropology. Pergamon Press, Oxford, pp. 75–86.

Kallay, J., 1970. A new classification of the taurodont teeth of the Krapina Neanderthal man. Bulletin Scientifique (Yugoslavie) 15, 2–3.

Keene, H., 1966. A morphologic and biometric study of taurodontism in a contemporary population. American Journal of Physical Anthropology 25, 208–209.

Keith, A., 1913. Problems relating to the teeth of the earlier forms of prehistoric man. Proceedings of the Royal Society of Medicine 6, 103–124.

Keith, A., Knowles, F.H., 1911. A description of teeth of Palaeolithic man from Jersey. Journal of Anatomy and Physiology 46, 12–27.

Keith, A., Knowles, F.H., 1912. A description of teeth of Palaeolithic man from Jersey. Bulletin Société Jersiaise 37, 222–240.

Krenn, V.A., Fornai, C., Wurm, L., Bookstein, F.L., Haeusler, M., Weber, G.W., 2019. Variation of 3D outer and inner crown morphology in modern human mandibular premolars. American Journal of Physical Anthropology 169, 646–663.

Kupczik, K., Hublin, J.J., 2010. Mandibular molar root morphology in Neanderthals and Late Pleistocene and recent *Homo sapiens*. Journal of Human Evolution 59, 525–541.

Kupczik, K., Delezene, L.K., Skinner, M.M., 2019. Mandibular molar root and pulp cavity morphology in *Homo naledi* and other Plio-Pleistocene hominins. Journal of Human Evolution 130, 83–95.

Lebel, S., Trinkaus, E., Faure, M., Fernandez, P., Guérin, C., Richter, D., Mercier, N., Valladas, H., Wagner, G.A., 2001. Comparative morphology and paleobiology of Middle Pleistocene human remains from the Bau de l'Aubesier, Vaucluse, France. Proceedings of the National Academy of Sciences USA 98, 11097–11102.

Le Cabec, A., 2013. Anterior dental loading and root morphology in Neanderthals. Ph.D. Dissertation, Université Toulouse III-Paul Sabatier.

Le Cabec, A., Gunz, P., Kupczik, K., Braga, J., Hublin, J.-J., 2013. Anterior tooth root morphology and size in Neanderthals: Taxonomic and functional implications. Journal of Human Evolution 64, 169–193.

McCown, T.D., Keith, A., 1939. The Stone Age of Mount Carmel II. Clarendon Press, Oxford.

Marett, R.R., 1911. XX.—Pleistocene man in Jersey. Archaeologia 62, 449–480.

Marett, R.R., 1916. IV.—The site, fauna, and industry of La Cotte de St. Brelade, Jersey. Archaeologia 67, 75–118.

Martin, R.M., Hublin, J.-J., Gunz, P., Skinner, M.M., 2017. The morphology of the enamel–dentine junction in Neanderthal molars: gross morphology, non-metric traits, and temporal trends. Journal of Human Evolution 103, 20–44.

Martinón-Torres, M., Bermúdez de Castro, J.M., Gómez-Robles, A., Prado-Simón, L., Arsuaga, J.L., 2012. Morphological description and comparison of the dental remains from Atapuerca-Sima de los Huesos site (Spain). Journal of Human Evolution 62, 7–58.

Martinón-Torres, M., Spěváčková, P., Gracia-Téllez, A., Martínez, I., Bruner, E., Arsuaga, J.L., Bermúdez de Castro, J.M., 2013. Morphometric analysis of molars in a Middle Pleistocene population shows a mosaic of 'modern' and Neanderthal features. Journal of Anatomy 223, 353–363.

Matiegka, J., 1934. *Homo předmostensis* – Fosilní Člověk z Předmostí Na Morarě I Lebky. Česká Akademie Věd a Umění, Prague.

Maureille, B., Rougier, H., Houêt, F., Vandermeersch, B., 2001. Les dents inférieures du Néandertalien Regourdou 1 (site de Regourdou, commune de Montignac, Dordogne): analyses métriques et comparatives. Paléo 13, 183–200.

Maureille, B., Djindjian, F., Garralda, M.D., Mann, A., Vandermeersch, B., 2008. Les dents moustériennes de la grotte Boccard, lieu-dit Bas-de-Morant (commune de Créancey, Côte-d'Or, Bourgogne). Bulletins et Mémoires de la Société d'Anthropologie de Paris 20, 59–78.

Moorrees, C.F.A., 1957. The Aleut Dentition. Harvard University Press, Cambridge.

NESPOS, 2013. NESPOS – Pleistocene People and Places. https://www.nespos.org/display/openspace/Home (last accessed on 20/12/2013).

Nicolle, E.T., Sinel, J., 1910. 102. Report on the exploration of the Palaeolithic cave-dwelling known as La Cotte, St. Brelade, Jersey. Man 10, 185–188.

Nicolle, E.T., Sinel, J., 1912. 88. Report on the resumed exploration of "La Cotte", St. Brelade, by the Societe Jersiaise. Man 12, 158–162.

Oakley, K.P., Campbell, B.G., Molleson, T.I., 1975. Catalogue of Fossil Hominids (Vol. 2). British Museum (Natural History), London.

Ortiz, A., Bailey, S.E., Hublin, J.J., Skinner, M.M., 2017. Homology, homoplasy and cusp variability at the enamel–dentine junction of hominoid molars. Journal of Anatomy 231, 585–599.

Patte, É., 1962. La Dentition des Néanderthaliens. Masson et Cie, Paris.

Peter, B., 2019. Gene flow between hominins was common. Proceedings of the European Society for the Study of Human Evolution 8, 147.

Pinilla, B., Trinkaus, E., 2017. The Palomas dental remains: Size and proportions. In: Trinkaus, E., Walker, M.J. (Eds.), The People of Palomas: Neandertals from the Sima de las Palomas del Cabezo Gordo, Southeastern Spain. Texas A&M University Press, College Station, pp. 89–104.

Prado-Simón, L., Martinón-Torres, M., Baca, P., Olejniczak, A.J., Gómez-Robles, A., Lapresa, M., Arsuaga, J.L., Bermúdez de Castro, J.M., 2012. Three-dimensional evaluation of root canal morphology in lower second premolars of Early and Middle Pleistocene human populations from Atapuerca (Burgos, Spain). American Journal of Physical Anthropology 147, 452–461.

Quam, R., Bailey, S., Wood, B., 2009. Evolution of M^1 crown size and cusp proportions in the genus *Homo*. Journal of Anatomy 214, 655–670.

Radovčić, J., Smith, F.H., Trinkaus, E., Wolpoff, M.H., 1988. The Krapina Hominids an Illustrated Catalog of Skeletal Collection. Mladost, Zagreb.

Rasband, W.S., 2008. ImageJ. U. S. National Institutes of Health, Bethesda, Maryland, http://rsb.info.nih.gov/ij/.

Reid, C., Reenen, J.F. Van, 1995. Remnants of the metaconule in recent man. In: Radlanski, R.J., Renz, H. (Eds.), Proceedings of the 10th International Symposium on Dental Morphology. C. and M. Brunne, Berlin, pp. 172–176.

Scott, B., Bates, M., Bates, R., Conneller, C., Pope, M., Shaw, A., Smith, G., 2014. A new view from la Cotte de St Brelade, Jersey. Antiquity 88, 13–29.

Scott, G.R., Turner II, C.G., 1997. The Anthropology of Modern Human Teeth. Cambridge Studies in Biological Anthropology, Cambridge University Press, Cambridge.

Scott, G.R., Irish, J.D., 2017. Human Tooth Crown and Root Morphology. Cambridge University Press, Cambridge.

Scott, G.R., Turner, C.G. II, Townsend, G.C., Martinón-Torres, M., 2018. The Anthropology of Modern Human Teeth: Dental Morphology and its Variation in Recent and Fossil *Homo sapiens*. 2nd ed. Cambridge University Press, Cambridge.

Semal, P., Hauzeur, A., Rougier, H., Crevecoeur, I., Germonpré, M., Pirson, S., Haesaerts, P., Jungels, C., Flas, D., Toussaint, M., Maureille, B., 2013. Radiocarbon dating of human remains and associated archaeological material. In: Rougier, H., Semal, P. (Eds), Spy Cave: 125 Years of Multidisciplinary Research at the Betche Aux Rotches (Jemeppe-sur-Sambre, Province of Namur, Belgium). Société Royale Belge d'Anthropologie et de Préhistoire, Brussels, pp. 331–356.

Shaw, A., Bates, M., Conneller, C., Gamble, C., Julien, M.A., McNabb, J., Pope, M., Scott, B., 2016. The archaeology of persistent places: the Palaeolithic case of La Cotte de St Brelade, Jersey. Antiquity 90, 1437–1453.

Shields, E.D., 2005. Mandibular premolar and second molar root morphological variation in modern humans: What root number can tell us about tooth morphogenesis. American Journal of Physical Anthropology 128, 299–311.

Shifman, A., Chananel, I., 1978. Prevalence of taurodontism found in radiographic dental examination of 1,200 young adult Israeli patients. Community Dental Oral Epidemiology 6, 200–203.

Skinner, M.M., Gunz, P., 2010. The presence of accessory cusps in chimpanzee lower molars is consistent with a patterning cascade model of development. Journal of Anatomy 217, 245–253.

Skinner, M.M., Wood, B.A., Boesch, C., Olejniczak, A.J., Rosas, A., Smith, T.M., Hublin, J.J., 2008. Dental trait expression at the enamel-dentine junction of lower molars in extant and fossil hominoids. Journal of Human Evolution 54, 173–186.

Skinner, M.M., Wood, B.A., Hublin, J.-J., 2009. Protostylid expression at the enamel-dentine junction and enamel surface of mandibular molars of *Paranthropus robustus* and *Australopithecus africanus*. Journal of Human Evolution 56, 76–85.

Skinner, M.M., Evans, A., Smith, T., Jernvall, J., Tafforeau, P., Kupczik, K., Olejniczak, A.J., Rosas, A., Radovčić, J., Thackeray, J.F., Toussaint, M., 2010. Brief communication: Contributions of enamel-dentine junction shape and enamel deposition to primate molar crown complexity. American Journal of Physical Anthropology 142, 157–163.

Smith, B.H., 1984. Patterns of molar wear in hunter–gatherers and agriculturalists. American Journal of Physical Anthropology 63, 39–56.

Smith, F.H., 1976. The Neandertal remains from Krapina: a descriptive and comparative study. Ph.D. Dissertation, University of Tennessee.

Smith, P., 1989. Dental evidence for phylogenetic relationships of Middle Palaeolithic hominids. In: Vandermeersch, B. (Ed.), L'Homme de Neandertal Vol 7. L'Extinction. Université de Liège, pp. 111–120.

Stringer, C.B., 2006. The Neanderthal-*H. sapiens* interface in Eurasia. In: Harvati, K., Harrison, T. (Eds.), Neanderthals Revisited: New Approaches and Perspectives. Springer, Dordrecht, pp. 315–323.

Stringer, C.B., Currant, A.P., 1986. Hominid specimens from La Cotte de St. Brelade. In: Callow, P., Cornford, J.M. (Eds.), La Cotte de St. Brelade 1961–1978. Excavations by C.B.M. McBurney. Geo Books, Norwich, pp. 155–158.

Tarli, S.M.B., 1983. A Neanderthal lower molar from Fondo Cattíe (Maglie, Lecce). Journal of Human Evolution 12, 383–401.

Trinkaus, E., 1995. Neanderthal mortality patterns. Journal of Archaeological Science 22, 121–142.

Trinkaus, E., 2007. European early modern humans and the fate of the Neandertals. Proceedings of the National Academy of Sciences USA 104, 7367–7372.

Trinkaus, E., 2017. The people of Palomas. In: Trinkaus, E., Walker, M.J. (Eds.), The People of Palomas: Neandertals from the Sima de las Palomas del Cabezo Gordo, Southeastern Spain. Texas A&M University Press, College Station, pp. 245–247.

Trinkaus, E., Moldovan, O., Bîlgăr, A., Sarcina, L., Athreya, S., Bailey, S.E., Rodrigo, R., Mircea, G., Higham, T., Ramsey, C.B., van der Plicht, J., 2003. An early modern human from the Peştera cu Oase, Romania. Proceedings of the National Academy of Sciences USA 100, 11231–11236.

Trinkaus, E., Bailey, S., Rougier , H., 2012. The dental and alveolar remains of Oase 1 and 2. In: Trinkaus, E., Constantin, S., Zilhão, J. (Eds.), Life and Death at the Pestera cu Oase: A

Setting for Modern Human Emergence in Europe. Oxford University Press, New York, pp. 781–851.

Turner, C.G., Nichol, C.R., Scott, G.R., 1991. Scoring procedures for key morphological traits of the permanent dentition. In: Kelley, M.A., Larsen, C.S. (Eds.), Advances in Dental Anthropology. Wiley-Liss, New York, pp. 13–31.

Van Beek, G.C., 1983. Dental Morphology: an Illustrated Guide. Wright, Oxford.

Vandermeersch, B., 1981. Les Hommes Fossiles de Qafzeh (Israel). CNRS, Paris.

Walker, M.J., Gibert, J., López, M.V., Lombardi, A.V., Pérez-Pérez, A., Zapata, J., Ortega, J., Higham, T., Pike, A., Schwenninger, J.L., Zilhão, J., 2008. Late Neandertals in southeastern Iberia: Sima de las Palomas del Cabezo Gordo, Murcia, Spain. Proceedings of the National Academy of Sciences USA 105, 20631–20636.

Walker, M.J., López, M.V., Haber, M., Trinkaus, E., 2017. The context of the Sima de las Palomas Neandertals. In: Trinkaus, E., Walker, M.J. (Eds.), The People of Palomas: Neandertals from the Sima de las Palomas del Cabezo Gordo, Southeastern Spain. Texas A&M University Press, College Station, pp. 4–18.

Wollny, G., Kellman, P., Ledesma-Carbayo, M.J., Skinner, M.M., Hublin, J.-J., Hierl, T., 2013. MIA-A free and open source software for gray scale medical image analysis. Source Code for Biology and Medicine 8, 20.

Wood, B.A., Abbott, S.A., 1983. Analysis of the dental morphology of Plio–Pleistocene hominids. I. Mandibular molars: crown area measurements and morphological traits. Journal of Anatomy 136, 197–219.

Zapata, J., Bayle, P., Lombardi, A.V., Pérez-Pérez, A., Trinkaus, E., 2017. The Palomas dental remains: preservation, wear, and morphology. In: Trinkaus, E., Walker, M.J. (Eds.), The People of Palomas: Neandertals from the Sima de las Palomas del Cabezo Gordo, Southeastern Spain. Texas A&M University Press, College Station, pp. 52–88.

Zeuner, F.E., 1940. The age of Neanderthal man, with notes on the Cotte de St Brelade, Jersey, C.I. London University Institute of Archaeology, London.

Zilhão, J., Trinkaus, E., Constantin, S., Milota, S., Gherase, M., Sacrina, L., Danciu, A., Rougier, H., Quilès, J., Rodrigo, R., 2007. The Peştera cu Oase people, Europe's earliest modern humans. In: Mellars, P.M., Bar-Yosef, O., Stringer, C., Boyle, K.V. (Eds.), Rethinking the Human Revolution: New Behavioural and Biological Perspectives on the Origin and Dispersal of Modern Humans. McDonald Institute for Archaeological Research, Cambridge, pp. 249–262.

Figure legends

Figure 1. Location of La Cotte de St Brelade (from Shaw et al., 2016). A) Channel Islands within north-western Europe. B) Jersey in relation to other Channel Islands and the French coast, showing the ~7 m drop in sea level necessary to reconnect to the continent. C) simplified geological map of Jersey showing main sites. Based on an image supplied by John Renouf, with permission.

Figure 2. Site plan (A) and cross-section (B) of La Cotte de St. Brelade.

Figure 3. E.T. Nicolle shown standing on the level of the hearth, with what might be the ledge on which the teeth were found on the left-hand side. Photograph by R. Mollet. Reproduced with the kind permission of the Société Jersiaise.

Figure 4. SJMJ2463, left C_1. a–c) Photographs in occlusal (a), distal (b), and mesial (c) views. d–f) Surface models in occlusal (d), distal (e), and mesial (f) views. g) EDJ in lingual view. h) CT cross-section (plane of section shown in d); i) CT cross-section (plane of section shown in f). Abbreviations: B = buccal; D = distal; L = lingual; M = mesial.

Figure 5. SJMJ2457, left P^4. a–c) Photographs in occlusal (a), distal (b), and mesial (c) views. d–f) Surface models in occlusal (d), distal (e), and mesial (f) views. g) EDJ in occlusal view. h) CT cross-section (plane of section shown in d); i) CT cross-section (plane of section shown in f). Abbreviations: B = buccal; D = distal; L = lingual; M = mesial.

Figure 6. SJMJ2464, left P_3. a–c) Photographs in occlusal (a), distal (b), and mesial (c) views. d–f) Surface models in occlusal (d), distal (e), and mesial (f) views. g) EDJ in occlusal view. h) CT cross-section (plane of section shown in d); i) CT cross-section (plane of section shown in f). Abbreviations: B = buccal; D = distal; L = lingual; M = mesial.

Figure 7. SJMJ2465, left P_4. a–c) Photographs in occlusal (a), distal (b), and mesial (c) views. d–f) Surface models in occlusal (d), distal (e), and mesial (f) views. g) EDJ in occlusal view. h) CT cross-section (plane of section shown in d); i) CT cross-section (plane of section shown in f). Abbreviations: B = buccal; D = distal; L = lingual; M = mesial.

Figure 8. SJMJ2456, right M^1. a–c) Photographs in occlusal (a), distal (b), and mesial (c) views. d–f) Surface models in occlusal (d), distal (e), and mesial (f) views. g) EDJ in occlusal view. h) CT cross-section (plane of section shown in d); i) CT cross-section (plane of section shown in f). Occlusal polygon shape shown on occlusal photograph. Abbreviations: B = buccal; D = distal; L = lingual; M = mesial.

Figure 9. SJMJ2458, left M^2. a–c) Photographs in occlusal (a), distal (b), and mesial (c) views. d–f) Surface models in occlusal (d), distal (e), and mesial (f) views. g) EDJ in occlusal view. h) CT cross-section (plane of section shown in d); i) CT cross-section (plane of section shown in f). Abbreviations: B = buccal; D = distal; L = lingual; M = mesial.

Figure 10. SJMJ2459, right M^3. a–c) Photographs in occlusal (a), distal (b), and mesial (c) views. d–f) Surface models in occlusal (d), distal (e), and mesial (f) views. g) EDJ in occlusal view. h) CT cross-section (plane of section shown in d); i) CT cross-section (plane of section shown in f). Abbreviations: B = buccal; D = distal; L = lingual; M = mesial.

Figure 11. Cast of SJMJ2467, left M^3. a–f) Photographs in occlusal (a), mesial (b), buccal (c), apical (d), distal (e), lingual (f) views. Note that a black and white photo of the original tooth taken after casting is provided in distal view. Abbreviations: B = buccal; D = distal; L = lingual; M = mesial.

Figure 12. SJMJ2461, right M_2. a–c) Photographs in occlusal (a), distal (b), and mesial (c) views. d–f) Surface models in occlusal (d), distal (e), and mesial (f) views. g) EDJ in occlusal view. h) CT cross-section (plane of section shown in d); i) CT cross-section (plane of section shown in f). Letters (a and b) on occlusal image denote mesiodistally concave/convex facets. Abbreviations: B = buccal; D = distal; L = lingual; M = mesial.

Figure 13. SJMJ2455, left M_2. a–c) Photographs in occlusal (a), distal (b), and mesial (c) views. d–f) Surface models in occlusal (d), distal (e), and mesial (f) views. g) EDJ in occlusal view. h) CT cross-section (plane of section shown in d). i) occlusion of SJMJ2455 and SJMJ2458 (not to scale). Abbreviations: B = buccal; D = distal; L = lingual; M = mesial.

Figure 14. SJMJ2460, right M_3. a–c) Photographs in occlusal (a), distal (b), and mesial (c) views. d–f) Surface models in occlusal (d), distal (e), and mesial (f) views. g) EDJ in occlusal view showing numerous accessory dentine horns (*). h) CT cross-section (plane of section shown in d). i) articulation of SJMJ2460 and SJMJ2461 (not to scale). Abbreviations: B = buccal; D = distal; L = lingual; M = mesial.

Figure 15. La Cotte SJMJ2452 occipital fragment (right) compared to a modern child aged about 6 years. A) ectocranial surface; B) endocranial surface, dotted lines indicating the pathway of the transverse sulcus, which passes directly across the asterion in both bones.

Figure 16. Comparison of M^1 occlusal polygon shapes. Neanderthal: Krapina D161; La Cotte: SJMJ2456; fossil *H. sapiens*: La Madeleine. Abbreviations: B = buccal; D = distal; L = lingual; M = mesial.

Figure 17. Results of the principal components analysis of cervix shape landmarks in P^4 in shape (a) and form (b) space, and wireframe models of mean cervix shape in shape (c) and form (d) space. The percentage of variance depicted by each principal component (PC) is indicated. Abbreviations: Hn = *Homo neanderthalensis*; Hs = *Homo sapiens.*

Figure 18. Results of the principal components analysis of cervix shape landmarks in P_3 in shape (a) and form (b) space, and wireframe models of mean cervix shape in shape (c) and form (d) space. The percentage of variance depicted by each principal component (PC) is indicated. Abbreviations: Hn = *Homo neanderthalensis*; Hs = *Homo sapiens.*

Figure 19. Results of the principal components analysis of cervix shape landmarks in P_4 in shape (a) and form (b) space, and wireframe models of mean cervix shape in shape (c) and form (d) space. The percentage of variance depicted by each principal component (PC) is indicated. Abbreviations: Hn = *Homo neanderthalensis*; Hs = *Homo sapiens.*

Figure 20. Results of the principal components analysis of cervix shape landmarks in M^1 in shape (a) and form (b) space, and wireframe models of mean cervix shape in shape (c) and form (d) space. The percentage of variance depicted by each principal component (PC) is indicated. Abbreviations: Hn = *Homo neanderthalensis*; Hs = *Homo sapiens.*

Figure 21. Results of the principal components analysis of cervix shape landmarks in M^2 in shape (a) and form (b) space, and wireframe models of mean cervix shape in shape (c) and form (d) space. The percentage of variance depicted by each principal component (PC) is indicated. Abbreviations: Hn = *Homo neanderthalensis*; Hs = *Homo sapiens.*

Figure 22. Results of the principal components analysis of cervix shape landmarks in M^3 in shape (a) and form (b) space, and wireframe models of mean cervix shape in shape (c) and form (d) space. The percentage of variance depicted by each principal component (PC) is indicated. Abbreviations: Hn = *Homo neanderthalensis*; Hs = *Homo sapiens.*

Figure 23. Results of the principal components analysis of cervix shape landmarks in M_2 in shape (a) and form (b) space, and wireframe models of mean cervix shape in shape (c) and form (d) space. The percentage of variance depicted by each principal component (PC) is indicated. Abbreviations: Hn = *Homo neanderthalensis*; Hs = *Homo sapiens.*

Figure 24. Crown area adjusted Z scores; distances of La Cotte dimensions from comparative sample means of late Neanderthal, fossil *Homo sapiens* and Krapina. Abbreviations: Hs = *H. sapiens*; U = upper; L = lower; C = canine; P = premolar; M = molar; UM3a = SJMJ2467; UM3b = SJMJ2459. P^4: buccolingual dimension only.

Figure 25. Crown index adjusted Z scores; distances of La Cotte dimensions from comparative sample means of late Neanderthal, fossil *Homo sapiens* and Krapina. Abbreviations: Hs = *H. sapiens*; U = upper; L = lower; C = canine; P = premolar; M = molar; UM3a = SJMJ2467; UM3b = SJMJ2459.

Response to reviewers

A number of minor clarifications have been made to the ms, identified in the cover letter and the tracked version of the ms.

There are three minor factual corrections and some grammatical corrections, not tracked. The factual corrections are:

Line 43; 40.6 in place of 40.5

Line 616; '39% and 13%' in place of '13% and 39%'

Line 890; 'P_3 and' deleted.

Also, in Table 6, hypocone size for SJMJ2459 changed from (3.5) to (>2).

The morphology of the Late Pleistocene hominin remains from the site of La Cotte de St Brelade, Jersey (Channel Islands)

Tim Compton[a,*], Matthew M. Skinner[b,c], Louise Humphrey[a], Matthew Pope[d], Martin Bates[e], Thomas W. Davies[c], Simon A. Parfitt[a,d], William P. Plummer[b], Beccy Scott[f], Andrew Shaw[g], Chris Stringer[a]

[a] *Centre for Human Evolution Research, Department of Earth Sciences, Natural History Museum, Cromwell Road, London SW7 5BD, UK*

[b] *School of Anthropology and Conservation, University of Kent, Canterbury CT2 7NR, UK*

[c] *Department of Human Evolution, Max Planck Institute for Evolutionary Anthropology, Deutscher Platz 6, 04103 Leipzig, Germany*

[d] UCL *Institute of Archaeology, University College London, 31-34 Gordon Square, London WC1H 0PY, UK*

[e] *Faculty of Humanities and Performing Arts, University of Wales Trinity St David, Lampeter, Ceredigion SA48 7ED, UK*

[f] *Directorate, The British Museum, Great Russell Street, London WC1B 3DG, UK*

[g] *Wessex Archaeology, Portway House, Old Sarum Park, Salisbury, Wiltshire SP4 6EB, UK*

* Corresponding author.

E-mail address: t.compton@nhm.ac.uk (T. Compton).

Acknowledgements

We would like to thank Shara Bailey, Silvia Bello, Emmy Bocaege, Christopher Dean, Brenna Hassett, Robert Kruszynski, Helen Liversidge, Theya Molleson and Carina Phillips for help and advice; Robert Kruszynski and Rachel Ives for access to the Natural History Museum collections; Harry Taylor for photographing the La Cotte teeth; Laura Buck for producing the CT scans; Vida Milovanovic for access to the Royal College of Surgeons archives; Ruth Benny and Katie Ormerod for access to the Natural History Museum archives. We would also like to thank Jersey Heritage for facilitating the research loan of the material, and for giving their permission for online open-access to scans of the material. In addition we would like to thank the Calleva Foundation and Human Origins Research Fund for funding parts of the NHM-based research. For access to comparative CT scans we thank Jean-Jacques Hublin, Department of Human Evolution, Max Planck Institute for Evolutionary Anthropology, Leipzig. This project has received support from the European Union's Horizon 2020 research and innovation programme (grant agreement No. 819960). Our initial reinvestigation and dating of La Cotte de St Brelade was made possible through a grant by the Natural Environment Research Council and with the kind permission of the Société Jersiaise, who own the site.

The morphology of the Late Pleistocene hominin remains from the site of La Cotte de St Brelade, Jersey (Channel Islands)

ABSTRACT

Thirteen permanent fully-erupted teeth were excavated at the Paleolithic site of La Cotte de St Brelade in Jersey in 1910 and 1911. These were all found in the same location, on a ledge behind a hearth in a Mousterian occupation level. They were originally identified as being Neanderthal. A fragment of occipital bone was found in a separate locality in a later season. Recent dating of adjacent sediments gives a probable age of <48 ka. The purpose of this paper is to provide an updated description of the morphology of this material, and consider its likely taxonomic assignment from comparison with Neanderthal and *Homo sapiens* samples. One of the original teeth has been lost, and we identify one as non-hominin. At least two adult individuals are represented. Cervix shape and the absence of common Neanderthal traits in several teeth suggest affinities with *H. sapiens* in both individuals, while crown and root dimensions and root morphology of all the teeth are entirely consistent with a Neanderthal attribution, pointing towards a possible shared Neanderthal and *H. sapiens* ancestry (the likely date of this material corresponds with the time in which both Neanderthals and *H. sapiens* were present in Europe). The occipital fragment is stratigraphically more recent and does not exhibit any diagnostic Neanderthal features.

Keywords: Hominin teeth; Late Pleistocene; Neanderthal; European Pleistocene *Homo sapiens*; La Cotte de St. Brelade; Hominin morphology.

1. Introduction

The timing and duration of overlaps between *Homo sapiens* and Neanderthals in Europe, and the nature of their interaction, have long been debated by archaeologists and anthropologists (e.g., Stringer, 2006; Hoffecker, 2009). Recent evidence points towards contemporaneity or alternation of occupation of the two populations (Benazzi et al., 2011; Harvati et al., 2019). The application of improved radiocarbon dating methods has shown that the Mousterian ended by ~41–39 ka cal BP across much of Europe (Higham et al., 2014). Furthermore, new data from Bulgaria suggest that *H. sapiens* were already in Eastern Europe by ~45 ka, several millennia before the physical disappearance of the Neanderthals from the region. Hominin fossils from Bacho Kiro were identified as *H. sapiens* from morphology and mtDNA analysis, and directly dated to ~46.8–42.8 ka cal BP (Fewlass et al., 2020; Hublin et al., 2020). Radiocarbon dating shows a clear overlap of the initial Upper Paleolithic at Bacho Kiro with the late Mousterian and Châtelperronian attributed to late Neanderthal populations (Fewlass et al., 2020). In central and northwestern Europe, the Châtelperronian (~44–40 ka) overlaps with both the Early Aurignacian, starting at ~43–42 ka, and the Proto-Aurignacian, starting at ~42 ka (Hublin, 2015). In Western Europe, there is direct fossil evidence for the presence of both *H. sapiens* and Neanderthals at ~41–40.4 ka. A tooth discovered in a Proto-Aurignacian context at the site of Grotta di Fumane in northern Italy and dated to ~41–38.5 ka cal BP was found to have *H. sapiens* DNA (Benazzi et al., 2015), while a Neanderthal tibia from Saint-Césaire in western France was directly dated to ~42–40.6 ka cal BP (Hublin et al., 2012) and Neanderthal fossils from Spy in Belgium have been directly dated to ~42.2–40.4 ka cal BP (Semal et al., 2013). The Oase 1 *H. sapiens* from Romania, dated to ~42.5–40.5 ka cal BP (Zilhão et al., 2007), had a Neanderthal ancestor within the previous six generations (Fu et al., 2015), which demonstrates that these populations probably did overlap in Europe before 40 ka. In support of this, Peter (2019) has determined that, while the majority of Neanderthal ancestry entered *H. sapiens* populations between ~55 and ~48 ka,

there was a lesser amount of gene flow within Europe, ending at ~40 ka. Interestingly, Hajdinjak et al. (2018) found no evidence of recent gene flow from *H. sapiens* in four very late Neanderthals, dated to <45 ka cal BP, from Goyet, Spy, Les Cottes and Mezmaiskaya.

The hominin remains from La Cotte de St Brelade on Jersey (Fig. 1) probably fall within this key time period when both Neanderthals and *H. sapiens* were present in Western Europe. Their taxonomic status is therefore of considerable interest. The hominin remains originate from an area of complex sedimentation close to where the North and West Ravines meet (Fig. 2). Members of the Société Jersiaise undertook excavation in this area in 1910–1911 after the cave entrance had been cleared of clay and granite rubble deposits. The investigators located a series of fine-grained deposits, some of which were rich in ash and carbonized wood, which they described as hearths (Nicolle and Sinel, 1910). The excavations of these deposits continued until 1920 and produced at least 20,000 stone artifacts (Callow, 1986a), but it appears that smaller debitage elements were largely discarded during the initial seasons. These artifacts were described at the time as Mousterian in character (Marett, 1916), and more recent analysis has confirmed that all the stone artifacts are consistent with Late Middle Paleolithic technological practices (Callow, 1986a). The assemblage contains both Levallois and discoidal production elements, as well as formal tools, including side scrapers and two bifaces. No artifacts consistent with Upper Paleolithic technology have been identified among the artifact collections of La Cotte de St Brelade.

It is not possible to determine what fauna were found within deposits directly associated with the hominin remains from the surviving archive of the excavations carried out between 1910 and 1920. However, the faunal material recovered from 'Weichselian' units as a whole includes *Mammuthus primigenius*, *Coelodonta antiquitatis*, *Equus* sp., *Rangifer tarandus*, *Crocuta crocuta*, and *Vulpes vulpes* (see Callow, 1986b), species which would be consistent with a Marine Isotope Stage (MIS) 3 attribution in northern France (Auguste, 2009).

Mammoth, woolly rhinoceros and horse are specifically mentioned as coming from the same general area as the hominin teeth (Nicolle and Sinel, 1910; Keith and Knowles, 1911).

The hominin teeth were discovered over two seasons. In 1910, nine teeth were found in a mass of poorly preserved bone (for which no identifications are recorded) on a rock ledge above the layer identified as a hearth (Fig. 3; Nicolle and Sinel, 1910). They were described as lying side by side in original position, but with no trace of once supporting bone apparent. A further four teeth were found in clay adhering to the rock at the same location in 1911 (Nicolle and Sinel, 1912). An occipital fragment, together with two other bone fragments, were discovered in a ravine 6 ft (1.8 m) beyond the entrance of the cave and 18 ft (5.4 m) above the Mousterian cave floor level by Ernest Daghorn in 1915 (Marett, 1916).

Analysis of the surviving archive and a modern survey of the site have allowed us to broadly identify the location and position in the stratigraphic succession from which the hominin teeth were recovered and, more generally, the position and context of the hominin occipital fragment (Table 1). Although the deposits from this part of the site were removed during the early 20th century, their stratigraphic equivalents appear to extend into areas of remaining sediment within the main West Ravine (Bates et al., 2013). Optically stimulated luminescence (OSL) dating undertaken in 2011 within the middle parts of this sequence, approximately 4 m below the location where the teeth were discovered, suggests that the deposits containing the teeth and the occipital fragment both postdate ~48 ka (Bates et al., 2013). In view of the vertical extent of sediments between the lower dated horizon and the location from which we understand the teeth to have been discovered, a date that is clearly younger than 48 ka for the teeth is the only tenable proposition. It is plausible that these deposits span a period in which both late Neanderthal populations and those of *H. sapiens* were present in Western Europe, and during which sea levels were low enough for Jersey to be part of a continuous landmass with France (Fig. 1B; Scott et al., 2014; Shaw et al., 2016).

Consequently, understanding the exact date and taxonomic affinity of these hominin fossils is important for understanding Pleistocene population replacement at a regional scale.

The teeth were originally described by Keith and Knowles (1911, 1912). The 1912 paper is a reprint of the 1911 paper, with additional details of the four teeth found in 1911. Keith (1913) further addressed the considerable level of taurodontism in the molar teeth. The teeth were briefly described in Marett (1911) and Oakley et al. (1975), and more recently were studied by Stringer and Currant (1986), who noted that by this date two of the teeth were only represented by casts and one other tooth was missing. The missing tooth was a left I^1, represented only by the root. The crown of this tooth had disintegrated before it was seen by Arthur Keith, as the result of an accident during conservation (letter from J. Sinel to Keith dated 1st September 1911, in the archives of the Royal College of Surgeons). In 1929 Tom Watson, an amateur paleontologist/archaeologist on Jersey, sent a hominin lower canine that he had found at La Cotte to Arthur Keith for identification (letter dated 17th January 1929, in the archives of the Royal College of Surgeons). Although Tom Watson left all his finds to the Jersey Museum, this tooth has not come to light. This letter also states that Tom Watson had previously sent teeth and bones that he had discovered at La Cotte to Arthur Keith for identification, but no record of these has been found. The three bone fragments recovered in 1915 were initially identified as parts of an occipital, malar and mandible from a single juvenile skull (Marett, 1916). Angel and Coon (1954) reanalyzed the material and concluded that only the occipital fragment was human, and that it belonged to a child about 5 years old. This opinion was supported by Stringer and Currant (1986), who agreed that the other two fragments did not represent any part of the human skeleton.

The purpose of this paper is to provide an updated description of the morphology of the La Cotte teeth and the occipital fragment, and present data relevant to their taxonomic attribution.

2. Materials and methods

2.1. Described material from La Cotte

The material available for study consists of ten isolated permanent fully erupted teeth (Table 2), and a fragment of occipital. These are held by the Jersey Museum, and were temporarily loaned to the Natural History Museum, London, in 2015. Two other teeth, SJMJ2462 (right I_1) and SJMJ2467 (left M^3), are represented by casts. The casts made in 1911 and now held by the Natural History Museum, London, were used in this study because, of several casts available, they are the most similar to the teeth described and illustrated by Keith and Knowles (1912). The right I_1 (SJMJ2462) is thought to be non-hominin and is not included in the analysis (see Supplementary Online Material [SOM] S1). With permission of Jersey Heritage, the microtomographic scans of the La Cotte de St Brelade specimens published in this paper are publically available (under a CC BY-NC 4.0 license) through the Human Fossil Record online archive (https://human-fossil-record.org/).

2.2. Comparative material

Comparative samples for morphological traits scored at the outer enamel surface (OES) principally come from Bailey (2006a) and, where the trait is not scored by Bailey (2006a), from Martinón-Torres et al. (2012)—see SOM Tables S1 and S2. These samples consist of Neanderthals and fossil (primarily European Late Pleistocene) *H. sapiens*. Comparative CT-scan samples employed for geometric morphometrics, and occurrence of Tomes' root (Arizona State University dental anthropology system [ASUDAS] grades 4–5: Turner et al., 1991) and taurodontism in P_3 and P_4, consist of Neanderthals, fossil (Pleistocene) *H. sapiens* and recent (Holocene) *H. sapiens* (SOM Tables S1, S3, S4). Comparative metrics data for the early Neanderthal site of Krapina, late Neanderthals and fossil (European Late Pleistocene)

H. sapiens were taken from the literature and the NESPOS database (2013), identified in table legends and in SOM Tables S1–S3, S5, S6. For crown dimensions, the site of Krapina was separated from late Neanderthals because of the distorting effect caused by the relatively large size of the Krapina tooth crowns, and in some cases their different shape, together with the fact that the Krapina teeth make up approximately one third of the total Neanderthal sample.

2.3. Methods

Definitions We use the terms pre-Neanderthal (e.g., Atapuerca-SH, Pontnewydd), early Neanderthal (e.g., Krapina, Bourgeois-Delaunay), and classic/late Neanderthal, as proposed by Dean et al. (1998). Although this assumed a linear and almost certainly oversimplified model of Neanderthal evolution (Hublin and Roebroeks, 2009), Compton and Stringer (2015) found it useful in classifying morphological differences observed in Neanderthal dentitions.

Dental morphological traits Most of the morphological traits were assessed using the Arizona State University Dental Anthropology System (ASUDAS), and associated reference plaques (Turner et al., 1991; Scott and Turner, 1997; Scott et al., 2018). Additional traits described by other authors and not included in the ASUDAS were also utilized (see SOM S2 for descriptions of the traits studied). Wherever possible, traits were scored at the OES but, due to wear, some traits could only be scored at the enamel dentine junction (EDJ). There are few comparative data available for the frequency of traits at the EDJ, and they are only provided here for P^4. In other cases, traits scored at the EDJ were compared to frequencies of traits at the OES. Several authors have found a strong positive correlation between the EDJ and the OES in the expression of morphological traits in hominins (Krenn et al., 2019 for lower premolars; Guy et al., 2015 for upper molars; Skinner et al., 2008, 2010 for lower molars) but we recognize that wear obscures the OES and can lead to misidentification of trait

expression. For each trait, 95% confidence limits were calculated for trait frequency in each taxon, and for the difference in frequencies between the two taxa (SOM S3). Traits that are of potential use in making inferences about taxonomic affiliation are those where the confidence intervals for the two comparative samples do not overlap, or where the confidence limits for the difference in frequencies between the two comparative samples are both either above or below zero (i.e., do not include zero; Altman et al., 2000).

Relative cusp areas and occlusal polygon Relative cusp areas, and the angles and relative size of the occlusal polygon, on SJMJ2456 (right M^1) were measured from a high definition photograph of the occlusal surface taken perpendicular to the plane of the cervix, using ImageJ software (Rasband, 2008), according to the methodology described by Bailey (2004). The original positions of the cusp tips were estimated by determining the point of intersection of the principal ridges of each cusp visible at the EDJ,

Taurodontism The degree of taurodontism of the molars was determined using the method of Shifman and Chananel (1978). Shifman and Chananel's (1978) method was employed (SOM S2) because it provides an absolute measurement, rather than a relative measurement that requires complete roots. The distance between the bicervical line and the highest point on the floor of the pulp cavity of the molar teeth was measured from the CT scans (Table 2: pulp chamber height). This is preferable to taking the measurement from the roof of the pulp chamber, where secondary dentine may form as the tooth wears. The method presented by Keene (1966; see SOM S2) was used to measure the degree of taurodontism in SJMJ2461 (right M_2), because the original root length could be estimated. The original length of the root of this tooth, where the broken sides of the tooth's root are converging, was estimated by extending these on a scaled photograph, and assuming a rounded tip.

Geometric morphometrics of cervix shape Microtomography was used to examine the internal structures of the teeth. Specimens were scanned at the Natural History Museum using

an XTekCT scanner (180 kV, 205 µA, 0.25mm copper filter, 3000 projections) with a resultant isometric voxel size of ~30 µm. To facilitate segmentation, each image stack was filtered using a mean-of-least-variance filter (kernel size one) or a median and mean-of least variance filter (each with kernel size three; Wollny et al., 2013). Each tooth was segmented into its enamel and dentine components in Avizo 6.3 (ThermoFisher Scientific, Waltham). Surface models of the EDJ were produced using the surface generation module (unconstrained smoothing) and saved as PLY files.

Geometric morphometric analysis of cervix shape (in almost all cases the dentine horns, and the ridges between, were too worn for landmark-based measurement) was conducted in Mathematica 10 (Wolfram, Long Hanborough) following protocols outlined in previous publications (Skinner and Gunz, 2010; Martin et al., 2017). Thirty semilandmarks were placed around the cervix of each tooth. For the mandibular molars, the initial cervix landmark was placed on the mesiobuccal corner of the crown (beneath the protoconid) and continued mesially. In the maxillary molars, the initial landmark was placed on the middle part of the buccal face of the crown (between the paracone and metacone) and continued mesially. For mandibular and maxillary premolars the initial landmark was placed at the mid-point of the buccal face and continued mesially. Estimations of missing portions of the cervix were made for SJMJ 2457 (left P^4), 2456 (right M^1) and 2461 (right M_2; SOM Fig. S1), and subjected to Procrustes superimposition and then slid (Gunz and Mitteroecker, 2013) to create a geometrically homologous set of shape variables. Principal components analysis (PCA) was conducted to assess variation in cervix shape. Canonical variate analysis (CVA) was conducted to assess taxonomic affinity using inclusive sets of principal component scores (i.e., first set using 1–5 PCs, second set using 1–6 PCs, etc.) that represented ~95% of overall shape variation. PCA was conducted in both shape space and form space; the latter including

the log of centroid size as a variable. CVA was only conducted in shape space and attempted to assign La Cotte teeth to either Neanderthals or *H. sapiens*.

Crown and root measurements Measurements of the La Cotte teeth were taken with sliding calipers to the nearest 0.1 mm. The crown dimensions and root lengths were measured using the method of Moorrees (1957): crown = maximum dimensions parallel to and at right angles to the buccal surface; root = maximum vertical dimension from the cervix of the mesiobuccal root on the buccal aspect. In multirooted teeth, the term 'trunk' is used to describe the portion of the root between the cervix and the point at which the individual roots furcate, and root trunk length was measured as the distance between the cervix and the root furcation on the aspect of the tooth on which this was at a minimum. The dimensions of the root at the cervix were measured as the maximum dimensions at right angles to the mesial and buccal surfaces. This definition was also used to measure cervical dimensions from CT scans of comparative samples. Where the measurements for both left and right antimeres are available, the average was used. Mesiodistal crown dimensions of the La Cotte teeth were adjusted for wear using the method of Wood and Abbott (1983), in which the estimated original margins of the tooth are drawn on a scaled photograph of the occlusal surface and the difference between these and the actual margins measured. The adjusted measurements were used for comparisons with other teeth. Where the length of the La Cotte teeth could not be estimated, only the buccolingual dimension is used for comparison with other teeth. The level of occlusal wear was quantified using Murphy's method, as summarized by Smith (1984; Table 2).

An adjusted z-score method, using Student's t inverse distribution (Maureille et al., 2001), was employed to compare each of the La Cotte measurements with the means and standard deviations of comparative groups. The formula applied was:

$$\frac{\text{La Cotte dimension} - X}{\text{Invt}_{0.975;\, n\text{-}1} * \text{SD}}$$

where X, SD and *n* represent the mean, sample standard deviation and sample size respectively of the comparative sample. The interval between -1 and +1 comprises 95% of the variation in the comparative sample. A value of zero denotes that the La Cotte dimension equals the mean of the comparative sample. A positive adjusted Z score indicates a La Cotte dimension above the mean value and vice versa. All measurements and observations on the La Cotte teeth were repeated by the same observer after an interval of one month.

3. Results

3.1. Descriptions

The tooth crown and roots appear to not have undergone any erosive taphonomic processes. However, cracking and areas of taphonomic reworking of the dentine are evident in the CT scans. Layers of cementum are apparent on the apical half of the root surfaces, with the exception of SJMJ2459 (right M^3), but hypercementosis is not present. The pulp chambers of the teeth exhibit what appears to be demineralisation and subsequent desiccation of the circumpulpal primary dentine, leading to it having a 'feathered' appearance (C. Dean, pers. comm.). There are deposits of secondary dentine in the molar pulp chambers. All the teeth show some wear and this is generally flat and near horizontal. Most tooth crowns have dentine exposed on individual cusps, and the surface morphology has largely been obliterated.

Our identifications of tooth type are in agreement with those given by Keith and Knowles (1912). Traits are described using the ASUDAS grades (Turner et al., 1991) unless otherwise stated. X-ray photographs of the teeth are shown in SOM Figures S2 and S3. Discrete morphological traits of the teeth, along with comparative data, are reported in Tables 3–7.

<u>Lower left permanent canine (SJMJ2463)</u> See Figure 4. The crown is complete, but the apex of the root is missing. Severe cracking is evident on the buccal surface of the root below the

cervix and running down the distal surface from this point to the apex. This is also evident in the buccolingual CT slice (Fig. 4h).

There is moderate (grade 2) shoveling (Fig. 4a), trace (grade 1) double shoveling (Fig. 4a), a grade 4 distal accessory ridge (Fig. 4g), and a mesiobuccal bulge viewed occlusally. Lingually, a tuberculum dentale is present as a mild medially placed bulge without a free apex and there is a faint, wide but low, lingual medial ridge (Fig. 4g). The root is labiolingually wide, with deep mesial and distal longitudinal grooves. The mesial groove is particularly marked. The pulp canal is single and ovoid throughout the root, wide viewed distally, and mesiodistally flattened (Fig. 4h, i). There is distinct vertical convex curvature of the buccal aspect of the root, particularly towards the apex, and vertical convexity of the lingual aspect.

Upper left fourth premolar (SJMJ2457) See Figure 5. The preserved morphology (narrow and ovoid, rather than a more triangular crown shape) is consistent with a P^4. The tooth has matching occlusion (facets, wear shape and level of wear) with the left P_4 (SJMJ2465). The crown has a postmortem chip on the distolingual corner of the occlusal rim, at the edge of a large double fracture, and the root apices are missing. The distal aspect of the crown must have broken off in life, since there is rounding and vertical striations on the occlusal edge of the fracture.

The buccal surface of the crown is swollen, viewed mesially. The sagittal sulcus is visible at the OES, curved lingually at the distal end (Fig. 5d) and, from the EDJ, it can be seen that it terminates at the mesial margin (Fig. 5g). The EDJ reveals a small mesial accessory crest (Fig. 5g), that likely delineated a small mesial fovea in the unworn tooth. A small pit is still visible in this location on the worn occlusal surface (Fig. 5d). There are two robust roots, with separate root canals, linked mesially by a radicular plate, creating a deep groove on the distal root surface (cross-section in Fig. 5i). The buccal root is vertically convex. The pulp

chamber is taurodont, extending to the root furcation. It is mildly ovoid in distal and buccal views (Fig. 5h; SOM Fig. S4).

Lower left third premolar (SJMJ2464) See Figure 6. The large size of the buccal cusp, and its more lingual placement than in SJMJ2465 (left P_4), and our analysis of cervix shape (SOM Fig. S5) indicate a P_3. Additionally, a buccal cingulum is present at the EDJ, which occurs only on the P_3 in the comparative samples. The crown is complete, but the root apices are missing.

The occlusal crown outline is buccolingually oblong, with slight mesiolingual truncation (insufficient to score tooth as asymmetric) and the mesiodistal dimension greatest buccally. Viewed mesially, the upper part of the buccal surface is curved sharply lingually and the lingual surface is swollen. The bulbous metaconid is mesially placed, and there are two smaller distolingual cusps observable at the OES (Fig. 6a). The Y-shaped mesiobuccally slanted sagittal sulcus is not interrupted (Fig. 6a). It is narrow and the two foveae are insignificant, the distal being the deepest. Traces of mesial and distal accessory ridges can be seen on the buccal cusp at the OES, and are clearly visible at the EDJ (Fig. 6d, g). A faint distolingual groove is present at the OES (Fig. 6a, d), but the lingual margin is uninterrupted at the EDJ (Fig. 6g; Davies et al., 2019). The mesial and distal margins also both appear to have been uninterrupted (there is no evidence of interruption at the EDJ). Examination of the EDJ (Fig. 6g) indicates no evidence of a transverse crest. Small dentine horns underlie the two accessory cusps distal to the metaconid (Fig 6g). Although not visible at the enamel surface, there is a faint buccal cingulum at the EDJ, consisting of a mesially placed horizontal ridge continuing from a slight mesial vertical groove/ridge (not shown).

There is a grade 4 Tomes' root (cross-section in Fig. 6i), with partial division into two roots, each with a single root canal. In the mesiobuccal root there is a vertical mesial groove and a prominent buccal groove. The buccal aspect of this root is vertically convex. The

taurodont pulp chamber extends to the root furcation and is mildly ovoid in lingual view (SOM Fig. S6). In distal view it is convex lingually on the lingual side at the cervix, and is hourglass shaped below this. The root canal in the buccal root is enlarged buccolingually (Fig. 6h, i).

Lower left fourth premolar (SJMJ2465) See Figure 7. Morphological identification as a P_4 is confirmed by analysis of cervix shape (SOM Fig. S5). The tooth cannot be a metamere of SJMJ2464 (left P_3) because the interproximal facets do not match. The tooth is complete apart from the apex of the root, which is chipped. Severe cracking can be seen on the lingual side of the root in the buccolingual CT slice (Fig. 7h).

The occlusal outline is oblong, with very slight mesiolingual truncation. The worn down buccal surface of the crown lacks the convexity and lingual inclination observed in SJMJ2464 (left P_3), and the lingual face is less swollen. The narrow sagittal sulcus has a small bridge of enamel centrally (Fig 7d). However, examination of the EDJ reveals no evidence of a transverse crest (Fig. 7g). As with SJMJ2464 (left P_3), the mesial and distal foveae (distal deepest) do not appear to have been large. The sagittal sulcus does not interrupt either margin at the OES at this level of wear (Fig. 7d); and neither margin is interrupted at the EDJ. The EDJ reveals a distolingual cusp, in addition to the metaconid, as well as a small dentine horn on the mesial marginal ridge, and confirms the presence of a distal accessory ridge on the buccal cusp (Fig. 7g).

There is a single straight-sided root, mesially convex viewed apically, with a longitudinal groove in the apical half of the distal surface. The root is taurodont, with the pulp chamber extending to the apex (SOM Fig. S6). In distal view it can be seen that there has been considerable taphonomic alteration of the dentine towards the centre of the root, so that it is difficult to determine the original shape of the pulp chamber but, as with the left P_3 (SJMJ2464), the lingual side appears to be convex at the cervix (Fig. 7h; SOM Fig. S6).

Molars The molar buccal and lingual faces are mildly convex viewed mesially. The buccal surface grooves on upper molars are weak, and they are absent on lower molars. The loss of occlusal surface morphology on the molars, despite a relatively low level of wear, suggests that the unworn cusps were low. All the molar roots exhibit supraradicular taurodontism (Kallay, 1970), where the pulp chamber is enlarged before the furcation of the roots.

Upper right permanent first molar (SJMJ2456) See Figure 8. The low crown index value (equal mesiodistal and buccolingual measurements), particularly in relation to the other upper molars in the comparative samples, and our analysis of cervix shape among Neanderthal and *H. sapiens* M^1–M^3, indicate an M^1 (SOM Fig. S7). Additionally, the oblique ridge at the EDJ is type 1, running from the metacone dentine horn tip to the lingual marginal ridge distal to the protocone. Type 1 is typical of M^1, but not of M^2 and M^3 (Martin et al., 2017). The crown is complete, but the roots are missing above the trunk. Part of the distal margin of the crown broke off antemortem, as indicated by the presence of regular minor chipping along the occlusal edge of the fracture.

The occlusal shape is a rounded and slightly skewed rhomboid, with a metacone that is mesiolingually placed, resulting in distobuccal truncation, and a buccally protruding paracone (Fig. 8a). Taking into account corrections for the missing fractured areas, the metacone and hypocone are of similar size. Although worn, there appears to be a grade 2 metaconule (Fig. 8a; mesial and distal enamel protrusions from the uninterrupted oblique ridge: Reid and Van Reenen, 1995). Examination of the EDJ (Fig. 8g) indicates no cusp 5 (hypoconule), two small accessory dentine horns on the mesial marginal ridge, and a grade 3 post-paracone tubercle (Ortiz et al., 2017) that cannot be detected at the enamel surface due to wear. The root is hypertaurodont. The lingual aspect of the root trunk is flared lingually, and there is a vertical groove reaching the cervix. At the broken root surface there is no evidence of separated roots

buccally or mesially, but the base of the trunk is visible distally. Due to taphonomic alteration of the dentine it is difficult to determine the original shape of the pulp chamber.

Upper left permanent second molar (SJMJ2458) See Figure 9. The distal reduction in the crown and presence of a distal interproximal facet indicate an M^2. This tooth occludes with the left M_2 (SJMJ2455; Keith and Knowles, 1912). The tooth is complete apart from the root apices.

The occlusal outline is near triangular, convex mesially and distally, and flattened buccally. The tooth has a deep central fossa and no oblique ridge (Fig. 9a). No hypocone is visible on the worn OES. There is a hypocone dentine horn at the EDJ (Fig. 9g), which is likely to have been below grade 3 (reduced) on the original enamel surface due to its small size. The presence of a cusp 5 is indicated by dentine exposure on the distal margin of the OES (Fig. 9a). A grade 2 post-paracone tubercle (Ortiz et al., 2017) and a mesial marginal ridge accessory tubercle are visible at the EDJ (Fig. 9g). The root is hypertaurodont. The individual roots are furcated mesially at the level at which they are preserved, but with both buccal and distal radicular plates (cross-section in Fig. 9i). Three individual root canals are evident. The roots curve inwards in the apical half viewed distally (Fig. 9b), and both root trunk and individual roots have a pronounced distal inclination. Though taphonomically altered buccally, the pulp chamber appears to have been hour glass shaped in distal view (Fig. 9h).

Upper right third molar (SJMJ2459) See Figure 10. The diminutive distal portion of the crown, and the lack of a distal interproximal facet despite the presence of substantial occlusal wear, indicate an M^3. The crown is complete, but the lingual root has been broken off at the trunk, and the buccal roots are missing above the trunk.

Viewed occlusally, the mesial aspect of the tooth, including the root trunk, is markedly concave, and the remainder of the tooth is near circular (Fig. 10a). Most surface morphology

has been obliterated due to wear. It is unclear which cusps were present in the large distal area of dentine exposure, even at the EDJ (Fig. 10g). There are two dentine horns evident at the EDJ between this area and the protocone (Fig 10g). If one of these is the hypocone, it is most likely to be the more distally placed of the two, both from its position and its larger size. If this is the case, it implies the presence of multiple lingual cusps along the distal rim of the unworn tooth in addition to metacone, hypocone and cusp 5. No oblique ridge is evident at the EDJ. There is a faint horizontal ridge on the buccal OES of the paracone (Fig. 10a), not seen at the EDJ. The root is mesotaurodont. The lingual root is separated from the buccal root mesially and distally just below the fragmented root surface. The buccal root is not bifurcated at this level, though separate root canals are apparent.

Upper left third molar (SJMJ2467, cast) See Figure 11. The description is based on the 1911 Natural History Museum cast, and published details (Keith and Knowles, 1912; see SOM Fig. S8B). The crown appears to have been complete. Only part of the root trunk is present in the cast, but the root appears to have been complete in the original tooth according to the photograph in Keith and Knowles (1912; Fig. 11e).

Viewed occlusally, the crown is strongly tapered distally, and flattened mesially. Details of morphology are not clear due to the poor quality of the cast. There is a deep central fossa and no oblique ridge (Fig. 11a). Keith and Knowles (1912) described the tooth as three-cusped, lacking the hypocone. There is no evidence of a cusp 5 (Fig. 11e). The roots were described as more compressed together than in the left M^2, but otherwise similar in form to those of the molars found previously (Keith and Knowles, 1911, 1912). The roots appear to have been hypertaurodont, with a greater degree of taurodontism than the other La Cotte molars (Fig. 11e).

Lower right permanent second molar (SJMJ2461) See Figure 12. This tooth is identified as an antimere of SJMJ2455 (left M_2). It has a distal interproximal facet, which is located

lingually, implying lingual displacement of the adjacent tooth. Displacement of this nature is more likely to occur in an M_3 than in an M_2. The tooth is complete apart from the root apices.

The occlusal shape is rectangular, wider distally than mesially. It has rounded buccal and distal aspects (mesial worn), and partial flattening lingually. There is a 'Y' groove pattern, and a large (grade 5) distally oriented hypoconulid (cusp 5) visible at the OES (Fig. 12a). A small dentine horn at the EDJ indicates that a cusp 6 (entoconulid) was present (Fig. 12g). The sagittal sulcus is uninterrupted at the OES and no mid-trigonid crest is evident. It is absent also at the EDJ, with only a weak crest on the protoconid (grade 0: Bailey et al., 2011). Traces of a wide mesial fovea (trait referred to as an anterior fovea in the ASUDAS: Turner et al., 1991; Scott and Turner, 1997; Scott and Irish, 2017; Scott et al., 2018) can be identified at the OES and it is present as a linear depression at the EDJ. The entoconid dentine horn tip is positioned on the margin of the tooth (Martin et al., 2017; Fig. 12g). There is a pit (grade 1) protostylid at the OES (Fig. 12a), with a corresponding horizontal cingular crest at the EDJ (Fig. 12g).

The mesial root is rectangular in shape and bifurcated at the apex, but fused to the distal root buccally. The lingual furcation of the mesial root is convex mesially. The buccal sides of both roots curve lingually. Marginal ridges are present mesially and distally on the mesial root, and mesially on the distal root. The root is classed as hypertaurodont using Shifman and Chananel's (1978) method but, with an estimated root length of 14.9 mm, Keene's (1966) method gives a figure of 37%, which is classed as hypotaurodont (25−49.9%). The pulp chamber is barrel shaped, viewed lingually, and widening of the mesial root canals is evident in the mesiodistal CT slices (Fig. 12h; SOM Fig. S9).

<u>Lower left permanent second molar (SJMJ2455)</u> See Figure 13. This tooth occludes with the left M^2 (SJMJ2458; Fig. 13i). It has mesial and distal interproximal wear facets, and, as with SJMJ2461 (right M_2), the distal interproximal facet is located lingually. Based on a similar

degree of wear, similar dimensions and crown morphology, and the description of the original root morphology (Keith and Knowles, 1912), this is likely to be the antimere to SJMJ2461 (right M_2). The crown is complete, but Keith and Knowles (1912) sectioned the root just below, and parallel to, the cervix (line visible in Fig. 13b). Part of the root has been restored with filler. Only 9 mm of the trunk remains and the apical part of the root has been lost. The tooth was described by Keith and Knowles (1912) as having roots of the same form as the right M_2, fused buccally but not lingually, inclined distally and lingually, and having a trunk length of 7 mm.

The occlusal shape is rectangular, with rounded margins (mesial worn), and partially flattened lingually. As with the right M_2, there is a 'Y' groove pattern, and a large (grade 5) distally placed hypoconulid is present (Fig. 13a, d). Unlike the right M_2 there is no cusp 6 dentine horn and no protostylid crest at the EDJ, though a trace protostylid is present on the hypoconid (Fig. 13g). However, as with the right M_2, there is no mid-trigonid crest at the EDJ (site worn at the OES; grade 0: Bailey et al., 2011) and only a weak crest evident on the protoconid. The entoconid dentine horn tip is positioned on the margin of the tooth (Martin et al., 2017).

<u>Lower right third molar (SJMJ2460)</u> See Figure 14. This tooth lacks a distal interproximal facet despite the presence of dentine exposure. This, together with its shape and the presence of a large number of accessory crests, indicates an M_3. The interproximal wear facet matches with that of the right M_2 (SJMJ2461) (Fig. 14i) and it is likely the teeth are metameres. Only the crown and less than one-quarter of the root are present. A portion of the mesial margin of the crown has broken off postmortem. A lingual crack can be seen in the CT slice (Fig. 14h).

The overall occlusal shape of the crown is near circular. The unworn lingual half of the tooth is very wrinkled, with multiple cusps present at the OES (Fig. 14a, d). There is an 'X' groove pattern (Fig. 14a). There are three crests running from the mesial margin into, and

filling, the mesial (anterior) fovea at the OES, but the presence of any associated mesial marginal ridge tubercles cannot be assessed because the mesial face of the tooth is missing (Fig. 14a). There is no mid-trigonid crest (grade 0 at the EDJ: Bailey et al., 2011). There is a single mesiodistal groove at the OES on the buccal slope of the hypoconid, and lingual to the dentine exposure, that delineates the large protostylid cingular crest seen at the EDJ (Fig. 14d, g). Examination of the EDJ (Fig. 14g) reveals the presence of numerous primary and accessory dentine horns. Some of these can be reasonably identified as cusps, while others reflect repeated enamel knot initiation (Martin et al., 2017). Moving distally from the metaconid dentine horn, there is a small (grade 3) cusp 7, the entoconid, an undulating ridge that potentially exhibits incipient dentine horns, a cusp 6, and then one additional dentine horn lingual to the grade 4 hypoconulid. Additionally, there is a small dentine horn on the protostylid ridge on the buccal aspect of the hypoconulid. The degree of internal placement of the hypoconid relative to the protostylid cingulum is uncommon (not seen in any of the CT-scan comparative samples), and may further reflect a general perturbation of the development of this tooth. The metaconid and entoconid dentine horn tips are positioned on the margin of the tooth (Martin et al., 2017).

<u>Occipital fragment (SJMJ2452)</u> See Figure 15. The occipital fragment comprises a small part of a left squamous, measuring 53 mm between the broken anterior and posterior edges, and 37 mm from the asterion to the broken medial edge. The endocranial and exocranial surfaces are weathered and marked by superficial cracks and abraded areas. One edge of the piece is defined by the lambdoid suture, which extends 45 mm from the asterion. All the other edges are defined by natural breaks. The thickness of the bone, and weak markings on the external surface, are consistent with an immature age at death. The lambdoid suture has several abraded patches but appears to be mostly open. An area of interdigitated bone, visible on the external surface located 35 mm from the asterion, may represent an early stage of fusion at

the lambdoid suture. A finger of bone projecting inwards from the lambdoid suture, situated 6 mm from the asterion, and measuring 6.2 by 2.6 mm, appears to be a small wormian bone. The endocranial surface has a well demarcated transverse sulcus that extends 35 mm from just below the asterion to the broken medial edge along the lower border, and 32 mm from the lambdoid suture to the broken medial edge along the upper border. The transverse sulcus passes directly across the asterion and would have crossed the posteroinferior (mastoid) corner of the parietal bone before reaching the temporal bone, instead of crossing directly onto the temporal bone (Fig. 15B, indicated by dotted lines). Taken together, the size and morphology of the occipital fragment are consistent with an immature individual who died in late childhood or adolescence.

3.2. Qualitative morphological comparisons

Trait frequencies for the tooth types found in the La Cotte material, and in comparative samples of Late Pleistocene hominins, are reported in Tables 3–7. Traits that show a significant difference between Neanderthal and fossil *H. sapiens* are identified: (1) where the 95% confidence interval for the difference between the proportions for the two samples is entirely above or below zero, i.e., does not include 0% difference; (2) where the 95% confidence intervals for the two sample proportions do not overlap (SOM S3). These are the traits principally discussed.

<u>Lower canine (SJMJ2463)</u> The characteristics of this tooth support a Neanderthal affinity. Shoveling is present in the entire Neanderthal comparative sample and most (88%) of the fossil *H. sapiens* sample (Table 3). The distal accessory ridge is more common in Neanderthals (78%) than fossil *H. sapiens* (42%; Table 3). It tends to be more strongly expressed in Neanderthals, as it is at La Cotte, than in fossil *H. sapiens* (50% compared to 8% at their grade 2 in Martinón-Torres et al.'s [2012: Table 17] samples). The mild expressions

of the tuberculum dentale and lingual medial ridge in SJMJ2463 (C_1) are the forms frequently found in both comparative samples (Martinón-Torres et al., 2012).

The buccal curvature of the root is typical of Neanderthals, but not of *H. sapiens* (Bilsborough and Thompson, 2005; Le Cabec et al., 2013), as is the convex buccal contour of crown and root together, known as 'cyrtodonty' (Patte, 1962; Brabant and Sahly, 1964). The wide root canal, as viewed distally, is unlike the narrow straight sided canals found in recent human teeth (van Beek, 1983).

Upper fourth premolar (SJMJ2457) The morphological traits of this tooth support a Neanderthal affinity. The swollen buccal surface, viewed mesially, and sharp lingual inclination from the point of maximum curvature, is typical of Neanderthals, and more pronounced than is generally found in *H. sapiens* (TC, personal observation). The absence of a buccal mesial accessory ridge is also typical of Neanderthals (83%) and less common in fossil *H. sapiens* (40%; Table 4).

The roots are robust compared to *H. sapiens*. The two-rooted form present is the most common type in Neanderthals (Maureille et al., 2008). The taurodontism, and a relatively longer root trunk before furcation of the roots than in recent humans, are also seen in some Neanderthal P^4 (Kallay, 1963).

Lower third (SJMJ2464) and fourth (SJMJ2465) premolars The characteristics of both premolars give an ambiguous picture. For the P_3 (SJMJ2464) the Neanderthal features are the large lingually placed buccal cusp (Gómez-Robles et al., 2008), and the presence of a buccal cingulum at the EDJ, which occurs frequently in the Neanderthal sample but is not seen in the recent human sample. For the P_4 (SJMJ2465) the Neanderthal features are the presence of multiple lingual cusps (94%), a mesially placed metaconid (97%), and a buccal distal accessory ridge (88%; Table 4). The corresponding figures for fossil *H. sapiens* are significantly lower (Table 4). The cusp on the mesial margin, represented by a dentine horn at

the EDJ, found on SJMJ2465 (left P_4), also occurs on three Krapina P_4 (Compton and Stringer, 2012). Three or more lingual cusps on P_4 (three at La Cotte) are present in 89% of Neanderthals but only 20% of fossil *H. sapiens* (Martinón-Torres et al 2012: Table 19).

In contrast, the absence of a transverse crest, and a symmetrical shape, found on both premolars, are rare in Neanderthal P_3 (3% and 6% respectively) and P_4 (both at 6%; Table 4). Additionally, Davies et al. (2019) recorded the presence of a transverse crest in their entire Neanderthal P_3 sample. Martinón-Torres et al. (2012: Tables 18 and 19), however, reported absence of a transverse crest in 15% of P_3 and 19% of P_4 in their Neanderthal sample. The absence of a transverse crest, and a symmetrical shape, are more frequently observed for P_3 and P_4 in fossil *H. sapiens* (Table 4). Bailey (2002) looked at the combination of three characteristics (well-developed metaconid, transverse crest and asymmetry) in P_4 and found that 98% of modern humans had only one of these traits, as at La Cotte, compared to only 6% of Neanderthals.

The robust roots of SJMJ2464 (left P_3) are more typical of Neanderthals than of *H. sapiens*. Interestingly, grade 4–5 Tomes' root, present on the P_3, occurs less frequently in the P_3 (12%) than in the P_4 (25%) in Neanderthals, the reverse of that found in fossil *H. sapiens* (38% and 23% respectively; Table 4) and recent humans. Tomes' root occurs less frequently in recent humans than in fossil *H. sapiens* (12.5% and 2.5% respectively for P_3 and P_4 in a large mixed sample; Shields, 2005). The wide root canal observed in SJMJ2465 (left P_4) is typical of Neanderthal P_4 but uncommon in recent humans (Prado-Simón et al., 2012). The extended taurodont pulp chambers in SJMJ2464 (left P_3) and SJMJ2465 (left P_4) are apparent as widening in both buccolingual and mesiodistal directions (SOM Fig. S6). In some teeth, in both comparative samples (Table 4), extension of the pulp chamber into the root is only apparent as widening in a buccolingual direction. Considering the small samples involved (Table 4), the frequency of taurodontism is similar between P_3 and P_4 and between

Neanderthals and fossil *H. sapiens*. Taken overall, widening in a buccolingual direction, with or without mesiodistal widening, occurs at approximately twice the frequency as widening in both directions together (51% against 23%; Table 4).

Molars The upper molar cusps are internally placed, as is often observed in Neanderthals. Carabelli's trait is absent in the upper molars. This was previously thought to be unusual in Neanderthals (McCown and Keith, 1939; Smith, 1989). More recently Martinón-Torres et al. (2012) reported 20% absence for M^1, 42% for M^2 and 80% for M^3, in their Neanderthal sample. The post-paracone dentine horn, which is present at the EDJ in SJMJ2456 (right M^1) and SJMJ2458 (left M^2) and could not be scored in SJMJ2459 (right M^3), was ubiquitous in a sample of Neanderthal maxillary molars and present in 86% of a recent human sample (Martin et al., 2017: Table 10). In contrast, Ortiz at al. (2017: Table 4) reported the presence of post-paracone dentine horns in 98% of a Neanderthal sample but only 25% of a recent human sample. Taurodontism is particularly associated with Neanderthals, but it is also found in fossil *H. sapiens* from Skhūl and Qafzeh (McCown and Keith, 1939; Vandermeersch, 1981) and in Aterians (Kupczik and Hublin, 2010). Kupczik et al. (2019: Table S1) found taurodontism (grades III and IV of their bifurcation index) in 88% (14 of 16) of their sample of Neanderthal M_2. Studies of recent Europeans have shown taurodontism is present in less than 10% of molars (Jafarzadeh et al., 2008: Table 3). The absence of enamel extensions above trace level on any of the molars is also typical of Neanderthals, and most *H. sapiens* outside Asia (Bailey, 2006b).

Upper first molar (SJMJ2456) The Neanderthal M^1 crown has a distinct shape (Bailey, 2004; Gómez-Robles et al., 2007; Martinón-Torres et al., 2013): The main cusp tips are more internally placed, leading to a relatively smaller occlusal polygon (formed by linking the tips of the four principal cusps) compared to the total occlusal area (Table 5). There is a statistically significant difference at $p \leq 0.01$ between Neanderthal and *H. sapiens* for this

percentage figure (Martinón-Torres et al., 2013). The occlusal shape is skewed and there is a large distally projected and swollen hypocone, leading to a narrow hypocone angle (Table 5; Fig. 16). The metacone is relatively smaller than the hypocone and mesiolingually oriented, leading to distobuccal truncation of the occlusal outline and a wide metacone angle (Table 5; Fig. 16). The hypocone is larger than the metacone in 14/16 molars in Bailey's (2004) Neanderthal sample. The occlusal polygon is narrower distally than mesially (Fig. 16).

The M^1 (SJMJ2456) shows clear Neanderthal affinities (see Table 5; Fig. 16). It has a relatively small occlusal polygon (24%), a mesiolingually placed metacone, along with a large metacone angle (116°), and an occlusal polygon that is narrower distally than mesially.

However, in contrast, the crown has only a mildly skewed appearance, with a small protocone angle (100°) compared to the means of both the comparative samples (106°). The relative size of the hypocone compared to total occlusal area (19%) is small in comparison to the Neanderthal sample mean (23.7%) and smaller than the metacone (21%), and the hypocone angle (76°) is large. While being within the Neanderthal range of variation, both of these features are more similar to the fossil *H. sapiens* sample. Additionally, the protocone is relatively large (33%) compared to Neanderthal (29.9%).

<u>Upper second molar (SJMJ2458)</u> The presence of a cusp 5 is common in Neanderthals (68%), and the presence of a mesial accessory cusp is ubiquitous. Both are less frequent in fossil *H. sapiens* (39% and 13% respectively; Table 6). The reduced hypocone is unusual, though, in both Neanderthals and fossil *H. sapiens*, occurring at frequencies of only 6% and 15% respectively (Table 6). It is, however, common in the pre-Neanderthal Atapuerca-SH sample (Martinón-Torres et al., 2012).

<u>Upper third molars (SJMJ2459 and SJMJ2467)</u> The concave mesial aspect, viewed occlusally, of SJMJ2459 (right M^3) is distinctly unusual. The presence of multiple cusps along the distal rim (i.e., in excess of metacone, hypocone and a single cusp 5), as inferred for

SJMJ2459 (right M^3), has been reported in Krapina M^3 (Compton and Stringer, 2012); and Martin et al. (2017) found considerable variation in distal cusp pattern in Neanderthal M^3. Multiple distal cusps and split hypocones occur in Aterian teeth (Bailey et al., 2017), and split hypocones have been reported in recent humans (Greene et al., 1967; Bermúdez de Castro and Martínez, 1986), but mention of multiple distal cusps in recent humans is rare in the literature. Ortiz et al. (2017: Table S3) found multiple cusp 5 at the EDJ in ~20% of Neanderthals but only in ~1% of recent humans.

<u>Lower molars (SJMJ2455 and SJMJ2461 M_2; SJMJ2460 M_3)</u> We did not observe the protostylid forms seen at the EDJ on SJMJ2461 (right M_2) and SJMJ2460 (right M_3) in our comparative samples. The hypoconulid expression in the M_2 (SJMJ2455 and SJMJ2461) is particularly large. Martinón-Torres et al. (2012: Table 21) found only 16.6% of Neanderthal and 4% of fossil *H. sapiens* M_2 with grade 5 hypoconulids. The characteristics of the La Cotte lower molars give an ambiguous picture. Neanderthal characteristics include the presence of a hypoconulid (found in the entire Neanderthal sample), a wide mesial (anterior) fovea (89% of M_2 and 93% of M_3), and a 'Y' groove pattern in M_2 (75%; Table 7). The corresponding figures for fossil *H. sapiens* are significantly lower (Table 7). Additionally, the multiple cusps and accessory crests found on SJMJ2460 (right M_3) have been observed in Neanderthals (McCown and Keith, 1939; Radovčić et al., 1988; Bailey and Hublin, 2006), as has the repeated enamel knot initiation seen at the EDJ (Martin et al., 2017).

In contrast, the absence of a mid-trigonid crest at the OES, observed in SJMJ2461 (right M_2) and SJMJ2460 (right M_3), is rare in Neanderthal M_2 and M_3 (4% and 7% respectively), but almost ubiquitous in the fossil *H. sapiens* sample, at 96% and 100% respectively (Table 7). At the EDJ, Bailey et al. (2011: Table 3) recorded the presence of a continuous mid-trigonid crest in their entire Neanderthal M_2 and M_3 sample (absent at La Cotte), but only 35.5% and 14.3% respectively of a recent European sample. Furthermore, the position of the

metaconid dentine horn tip on the occlusal margin of SJMJ2460 (right M_3) is rare in Neanderthals. The metaconid dentine horn was centrally placed in 95% of a late Neanderthal sample but only 36% of a recent human sample (Martin et al., 2017: Table 9).

The non-tapering shape and bifurcation of the mesial root, and the presence of longitudinal marginal ridges on mesial and distal roots, observed in SJMJ2461 (right M_2), are typical of Neanderthal M_2 (Compton and Stringer, 2015).

Occipital fragment (SJMJ2452) The occipital lacks any diagnostic Neanderthal anatomical features. The transverse sulcus pathway is typical of recent humans, and differs from the pathway observed in some Neanderthals, in which the transverse sulcus passes directly from the occipital to the temporal without crossing the parietal bone (Arsuaga et al., 2002).

3.3. Geometric morphometric analysis of cervix shape

Figures 17–23 illustrate PCAs of cervix morphology in shape and form (form including the log of centroid size as a variable) space for upper and lower molars and premolars.

The P^4 (SJMJ2457) falls closer to the *H. sapiens* samples (fossil and recent humans) in shape space but with the Neanderthals in form space, reflecting its large size (Fig. 17a, b). It differs from the mean Neanderthal cervix shape in being somewhat compressed mesiolingually and distobuccally (Fig. 17c, d). Using 11 shape PCs, attribution accuracy of the comparative P^4 sample is ~65% (i.e., the proportion of specimens of known taxonomic affiliation that are attributed correctly using cross-validated canonical variate analysis) and posterior probabilities of discriminant analysis consistently assign SJMJ2457 (P^4) to *H. sapiens* rather than Neanderthal.

The identification of SJMJ2464 as a P_3 and SJMJ2465 as a P_4 is supported by their cervix shape that groups them with the *H. sapiens* (fossil and recent humans) P_3 and P_4 samples (SOM Fig. S5). The P_3 falls with the *H. sapiens* samples in shape space but closer to the

Neanderthal sample in form space due to its large size (Fig 18a, b). Wireframe models indicate Neanderthals have a distally expanded cervix compared to the *H. sapiens* samples and SJMJ2464 (P_3; Fig. 18c, d). Using 11 shape PCs, attribution accuracy of the comparative P_3 sample is ~70% (with cross-validation), and posterior probabilities consistently assign SJMJ2464 (P_3) to *H. sapiens*. The P_4 falls with the *H. sapiens* samples in both shape and form space (Fig. 19a, b), sharing a buccolingually expanded cervix with both *H. sapiens* samples (Fig. 19c, d) but being more similar in size to the earlier sample. Using 9 shape PCs, attribution accuracy of the P_4 sample is ~90% (with cross-validation) and posterior probabilities consistently assign SJMJ2465 (P_4) to *H. sapiens*.

The SJMJ2456 M^1 plots with Neanderthals in both shape space and form space (Fig. 20a, b). It shares a distolingual expansion of the cervix with Neanderthals although it is not as marked as the average Neanderthal M^1 wireframe (Fig. 20c, d). Using 11 shape PCs, attribution accuracy of the comparative M^1 sample is ~90% (with cross-validation) and posterior probabilities consistently assign SJMJ2456 (M^1) to Neanderthals.

The SJMJ2458 M^2 falls on the margin of the overlapping distributions of the *H. sapiens* and Neanderthal samples in shape space, and the form analysis demonstrates it is larger than most of the *H. sapiens* comparative sample and of average size for a Neanderthal (Fig. 21a, b). The wireframe model highlights the unusually small hypocone of SJMJ2458 (M^2) compared to the mean *H. sapiens* and Neanderthal cervix shapes (Fig. 21c, d). Using 13 shape PCs, attribution accuracy of the comparative M^2 sample is ~70% (with cross-validation) and SJMJ2458 (M^2) assigns with near equal frequency as either a Neanderthal or *H. sapiens* (i.e., its taxonomic attribution cannot be determined based on cervix shape).

The SJMJ2459 M^3 falls well outside of both Neanderthal and *H. sapiens* ranges and it is considerably larger than the largest Neanderthals in this analysis (Fig 22a, b). As with the SJMJ2458 M^2, the wireframe comparisons of mean shape illustrate the particularly strange

contour of the SJMJ2459 M^3 (Fig. 22c, d). Using 9 shape PCs, attribution accuracy of the comparative M^3 sample is ~70% (with cross-validation) and SJMJ2459 (M^3) is consistently assigned to Neanderthals.

The two M_2 (SJMJ2455 and SJMJ2461) fall in an intermediate position between the Neanderthals and *H. sapiens* in shape space but fall closer to the fossil *H. sapiens* and Neanderthal samples when size is included (Fig. 23a, b). The M_2s are similar to the Neanderthal sample in having a buccally expanded cervix without the buccal pinching distal to the protoconid present in the *H. sapiens* samples (Fig. 23c, d). Using 14 shape PCs, attribution accuracy of the comparative sample is ~85% (with cross-validation) and posterior probabilities consistently assign both SJMJ2455 and SJMJ2461 (M_2) to Neanderthals.

Cervix shape alone tends to perform less well at taxonomic discrimination than analyzes that also incorporate the EDJ marginal ridge (Martin et al., 2017) and, at a number of tooth positions, attribution accuracy of the comparative sample (in which taxonomic affiliation is known) ranges between 60–90%. In summary, the P_3, P_4 and P^4 are consistently assigned as *H. sapiens*, while the two M_2, the M^1 and the M^3 are consistently assigned as Neanderthals. Attribution of the M^2 is less consistent and cervix shape cannot contribute strongly to its taxonomic assessment.

3.4. Metrical comparisons

Comparative data for crown dimensions are presented in SOM Tables S7 and S8, and adjusted Z scores for crown dimensions are illustrated in Figures 24 and 25.

<u>Crown area</u> See Figure 24. The crown areas of the La Cotte teeth are all close to or above the late Neanderthal comparative sample means, with associated adjusted Z scores under ±0.5, except for SJMJ2463 (left C_1) and SJMJ2464 (left P_3), which are particularly large. The C_1 crown area is above the range of the late Neanderthal comparative sample, and its

buccolingual dimension is only exceeded by Kebara 2 (10.2 mm). The buccolingual dimension of the P_3 is only exceeded by La Quina 9 (11.0 mm), and this is the only tooth in the late Neanderthal comparative sample with a larger crown area (99 sq mm). With the exception of these two teeth, the crown areas of the La Cotte teeth are all within the ranges of the other comparative samples, with associated adjusted Z scores up to ±0.7 (-0.8 for the Krapina P_4). In contrast, the adjusted Z scores for SJMJ2463 (left C_1) and SJMJ2464 (left P_3) are 0.8 and 0.7 respectively in relation to late Neanderthals, and 1.0 and 1.4 in relation to fossil *H. sapiens*.

Crown index See Figure 25. The crown indices of the La Cotte teeth all have adjusted Z scores under ±0.5 in relation to the late Neanderthal comparative sample except for the left M^3 SJMJ2467 (-0.7). The La Cotte M^1, M^2 and M^3 have crown indices below the means of all the comparative samples (SOM Table S7; with the lone exception of the right M^3 SJMJ2459 in relation to Krapina), indicating that they are squarer; and C_1, P_3 and P_4 have crown indices above the means of the comparative samples (SOM Table S8), indicating that they are relatively buccolingually expanded. Two large differences in the comparative samples stand out. The fossil *H. sapiens* M^1 has an adjusted Z score of -1.3, reflecting the more rectangular shape of these teeth compared to Neanderthals. The Krapina P_3 has an adjusted Z score of 2.2 due to the lower crown indices of these teeth and this is also apparent in the Krapina lower molars.

Cervical dimensions See Table 8. In all but one case (SJMJ2461, right M_2) the La Cotte dimensions are above the Neanderthal comparative sample means. The mesiodistal dimensions of SJMJ2463 (left C_1) and SJMJ2464 (left P_3), and the buccolingual dimension of SJMJ2457 (left P^4), at the cervix are either above or at the upper end of the Neanderthal ranges. SJMJ2464 (left P_3) has adjusted Z scores for Neanderthal of 1.5 for the mesiodistal dimension and 1.0 for the buccolingual dimension. Keith and Knowles (1912) noted the large

cervical dimensions; and the particularly high cervical dimensions of the La Cotte canine and premolars, other than SJMJ2465 (left P_4), is very distinctive. Fossil *H. sapiens* have smaller cervical dimensions than Neanderthals, and this difference is most pronounced in the P_4, M^2 and M_2. The fossil *H. sapiens* adjusted Z scores for SJMJ2463 (left C_1) and SJMJ2464 (left P_3) in both mesiodistal and buccolingual dimensions, and for SJMJ2458 (left M^2) in the mesiodistal dimension, are all at 1.0 or above.

<u>Root length</u> The only La Cotte tooth with a complete root is SJMJ2467 (LM^3), for which only a cast is now available (Keith and Knowles, 1912: preface). It has a length of 16.0 mm, which is within the Neanderthal range (13.5–16.7 mm, mean 15.2 mm; Bailey, 2005), and above the ranges for Předmostí (11.0–14.0 mm; Matiegka, 1934) and contemporary humans (8.0–15.0 mm; Black, 1902).

3.5. Number of individuals

Since all the teeth from La Cotte were found in one place, and are broadly similar in their degree of development and wear, the 'null hypothesis' would be that they all come from the same individual (Keith and Knowles, 1912). Our observations demonstrate that the eleven teeth from La Cotte represent a maximum of six individuals, made up of three groups of teeth that can be confidently associated with one another and three isolated teeth:

i) The largest group of unambiguously associated teeth comprises four molars, SJMJ 2455, 2458, 2460 and 2461 (referred to hereafter as individual A-1). SJMJ2455 (left M_2) and SJMJ2458 (left M^2) occlude (Fig. 13i). SJMJ2455 (left M_2) and SJMJ2461 (right M_2) are likely to be antimeres, due to the similarities of morphology and size, and the shared presence of lingually placed distal interproximal facets, a highly unusual pattern of distal wear (Fig. 12a, marked 'a') and unusually lingually inclined roots. SJMJ2461 (right M_2) and SJMJ2460 (right M_3) are likely metameres. The

lingual placement of the interproximal facet on SJMJ2461 suggests lingual displacement of the adjacent M_3, and the form of wear on SJMJ2460 is consistent with this (Fig. 14i). SJMJ2460 (right M_3) also has a prominent form of the protostylid, similar to, although larger than, that seen on SJMJ2461.

ii) The matching interproximal wear between SJMJ2463 (left C_1) and SJMJ2464 (left P_3), and their unusually large size, demonstrates that they are metameres (A-2)

iii) SJMJ2456, right M^1 (A-3)

iv) SJMJ2467, left M^3 (A-4)

v) SJMJ2457 (left P^4) and SJMJ2465 (left P_4) occlude (B-1)

vi) SJMJ2459, right M^3 (B-2).

The minimum number of individuals (MNI) represented by these eleven teeth is two, referred to as Individuals A and B. This can be confidently inferred from the fact that some of the groupings identified above cannot belong to the same dentition. Firstly, SJMJ2459 (right M^3; B-2) does not occlude with either the right M_2 or the right M_3 from A-1. Secondly, premolars SJMJ2464 (left P_3; A-2) and SJMJ2465 (left P_4; B-1) are not metameres, since the interproximal facets do not match, and their large difference in size is inconsistent with a single dentition.

Teeth from individual B (SJMJ2457 [left P^4; B-1] and SJMJ2465 [left P_4; B-1] and SJMJ2459 [right M^3; B-2]) exhibit a similar degree of wear that is proportionally greater than that of the other teeth and consistent with a single individual. The remaining four teeth, SJMJ 2456, 2467, 2463 and 2464, cannot with complete confidence be associated with either Individual A or B, but are tentatively included with Individual A on the basis of dental metrics. SJMJ2456 (right M^1; A-3), SJMJ2467 (left M^3; A-4) and SJMJ2458 (left M^2; A-1) have similar crown area and crown index values in relation to the Neanderthal means.

Likewise, the relationship of crown area to the Neanderthal mean in SJMJ2463 (left C_1) and SJMJ2464 (left P_3; A-2) is similar to that in M_2 SJMJ2461 and SJMJ2455 (A-1).

In summary, Individual A is represented by four teeth that are unambiguously associated and another four teeth that could belong to this individual, and Individual B is represented by three teeth. Based on the level of wear and the fact that there is dentine exposure on third molars in both individuals, it is likely that Individuals A and B were (young) adults. Trinkaus (1995) found a uniform pattern of wear in a sample of Neanderthals and noted that there was slight dentine exposure on first molars, as at La Cotte, in the third decade of life. However, the accumulation of cementum on the apical two thirds of the roots and the amount of secondary dentine in the pulp chambers of the molars, from both individuals, could indicate a greater age at death, as these are age related processes (Hillson, 1996; Guatelli-Steinberg and Huffman, 2012). The teeth found in the first season (1910) clearly did not all come from a right mandible as stated by Nicolle and Sinel (1910), but the fact that the teeth were in a row suggests that those from Individual A, at least, might have been originally deposited in anatomical association.

The occipital fragment came from an individual who died in late childhood or adolescence. It can therefore be concluded, from the degree of root development and wear on the teeth, that this fragment is not associated with the dental remains and therefore comes from a third individual.

4. Discussion

Individually, all of the La Cotte teeth have diagnostically Neanderthal characteristics and seven teeth also have *H. sapiens* characteristics. The teeth that lack *H. sapiens* characteristics are SJMJ2463 (left C_1), SJMJ2458 (left M^2), and the upper third molars, SJMJ2459 (right M^3) and SJMJ2467 (left M^3). Table 9 summarizes the mix of Neanderthal and *H. sapiens*

characteristics within the individual teeth, grouped according to the maximum number of six individuals (A-1, A-2, A-3, A-4, B-1 and B-2) and minimum number of two individuals (A and B).

Within A-1 (SJMJ2458, left M^2; SJMJ2461, right M_2; SJMJ2455, left M_2; SJMJ2460, right M_3), the M^2 has no *H. sapiens* characteristics and the other three molars have a mixture of characteristics. Within A-2 (SJMJ2463, left C_1; SJMJ2464, left P_3), the canine has entirely Neanderthal diagnostic characteristics but those of the premolar are mixed. A-3 (SJMJ2456, right M^1) has mixed characteristics. A-4 (SJMJ2467, left M^3) only has Neanderthal characteristics. Within B1, both premolars (SJMJ2457, left P^4; SJMJ2465, left P_4) have a mixture of characteristics. B-2 (SJMJ2459, right M^3) only has Neanderthal characteristics.

Traits that are specific to one of these six groups include absence of mid-trigonid crest in lower molars (A-1), and particularly large teeth compared to Neanderthal and *H. sapiens* (A-2). Traits that occur in more than one group include absence of transverse crest and mesiolingual truncation in lower premolars, and cervix shape of *H. sapiens* form (A-2 and B-1). It is notable that for teeth with multiple crown traits that show a significant difference in prevalence between Neanderthals and fossil *H. sapiens* (P_4, M_2, M_3) there is an ambiguous picture.

Four of the maximum of six individuals have a mixture of diagnostic Neanderthal, and *H. sapiens*, characteristics. Three of these sets of teeth could belong to the same dentition (Individual A) but the fourth belongs to a second dentition (Individual B). This suggests that the occurrence of mixed characteristics relates to a group of individuals, rather than being specific to one individual. The *H. sapiens* characteristics occur principally in the lower premolars, are less common in the P^4, M^1 and lower molars, and are reflected in cervix shape and crown morphological traits. The analysis of cervix shape gives a varied picture. The molars (other than M^2) are assigned to Neanderthals, while the premolars are assigned to *H.*

sapiens. The root forms and the tooth dimensions are entirely compatible with Neanderthals. Several traits that are considered to be particularly typical of Neanderthals (Bailey, 2002, 2004, 2006a; Martin et al., 2017) are absent in the La Cotte teeth. These are the presence of a transverse crest, and mesiolingual truncation in lower premolars; the presence of a mid-trigonid crest, and metaconid central dentine horn tip placement in lower molars; and peculiarities of the occlusal shape of M^1. The first four of these traits are not diagnostic of either Neanderthals or *H. sapiens*, but they are consistently present in Neanderthals and less common in *H. sapiens*. The small occlusal polygon of the M^1 from La Cotte is diagnostically Neanderthal, but other aspects of the M^1 morphology are more ambiguous.

Three aspects of the morphology of the La Cotte teeth are unusual in both Neanderthals and fossil *H. sapiens*. These are the reduced hypocone on SJMJ2458 (left M^2); the concave mesial surface and unusual cervical shape of SJMJ2459 (right M^3); and the protostylid form on SJMJ2461 (right M_2) and SJMJ2460 (right M_3). The protostylid form of SJMJ2461 (right M_2) is superficially similar to that observed in *Paranthropus robustus* (Skinner et al., 2009), although not identical. We consider the SJMJ2460 (right M_3) protostylid form to reflect abnormal development of the distal part of the crown and thus not useful for its taxonomic assessment.

With the exception of the possibly early form of the protostylid, there are no traits relating to earlier hominins in the La Cotte teeth. Traits that are only seen in *Homo heidelbergensis*, pre-Neanderthals or early Neanderthals (Compton and Stringer, 2015) are absent. These include a buccal cingulum at the enamel surface on P_3 (*H. heidelbergensis*); a distal occlusolingual cleft on P_3 (*H. heidelbergensis* and pre-Neanderthal); mesiobuccal swelling (viewed occlusally) of P_4 (*H. heidelbergensis*, pre-Neanderthal and early Neanderthal); and grade 2 buccal vertical grooves/cingula on lower molars (*H. heidelbergensis*, pre-Neanderthal and early Neanderthal). Multiple lingual cusps on the P_3 (present at La Cotte) are not found in

H. heidelbergensis (Compton and Stringer, 2015; M. Bermúdez de Castro, pers. comm. regarding Arago),

The dental morphology of at least two dental individuals from La Cotte therefore displays a mixture of Neanderthal and *H. sapiens* characteristics, with Neanderthal features more strongly represented, and is clearly distinct from earlier hominins. Since there is more than one individual involved, abnormality of development can be dismissed as a likely cause. This mix of features could suggest shared ancestry or, alternatively, a need to extend the phenotype of one or other species to accommodate this variation. If this combination of features is not the result of introgression, it could be due to genetic drift as a consequence of isolation, but this does not seem probable since, at the likely date of these fossils (<48 ka), sea levels were lower and Jersey was connected to mainland Europe. Another possibility is short term evolutionary pressures, although it is difficult to see what advantage would be conveyed by these minor morphological differences. The small sample of teeth from La Cotte does not enable us to determine which of these scenarios is more likely. Attempts to extract DNA and resolve the issue through genetic analysis have thus far proved unsuccessful.

The site of Palomas in southern Spain has hominin dental material from secure stratigraphic contexts dated to ~45–38 ka cal BP (Walker et al., 2017), which shows a comparable mix of dental features to those found at La Cotte. The traits of the Palomas teeth are primarily Neanderthal, but not all the P_4 exhibit asymmetry and a transverse crest (present in 50% and 75% respectively); only one of the eight lower molars has a mid-trigonid crest at the OES, and fewer than half (43%) have a mesial (anterior) fovea of grade >1 (Zapata et al., 2017). However, unlike La Cotte, the crown breadths of some of the anterior teeth, and crown areas of some of the lower molars, are more than two standard deviations below the Neanderthal mean (Pinilla and Trinkaus, 2017). Trinkaus (2017) concluded that the Palomas remains were Neanderthals, but acknowledged that the Neanderthal range of variation would

need to be extended to accommodate this group within Neanderthals because of differences in dental traits, their small size, and other aspects of their skeletal morphology. DNA analysis might help resolve the taxonomic ambiguity, but to date none has been reported.

Trinkaus (2007) identified distinct Neanderthal dental characteristics that appear in European Late Pleistocene *H. sapiens* dated earlier than 33 ka, and considered these to be due to the assimilation of Neanderthals into these populations. The characteristics listed involve: (1) morphological traits in I^1, C^1 and P_4 (multiple lingual cusps, mesially placed metaconid, and asymmetry for P_4) that are present in the earlier material and generally absent in later, post 33 ka, material; (2) relatively large anterior teeth; and (3) megadont distal molars. The only *H. sapiens* specimen known to have a high level of Neanderthal ancestry is the Oase 1 mandible and, by association, the Oase 2 cranium (Fu et al., 2015). Between 6 and 9% of its genome was derived from Neanderthals and it was concluded that there had been a Neanderthal ancestor 4–6 generations back (Fu et al., 2015). However, the Oase teeth (molars) do not exhibit any Neanderthal features. The lower molar mesial (anterior) foveae are small and there are no mid-trigonid crests; the M^1 is of *H. sapiens* form; and the teeth are non-taurodont. The complex crown morphology of the M^3 was considered unique (Trinkaus et al., 2012). The teeth, however, are very large, particularly the second and third molars. A discriminant function analysis of the lower molar crown dimensions plotted them with Neanderthals (Trinkaus et al., 2003).

There is no evidence of transitional or Upper Paleolithic characteristics in the stone artifacts retained from the excavations at La Cotte. However, the degree of association between the teeth and the Mousterian artifacts in the occupation level is uncertain because the teeth were found on a ledge above the occupation level (though clearly accessible). The stone artifacts recovered at Palomas are similarly described as Mousterian (Walker et al., 2017).

The supraradicular taurodontism found in the La Cotte molars is the type generally found in Neanderthals. The more extreme radicular or total taurodontism, where the pulp chamber extends to the tip of a single root, is only found at a few sites, e.g., Krapina (Smith, 1976); Fondo Cattíe (Tarli, 1983); Palomas (Walker et al., 2008). Pyramidal roots, defined by Kupczik and Hublin (2010) as fused roots that can have apical root canal branches in addition to radicular or total taurodontism, are found at Regourdou, Kebara and La Quina (Kupczik and Hublin, 2010) and Aubesier (Lebel et al., 2001). The description of SJMJ2461 (M_2), where both Shifman and Chananel's (1978) and Keene's (1966) methods are used to measure the degree of taurodontism, demonstrates that different methods can give very different results. The degree of taurodontism in the La Cotte premolars is particularly notable. The extent of taurodontism in molars can be identified by the type, the height of the pulp chamber, and its shape—hourglass or barrel. In the comparative samples of Neanderthal P_3 and P_4 there is considerably greater variation of form than is found in molars. There is variation in the degrees of buccolingual and mesiodistal widening, and in the overall shape and the degree of tapering, in addition to the extent to which the pulp chamber expands towards the root apex. Consideration is needed as to how this should be measured. A point of interest is that P_3 and P_4 show a similar degree and shape of the taurodontism when both teeth are present in a specimen in the comparative samples in six of nine cases, and the P_4 has a slightly greater level of taurodontism in the remainder. This contrasts with the situation in molars, where the degree of taurodontism frequently increases from first to third (Dumančić et al., 2001).

5. Conclusions

The crown and root dimensions for the La Cotte teeth fit well with the Neanderthal comparative samples, and the morphology of the crowns and roots are, in most aspects,

typical of Neanderthals. However, there are also *H. sapiens* characteristics, specifically the lack of asymmetry and absence of transverse crests in the lower premolars; the mixture of characteristics in the M^1; and the absence of mid-trigonid crests, and the marginal position of the metaconid dentine horn tip, in the lower molars. Furthermore, the cervix shape of molars and premolars gives a mixed picture, Neanderthal for molars and *H. sapiens* for premolars. The taxonomic attribution of the teeth is therefore ambiguous. Neanderthal characteristics are present in all eleven teeth, but seven of the teeth also have *H. sapiens* characteristics. *Homo sapiens* characteristics occur in teeth from both the minimum of two adult individuals identified, suggesting a group or kin with these characteristics. Also of note is the unusual form of the protostylids found at the EDJ on lower molars, which has not previously been observed in Neanderthal or *H. sapiens* teeth.

The occipital fragment, which was found in a stratigraphically higher archaeological horizon, is likely to be from an immature individual who died in late childhood or adolescence. Its taxonomic status cannot be determined with certainty, but there are no anatomical features preserved in the bone that clearly indicate a Neanderthal affinity.

Of the various scenarios that can be considered to explain the mix of features in the La Cotte teeth, we favor shared Neanderthal and *H. sapiens* ancestry. The likely dating of the fossils during a period of temporal overlap between these groups is consistent with this interpretation.

References

Altman, D.G., Machin, D., Bryant, T.N., Gardner, M.J., 2000. Statistics with Confidence: Confidence Intervals and Statistical Guidelines, 2nd ed. BMJ Books, London.

Angel, J.L., Coon, C.S., 1954. La Cotte de St. Brelade II: Present status. Man 54, 53–55.

Arsuaga, J.L., Villaverde, V., Quam, R., Gracia, A., Lorenzo, C., Martínez, I., Carretero, J.M., 2002. The Gravettian occipital bone from the site of Malladetes (Barx, Valencia, Spain). Journal of Human Evolution 43, 381–393.

Auguste, P., 2009. Évolution des peuplements mammaliens en Europe du Nord-Ouest durant le Pléistocène moyen et supérieur. Le cas de la France septentrionale. Quaternaire. Revue de l'Association Française pour l'étude du Quaternaire 20, 527–550.

Bailey, S.E., 2002. A closer look at Neanderthal postcanine dental morphology. I. The mandibular dentition. Anatomical Record 269, 148–156.

Bailey, S.E., 2004. A morphometric analysis of maxillary molar crowns of Middle–Late Pleistocene hominins. Journal of Human Evolution 47, 183–198.

Bailey, S.E., 2005. Diagnostic dental differences between Neandertals and Upper Paleolithic modern humans: Getting to the root of the matter. In: Zadzinska, E. (Ed.), Current Trends in Dental Morphology Research. University of Lodz Press, Lodz, pp. 201–210.

Bailey, S.E., 2006a. Beyond shovel-shaped incisors: Neandertal dental morphology in a comparative context. Periodicum Biologorum 108, 253–267.

Bailey, S.E., 2006b. The evolution of non-metric dental variation in Europe. Mitteilungen der Gesellschaft für Urgeschichte 15, 9–30.

Bailey, S.E., Hublin, J.J., 2006. Dental remains from the Grotte du Renne at Arcy-sur-Cure (Yonne). Journal of Human Evolution 50, 485–508.

Bailey, S.E., Glantz, M., Weaver, T.D., Viola, B., 2008. The affinity of the dental remains from Obi-Rakhmat Grotto, Uzbekistan. Journal of Human Evolution 55, 238–248.

Bailey, S.E., Skinner, M.M., Hublin, J.J., 2011. What lies beneath? An evaluation of lower molar trigonid crest patterns based on both dentine and enamel expression. American Journal of Physical Anthropology 145, 505–518.

Bailey, S.E., Weaver, T.D., Hublin, J.J., 2017. The dentition of the earliest modern humans: How 'modern' are they? In: Marom, A., Hovers, E. (Eds), Human Paleontology and Prehistory. Springer, Cham, pp. 215–232.

Bates, M., Pope, M., Shaw, A., Scott, B., Schwenninger, J.L., 2013. Late Neanderthal occupation in North-West Europe: rediscovery, investigation and dating of a last glacial sediment sequence at the site of La Cotte de Saint Brelade, Jersey. Journal of Quaternary Science 28, 647–652.

Becam, G., Verna, C., Gómez-Robles, A., Gómez-Olivencia, A., Albessard, L., Arnaud, J., Frelat, M.A., Madelaine, S., Schwab, C., Souday, C., Turq, A., 2019. Isolated teeth from La Ferrassie: Reassessment of the old collections, new remains, and their implications. American Journal of Physical Anthropology 169, 132–142.

Benazzi, S., Douka, K., Fornai, C., Bauer, C.C., Kullmer, O., Svoboda, J., Pap, I., Mallegni, F., Bayle, P., Coquerelle, M., Condemi, S., 2011. Early dispersal of modern humans in Europe and implications for Neanderthal behaviour. Nature 479, 525–528.

Benazzi, S., Slon, V., Talamo, S., Negrino, F., Peresani, M., Bailey, S.E., Sawyer, S., Panetta, D., Vicino, G., Starnini, E., Mannino, M.A., 2015. The makers of the Protoaurignacian and implications for Neandertal extinction. Science 348, 793–796.

Bermúdez de Castro, J.M., Martínez, I., 1986. Hypocone and metaconule: identification and variability on human molars. International Journal of Anthropology 1, 165–168.

Bilsborough, A., Thompson, J.L., 2005. The dentition of the Le Moustier 1 Neandertal. In: Ullrich, H. (Ed.), The Neandertal Adolescent Le Moustier 1 – New Aspects, New Results. Staatliche Museum, Berlin, pp. 157–186.

Black, G.V., 1902. Descriptive Anatomy of the Human Teeth, 4th ed. S White Dental Manufacturing Co., Philadelphia.

Brabant, H., Sahly, A., 1964. Étude des dents Néandertaliennes découvertes dans la Grotte du Portel, en Ariège (France). Bulletin du Groupement International pour la Recherche Scientifique en Stomatologie & Odontologie 7, 237–254.

Burdo, C., 1960. La Cotte-de-Saint-Brelade, Jersey, British Channel Islands: Excavation of a Pre-Mousterian Horizon, 1950-1958. Société Jersiaise, St. Helier.

Callow, P., 1986a. Appendix B: Artefacts from the Weichselian deposits. In: Callow, P., Cornford, J.M. (Eds.), La Cotte de St. Brelade 1961–1978. Excavations by C.B.M. McBurney. Geobooks, Norwich, pp. 397–408.

Callow, P., 1986b. Appendix F: Fauna from deposits of the last cold stage at La Cotte de St Brelade. In: Callow, P., Cornford, J.M. (Eds.), La Cotte de St. Brelade 1961–1978. Excavations by C.B.M. McBurney. Geobooks, Norwich, microfiche bound with book.

Callow, P., 1986c. Interpreting the La Cotte sequence. In: Callow, P., Cornford, J.M. (Eds.), La Cotte de St. Brelade 1961–1978. Excavations by C.B.M. McBurney. Geobooks, Norwich, pp. 73–82.

Compton, T., Stringer, C.B., 2012. The human remains. In: Aldhouse-Green, S., Peterson, R., Walker, E.A. (Eds.), Neanderthals in Wales: Pontnewydd and the Elwy Valley Caves. Oxbow Books, Oxford, pp. 118–230.

Compton, T., Stringer, C., 2015. The morphological affinities of the Middle Pleistocene hominin teeth from Pontnewydd Cave, Wales. Journal of Quaternary Science 30, 713–730.

Davies, T.W., Delezene, L.K., Gunz, P., Hublin, J.J., Skinner, M.M., 2019. Endostructural morphology in hominoid mandibular third premolars: Discrete traits at the enamel-dentine junction. Journal of Human Evolution 136, 102670.

Dean, D., Hublin, J.-J., Holloway, R., Ziegler, R., 1998. On the phylogenetic position of the pre-Neandertal specimen from Reilingen, Germany. Journal of Human Evolution 34, 485–508.

Dumančić, J., Kaić, Z., Petrovečki, M., 2001. Evaluation of taurodontism in Krapina Neanderthals. In: Brook, A. (Ed.), Dental Morphology 2001. Sheffield Academic Press, Sheffield, pp. 111–121.

Fewlass, H., Talamo, S., Wacker, L., Kromer, B., Tuna, T., Fagault, Y., Bard, E., McPherron, S.P., Aldeias, V., Maria, R., Martisius, N.L., 2020. A ^{14}C chronology for the Middle to Upper Palaeolithic transition at Bacho Kiro Cave, Bulgaria. Nature Ecology & Evolution 4, 794–801.

Fu, Q., Hajdinjak, M., Moldovan, O.T., Constantin, S., Mallick, S., Skoglund, P., Patterson, N., Rohland, N., Lazaridis, I., Nickel, B., Viola, B., Prüfer, K., Meyer, M., Kelso, J., Reich, D., Pääbo, S., 2015. An early modern human from Romania with a recent Neanderthal ancestor. Nature 524, 216–219.

Gómez-Robles, A., Martinón-Torres, M., Bermúdez de Castro, J.M., Margvelashvili, A., Bastir, M., Arsuaga, J.L., Pérez-Pérez, A., Estebaranz, F., Martínez, L.M., 2007. A geometric morphometric analysis of hominin upper first molar shape. Journal of Human Evolution 53, 272–285.

Gómez-Robles, A., Martinón-Torres, M., de Castro, J.M.B., Prado, L., Sarmiento, S., Arsuaga, J.L., 2008. Geometric morphometric analysis of the crown morphology of the lower first premolar of hominins, with special attention to Pleistocene *Homo*. Journal of Human Evolution 55, 627–638.

Greene, D.L., Ewing, G.H., Armelagos, G.J., 1967. Dentition of a Mesolithic population from Wadi Halfa, Sudan. American Journal of Physical Anthropology 27, 41–55.

Guatelli-Steinberg, D., Huffman, M., 2012. Histological features of dental hard tissues and their utility in forensic anthropology. In: Crowder, C., Stout, S.D. (Eds.), Bone Histology. An Anthropological Perspective. CRC Press, Boca Raton, pp. 91–107.

Gunz, P., Mitteroecker, P., 2013. Semilandmarks: a method for quantifying curves and surfaces. Hystrix 24, 103–109.

Guy, F., Lazzari, V., Gilissen, E., Thiery, G., 2015. To what extent is primate second molar enamel occlusal morphology shaped by the enamel-dentine junction? PLoS One 10, e0138802.

Hajdinjak, M., Fu, Q., Hübner, A., Petr, M., Mafessoni, F., Grote, S., Skoglund, P., Narasimham, V., Rougier, H., Crevecoeur, I., Semal, P., 2018. Reconstructing the genetic history of late Neanderthals. Nature 555, 652–656.

Harvati, K., Röding, C., Bosman, A.M., Karakostis, F.A., Grün, R., Stringer, C., Karkanas, P., Thompson, N.C., Koutoulidis, V., Moulopoulos, L.A., Gorgoulis, V.G., 2019. Apidima Cave fossils provide earliest evidence of *Homo sapiens* in Eurasia. Nature 571, 500–504.

Higham, T., Douka, K., Wood, R., Ramsey, C.B., Brock, F., Basell, L., Camps, M., Arrizabalaga, A., Baena, J., Barroso-Ruíz, C., Bergman, C., 2014. The timing and spatiotemporal patterning of Neanderthal disappearance. Nature 512, 306–309.

Hillson, S., 1996. Dental Anthropology. Cambridge University Press, Cambridge.

Hoffecker, J.F., 2009. The spread of modern humans in Europe**.** Proceedings of the National Academy of Sciences USA 106, 16040–16045.

Hublin, J.J., 2015. The modern human colonization of western Eurasia: when and where? Quaternary Science Reviews 118, 194–210.

Hublin, J-J., Roebroeks, W., 2009. Ebb and flow or regional extinctions? On the character of Neandertal occupation of northern environments. Comptes Rendus Palevol 8, 503–509.

Hublin, J.J., Talamo, S., Julien, M., David, F., Connet, N., Bodu, P., Vandermeersch, B., Richards, M.P., 2012. Radiocarbon dates from the Grotte du Renne and Saint-Césaire support a Neandertal origin for the Châtelperronian. Proceedings of the National Academy of Sciences USA 109, 18743–18748.

Hublin, J.J., Sirakov, N., Aldeias, V., Bailey, S., Bard, E., Delvigne, V., Endarova, E., Fagault, Y., Fewlass, H., Hajdinjak, M., Kromer, B., 2020. Initial Upper Palaeolithic *Homo sapiens* from Bacho Kiro Cave, Bulgaria. Nature 581, 299–302.

Jafarzadeh, H., Azarpazhooh, A., Mayhall, J.T., 2008. Taurodontism: a review of the condition and endodontic treatment challenges. International Endodontic Journal 41, 375–388.

Kallay, J., 1963. A radiographic study of the Neanderthal teeth from Krapina, Croatia. In: Brothwell, D.R. (Ed.), Dental Anthropology. Pergamon Press, Oxford, pp. 75–86.

Kallay, J., 1970. A new classification of the taurodont teeth of the Krapina Neanderthal man. Bulletin Scientifique (Yugoslavie) 15, 2–3.

Keene, H., 1966. A morphologic and biometric study of taurodontism in a contemporary population. American Journal of Physical Anthropology 25, 208–209.

Keith, A., 1913. Problems relating to the teeth of the earlier forms of prehistoric man. Proceedings of the Royal Society of Medicine 6, 103–124.

Keith, A., Knowles, F.H., 1911. A description of teeth of Palaeolithic man from Jersey. Journal of Anatomy and Physiology 46, 12–27.

Keith, A., Knowles, F.H., 1912. A description of teeth of Palaeolithic man from Jersey. Bulletin Société Jersiaise 37, 222–240.

Krenn, V.A., Fornai, C., Wurm, L., Bookstein, F.L., Haeusler, M., Weber, G.W., 2019. Variation of 3D outer and inner crown morphology in modern human mandibular premolars. American Journal of Physical Anthropology 169, 646–663.

Kupczik, K., Hublin, J.J., 2010. Mandibular molar root morphology in Neanderthals and Late Pleistocene and recent *Homo sapiens*. Journal of Human Evolution 59, 525–541.

Kupczik, K., Delezene, L.K., Skinner, M.M., 2019. Mandibular molar root and pulp cavity morphology in *Homo naledi* and other Plio-Pleistocene hominins. Journal of Human Evolution 130, 83–95.

Lebel, S., Trinkaus, E., Faure, M., Fernandez, P., Guérin, C., Richter, D., Mercier, N., Valladas, H., Wagner, G.A., 2001. Comparative morphology and paleobiology of Middle Pleistocene human remains from the Bau de l'Aubesier, Vaucluse, France. Proceedings of the National Academy of Sciences USA 98, 11097–11102.

Le Cabec, A., 2013. Anterior dental loading and root morphology in Neanderthals. Ph.D. Dissertation, Université Toulouse III-Paul Sabatier.

Le Cabec, A., Gunz, P., Kupczik, K., Braga, J., Hublin, J.-J., 2013. Anterior tooth root morphology and size in Neanderthals: Taxonomic and functional implications. Journal of Human Evolution 64, 169–193.

McCown, T.D., Keith, A., 1939. The Stone Age of Mount Carmel II. Clarendon Press, Oxford.

Marett, R.R., 1911. XX.—Pleistocene man in Jersey. Archaeologia 62, 449–480.

Marett, R.R., 1916. IV.—The site, fauna, and industry of La Cotte de St. Brelade, Jersey. Archaeologia 67, 75–118.

Martin, R.M., Hublin, J.-J., Gunz, P., Skinner, M.M., 2017. The morphology of the enamel–dentine junction in Neanderthal molars: gross morphology, non-metric traits, and temporal trends. Journal of Human Evolution 103, 20–44.

Martinón-Torres, M., Bermúdez de Castro, J.M., Gómez-Robles, A., Prado-Simón, L., Arsuaga, J.L., 2012. Morphological description and comparison of the dental remains from Atapuerca-Sima de los Huesos site (Spain). Journal of Human Evolution 62, 7–58.

Martinón-Torres, M., Spěváčková, P., Gracia-Téllez, A., Martínez, I., Bruner, E., Arsuaga, J.L., Bermúdez de Castro, J.M., 2013. Morphometric analysis of molars in a Middle

Pleistocene population shows a mosaic of ‘modern’ and Neanderthal features. Journal of Anatomy 223, 353–363.

Matiegka, J., 1934. *Homo předmostensis* – Fosilní Člověk z Předmostí Na Morarě I Lebky. Česká Akademie Věd a Umění, Prague.

Maureille, B., Rougier, H., Houêt, F., Vandermeersch, B., 2001. Les dents inférieures du Néandertalien Regourdou 1 (site de Regourdou, commune de Montignac, Dordogne): analyses métriques et comparatives. Paléo 13, 183–200.

Maureille, B., Djindjian, F., Garralda, M.D., Mann, A., Vandermeersch, B., 2008. Les dents moustériennes de la grotte Boccard, lieu-dit Bas-de-Morant (commune de Créancey, Côte-d'Or, Bourgogne). Bulletins et Mémoires de la Société d’Anthropologie de Paris 20, 59–78.

Moorrees, C.F.A., 1957. The Aleut Dentition. Harvard University Press, Cambridge.

NESPOS, 2013. NESPOS – Pleistocene People and Places. https://www.nespos.org/display/openspace/Home (last accessed on 20/12/2013).

Nicolle, E.T., Sinel, J., 1910. 102. Report on the exploration of the Palaeolithic cave-dwelling known as La Cotte, St. Brelade, Jersey. Man 10, 185–188.

Nicolle, E.T., Sinel, J., 1912. 88. Report on the resumed exploration of "La Cotte", St. Brelade, by the Societe Jersiaise. Man 12, 158–162.

Oakley, K.P., Campbell, B.G., Molleson, T.I., 1975. Catalogue of Fossil Hominids (Vol. 2). British Museum (Natural History), London.

Ortiz, A., Bailey, S.E., Hublin, J.J., Skinner, M.M., 2017. Homology, homoplasy and cusp variability at the enamel–dentine junction of hominoid molars. Journal of Anatomy 231, 585–599.

Patte, É., 1962. La Dentition des Néanderthaliens. Masson et Cie, Paris.

Peter, B., 2019. Gene flow between hominins was common. Proceedings of the European Society for the Study of Human Evolution 8, 147.

Pinilla, B., Trinkaus, E., 2017. The Palomas dental remains: Size and proportions. In: Trinkaus, E., Walker, M.J. (Eds.), The People of Palomas: Neandertals from the Sima de las Palomas del Cabezo Gordo, Southeastern Spain. Texas A&M University Press, College Station, pp. 89–104.

Prado-Simón, L., Martinón-Torres, M., Baca, P., Olejniczak, A.J., Gómez-Robles, A., Lapresa, M., Arsuaga, J.L., Bermúdez de Castro, J.M., 2012. Three-dimensional evaluation of root canal morphology in lower second premolars of Early and Middle Pleistocene human populations from Atapuerca (Burgos, Spain). American Journal of Physical Anthropology 147, 452–461.

Quam, R., Bailey, S., Wood, B., 2009. Evolution of M^1 crown size and cusp proportions in the genus *Homo*. Journal of Anatomy 214, 655–670.

Radovčić, J., Smith, F.H., Trinkaus, E., Wolpoff, M.H., 1988. The Krapina Hominids an Illustrated Catalog of Skeletal Collection. Mladost, Zagreb.

Rasband, W.S., 2008. ImageJ. U. S. National Institutes of Health, Bethesda, Maryland, http://rsb.info.nih.gov/ij/.

Reid, C., Reenen, J.F. Van, 1995. Remnants of the metaconule in recent man. In: Radlanski, R.J., Renz, H. (Eds.), Proceedings of the 10th International Symposium on Dental Morphology. C. and M. Brunne, Berlin, pp. 172–176.

Scott, B., Bates, M., Bates, R., Conneller, C., Pope, M., Shaw, A., Smith, G., 2014. A new view from la Cotte de St Brelade, Jersey. Antiquity 88, 13–29.

Scott, G.R., Turner II, C.G., 1997. The Anthropology of Modern Human Teeth. Cambridge Studies in Biological Anthropology, Cambridge University Press, Cambridge.

Scott, G.R., Irish, J.D., 2017. Human Tooth Crown and Root Morphology. Cambridge University Press, Cambridge.

Scott, G.R., Turner, C.G. II, Townsend, G.C., Martinón-Torres, M., 2018. The Anthropology of Modern Human Teeth: Dental Morphology and its Variation in Recent and Fossil *Homo sapiens*. 2nd ed. Cambridge University Press, Cambridge.

Semal, P., Hauzeur, A., Rougier, H., Crevecoeur, I., Germonpré, M., Pirson, S., Haesaerts, P., Jungels, C., Flas, D., Toussaint, M., Maureille, B., 2013. Radiocarbon dating of human remains and associated archaeological material. In: Rougier, H., Semal, P. (Eds), Spy Cave: 125 Years of Multidisciplinary Research at the Betche Aux Rotches (Jemeppe-sur-Sambre, Province of Namur, Belgium). Société Royale Belge d'Anthropologie et de Préhistoire, Brussels, pp. 331–356.

Shaw, A., Bates, M., Conneller, C., Gamble, C., Julien, M.A., McNabb, J., Pope, M., Scott, B., 2016. The archaeology of persistent places: the Palaeolithic case of La Cotte de St Brelade, Jersey. Antiquity 90, 1437–1453.

Shields, E.D., 2005. Mandibular premolar and second molar root morphological variation in modern humans: What root number can tell us about tooth morphogenesis. American Journal of Physical Anthropology 128, 299–311.

Shifman, A., Chananel, I., 1978. Prevalence of taurodontism found in radiographic dental examination of 1,200 young adult Israeli patients. Community Dental Oral Epidemiology 6, 200–203.

Skinner, M.M., Gunz, P., 2010. The presence of accessory cusps in chimpanzee lower molars is consistent with a patterning cascade model of development. Journal of Anatomy 217, 245–253.

Skinner, M.M., Wood, B.A., Boesch, C., Olejniczak, A.J., Rosas, A., Smith, T.M., Hublin, J.J., 2008. Dental trait expression at the enamel-dentine junction of lower molars in extant and fossil hominoids. Journal of Human Evolution 54, 173–186.

Skinner, M.M., Wood, B.A., Hublin, J.-J., 2009. Protostylid expression at the enamel-dentine junction and enamel surface of mandibular molars of *Paranthropus robustus* and *Australopithecus africanus*. Journal of Human Evolution 56, 76–85.

Skinner, M.M., Evans, A., Smith, T., Jernvall, J., Tafforeau, P., Kupczik, K., Olejniczak, A.J., Rosas, A., Radovčić, J., Thackeray, J.F., Toussaint, M., 2010. Brief communication: Contributions of enamel-dentine junction shape and enamel deposition to primate molar crown complexity. American Journal of Physical Anthropology 142, 157–163.

Smith, B.H., 1984. Patterns of molar wear in hunter–gatherers and agriculturalists. American Journal of Physical Anthropology 63, 39–56.

Smith, F.H., 1976. The Neandertal remains from Krapina: a descriptive and comparative study. Ph.D. Dissertation, University of Tennessee.

Smith, P., 1989. Dental evidence for phylogenetic relationships of Middle Palaeolithic hominids. In: Vandermeersch, B. (Ed.), L'Homme de Neandertal Vol 7. L'Extinction. Université de Liège, pp. 111–120.

Stringer, C.B., 2006. The Neanderthal-*H. sapiens* interface in Eurasia. In: Harvati, K., Harrison, T. (Eds.), Neanderthals Revisited: New Approaches and Perspectives. Springer, Dordrecht, pp. 315–323.

Stringer, C.B., Currant, A.P., 1986. Hominid specimens from La Cotte de St. Brelade. In: Callow, P., Cornford, J.M. (Eds.), La Cotte de St. Brelade 1961–1978. Excavations by C.B.M. McBurney. Geo Books, Norwich, pp. 155–158.

Tarli, S.M.B., 1983. A Neanderthal lower molar from Fondo Cattíe (Maglie, Lecce). Journal of Human Evolution 12, 383–401.

Trinkaus, E., 1995. Neanderthal mortality patterns. Journal of Archaeological Science 22, 121–142.

Trinkaus, E., 2007. European early modern humans and the fate of the Neandertals. Proceedings of the National Academy of Sciences USA 104, 7367–7372.

Trinkaus, E., 2017. The people of Palomas. In: Trinkaus, E., Walker, M.J. (Eds.), The People of Palomas: Neandertals from the Sima de las Palomas del Cabezo Gordo, Southeastern Spain. Texas A&M University Press, College Station, pp. 245–247.

Trinkaus, E., Moldovan, O., Bîlgăr, A., Sarcina, L., Athreya, S., Bailey, S.E., Rodrigo, R., Mircea, G., Higham, T., Ramsey, C.B., van der Plicht, J., 2003. An early modern human from the Peştera cu Oase, Romania. Proceedings of the National Academy of Sciences USA 100, 11231–11236.

Trinkaus, E., Bailey, S., Rougier , H., 2012. The dental and alveolar remains of Oase 1 and 2. In: Trinkaus, E., Constantin, S., Zilhão, J. (Eds.), Life and Death at the Pestera cu Oase: A Setting for Modern Human Emergence in Europe. Oxford University Press, New York, pp. 781–851.

Turner, C.G., Nichol, C.R., Scott, G.R., 1991. Scoring procedures for key morphological traits of the permanent dentition. In: Kelley, M.A., Larsen, C.S. (Eds.), Advances in Dental Anthropology. Wiley-Liss, New York, pp. 13–31.

Van Beek, G.C., 1983. Dental Morphology: an Illustrated Guide. Wright, Oxford.

Vandermeersch, B., 1981. Les Hommes Fossiles de Qafzeh (Israel). CNRS, Paris.

Walker, M.J., Gibert, J., López, M.V., Lombardi, A.V., Pérez-Pérez, A., Zapata, J., Ortega, J., Higham, T., Pike, A., Schwenninger, J.L., Zilhão, J., 2008. Late Neandertals in southeastern Iberia: Sima de las Palomas del Cabezo Gordo, Murcia, Spain. Proceedings of the National Academy of Sciences USA 105, 20631–20636.

Walker, M.J., López, M.V., Haber, M., Trinkaus, E., 2017. The context of the Sima de las Palomas Neandertals. In: Trinkaus, E., Walker, M.J. (Eds.), The People of Palomas: Neandertals from the Sima de las Palomas del Cabezo Gordo, Southeastern Spain. Texas A&M University Press, College Station, pp. 4–18.

Wollny, G., Kellman, P., Ledesma-Carbayo, M.J., Skinner, M.M., Hublin, J.-J., Hierl, T., 2013. MIA-A free and open source software for gray scale medical image analysis. Source Code for Biology and Medicine 8, 20.

Wood, B.A., Abbott, S.A., 1983. Analysis of the dental morphology of Plio–Pleistocene hominids. I. Mandibular molars: crown area measurements and morphological traits. Journal of Anatomy 136, 197–219.

Zapata, J., Bayle, P., Lombardi, A.V., Pérez-Pérez, A., Trinkaus, E., 2017. The Palomas dental remains: preservation, wear, and morphology. In: Trinkaus, E., Walker, M.J. (Eds.), The People of Palomas: Neandertals from the Sima de las Palomas del Cabezo Gordo, Southeastern Spain. Texas A&M University Press, College Station, pp. 52–88.

Zeuner, F.E., 1940. The age of Neanderthal man, with notes on the Cotte de St Brelade, Jersey, C.I. London University Institute of Archaeology, London.

Zilhão, J., Trinkaus, E., Constantin, S., Milota, S., Gherase, M., Sacrina, L., Danciu, A., Rougier, H., Quilès, J., Rodrigo, R., 2007. The Peştera cu Oase people, Europe's earliest modern humans. In: Mellars, P.M., Bar-Yosef, O., Stringer, C., Boyle, K.V. (Eds.), Rethinking the Human Revolution: New Behavioural and Biological Perspectives on the Origin and Dispersal of Modern Humans. McDonald Institute for Archaeological Research, Cambridge, pp. 249–262.

Figure legends

Figure 1. Location of La Cotte de St Brelade (from Shaw et al., 2016). A) Channel Islands within north-western Europe. B) Jersey in relation to other Channel Islands and the French coast, showing the ~7 m drop in sea level necessary to reconnect to the continent. C) simplified geological map of Jersey showing main sites. Based on an image supplied by John Renouf, with permission.

Figure 2. Site plan (A) and cross-section (B) of La Cotte de St. Brelade.

Figure 3. E.T. Nicolle shown standing on the level of the hearth, with what might be the ledge on which the teeth were found on the left-hand side. Photograph by R. Mollet. Reproduced with the kind permission of the Société Jersiaise.

Figure 4. SJMJ2463, left C_1. a–c) Photographs in occlusal (a), distal (b), and mesial (c) views. d–f) Surface models in occlusal (d), distal (e), and mesial (f) views. g) EDJ in lingual view. h) CT cross-section (plane of section shown in d); i) CT cross-section (plane of section shown in f). Abbreviations: B = buccal; D = distal; L = lingual; M = mesial.

Figure 5. SJMJ2457, left P^4. a–c) Photographs in occlusal (a), distal (b), and mesial (c) views. d–f) Surface models in occlusal (d), distal (e), and mesial (f) views. g) EDJ in occlusal view. h) CT cross-section (plane of section shown in d); i) CT cross-section (plane of section shown in f). Abbreviations: B = buccal; D = distal; L = lingual; M = mesial.

Figure 6. SJMJ2464, left P_3. a–c) Photographs in occlusal (a), distal (b), and mesial (c) views. d–f) Surface models in occlusal (d), distal (e), and mesial (f) views. g) EDJ in occlusal view. h) CT cross-section (plane of section shown in d); i) CT cross-section (plane of section shown in f). Abbreviations: B = buccal; D = distal; L = lingual; M = mesial.

Figure 7. SJMJ2465, left P_4. a–c) Photographs in occlusal (a), distal (b), and mesial (c) views. d–f) Surface models in occlusal (d), distal (e), and mesial (f) views. g) EDJ in occlusal view. h) CT cross-section (plane of section shown in d); i) CT cross-section (plane of section shown in f). Abbreviations: B = buccal; D = distal; L = lingual; M = mesial.

Figure 8. SJMJ2456, right M^1. a–c) Photographs in occlusal (a), distal (b), and mesial (c) views. d–f) Surface models in occlusal (d), distal (e), and mesial (f) views. g) EDJ in occlusal view. h) CT cross-section (plane of section shown in d); i) CT cross-section (plane of section shown in f). Occlusal polygon shape shown on occlusal photograph. Abbreviations: B = buccal; D = distal; L = lingual; M = mesial.

Figure 9. SJMJ2458, left M^2. a–c) Photographs in occlusal (a), distal (b), and mesial (c) views. d–f) Surface models in occlusal (d), distal (e), and mesial (f) views. g) EDJ in occlusal view. h) CT cross-section (plane of section shown in d); i) CT cross-section (plane of section shown in f). Abbreviations: B = buccal; D = distal; L = lingual; M = mesial.

Figure 10. SJMJ2459, right M^3. a–c) Photographs in occlusal (a), distal (b), and mesial (c) views. d–f) Surface models in occlusal (d), distal (e), and mesial (f) views. g) EDJ in occlusal view. h) CT cross-section (plane of section shown in d); i) CT cross-section (plane of section shown in f). Abbreviations: B = buccal; D = distal; L = lingual; M = mesial.

Figure 11. Cast of SJMJ2467, left M^3. a–f) Photographs in occlusal (a), mesial (b), buccal (c), apical (d), distal (e), lingual (f) views. Note that a black and white photo of the original tooth taken after casting is provided in distal view. Abbreviations: B = buccal; D = distal; L = lingual; M = mesial.

Figure 12. SJMJ2461, right M_2. a–c) Photographs in occlusal (a), distal (b), and mesial (c) views. d–f) Surface models in occlusal (d), distal (e), and mesial (f) views. g) EDJ in occlusal view. h) CT cross-section (plane of section shown in d); i) CT cross-section (plane of section shown in f). Letters (a and b) on occlusal image denote mesiodistally concave/convex facets. Abbreviations: B = buccal; D = distal; L = lingual; M = mesial.

Figure 13. SJMJ2455, left M_2. a–c) Photographs in occlusal (a), distal (b), and mesial (c) views. d–f) Surface models in occlusal (d), distal (e), and mesial (f) views. g) EDJ in occlusal

view. h) CT cross-section (plane of section shown in d). i) occlusion of SJMJ2455 and SJMJ2458 (not to scale). Abbreviations: B = buccal; D = distal; L = lingual; M = mesial.

Figure 14. SJMJ2460, right M_3. a–c) Photographs in occlusal (a), distal (b), and mesial (c) views. d–f) Surface models in occlusal (d), distal (e), and mesial (f) views. g) EDJ in occlusal view showing numerous accessory dentine horns (*). h) CT cross-section (plane of section shown in d). i) articulation of SJMJ2460 and SJMJ2461 (not to scale). Abbreviations: B = buccal; D = distal; L = lingual; M = mesial.

Figure 15. La Cotte SJMJ2452 occipital fragment (right) compared to a modern child aged about 6 years. A) ectocranial surface; B) endocranial surface, dotted lines indicating the pathway of the transverse sulcus, which passes directly across the asterion in both bones.

Figure 16. Comparison of M^1 occlusal polygon shapes. Neanderthal: Krapina D161; La Cotte: SJMJ2456; fossil *H. sapiens*: La Madeleine. Abbreviations: B = buccal; D = distal; L = lingual; M = mesial.

Figure 17. Results of the principal components analysis of cervix shape landmarks in P^4 in shape (a) and form (b) space, and wireframe models of mean cervix shape in shape (c) and form (d) space. The percentage of variance depicted by each principal component (PC) is indicated. Abbreviations: Hn = *Homo neanderthalensis*; Hs = *Homo sapiens.*

Figure 18. Results of the principal components analysis of cervix shape landmarks in P_3 in shape (a) and form (b) space, and wireframe models of mean cervix shape in shape (c) and form (d) space. The percentage of variance depicted by each principal component (PC) is indicated. Abbreviations: Hn = *Homo neanderthalensis*; Hs = *Homo sapiens.*

Figure 19. Results of the principal components analysis of cervix shape landmarks in P_4 in shape (a) and form (b) space, and wireframe models of mean cervix shape in shape (c) and form (d) space. The percentage of variance depicted by each principal component (PC) is indicated. Abbreviations: Hn = *Homo neanderthalensis*; Hs = *Homo sapiens.*

Figure 20. Results of the principal components analysis of cervix shape landmarks in M^1 in shape (a) and form (b) space, and wireframe models of mean cervix shape in shape (c) and form (d) space. The percentage of variance depicted by each principal component (PC) is indicated. Abbreviations: Hn = *Homo neanderthalensis*; Hs = *Homo sapiens.*

Figure 21. Results of the principal components analysis of cervix shape landmarks in M^2 in shape (a) and form (b) space, and wireframe models of mean cervix shape in shape (c) and form (d) space. The percentage of variance depicted by each principal component (PC) is indicated. Abbreviations: Hn = *Homo neanderthalensis*; Hs = *Homo sapiens.*

Figure 22. Results of the principal components analysis of cervix shape landmarks in M^3 in shape (a) and form (b) space, and wireframe models of mean cervix shape in shape (c) and form (d) space. The percentage of variance depicted by each principal component (PC) is indicated. Abbreviations: Hn = *Homo neanderthalensis*; Hs = *Homo sapiens.*

Figure 23. Results of the principal components analysis of cervix shape landmarks in M_2 in shape (a) and form (b) space, and wireframe models of mean cervix shape in shape (c) and form (d) space. The percentage of variance depicted by each principal component (PC) is indicated. Abbreviations: Hn = *Homo neanderthalensis*; Hs = *Homo sapiens.*

Figure 24. Crown area adjusted Z scores; distances of La Cotte dimensions from comparative sample means of late Neanderthal, fossil *Homo sapiens* and Krapina. Abbreviations: Hs = *H. sapiens*; U = upper; L = lower; C = canine; P = premolar; M = molar; UM3a = SJMJ2467; UM3b = SJMJ2459. P^4: buccolingual dimension only.

Figure 25. Crown index adjusted Z scores; distances of La Cotte dimensions from comparative sample means of late Neanderthal, fossil *Homo sapiens* and Krapina. Abbreviations: Hs = *H. sapiens*; U = upper; L = lower; C = canine; P = premolar; M = molar; UM3a = SJMJ2467; UM3b = SJMJ2459.

Figure

Click here to access/download;Figure;Figure 1 Location of La Cotte de St Brelade.jpg

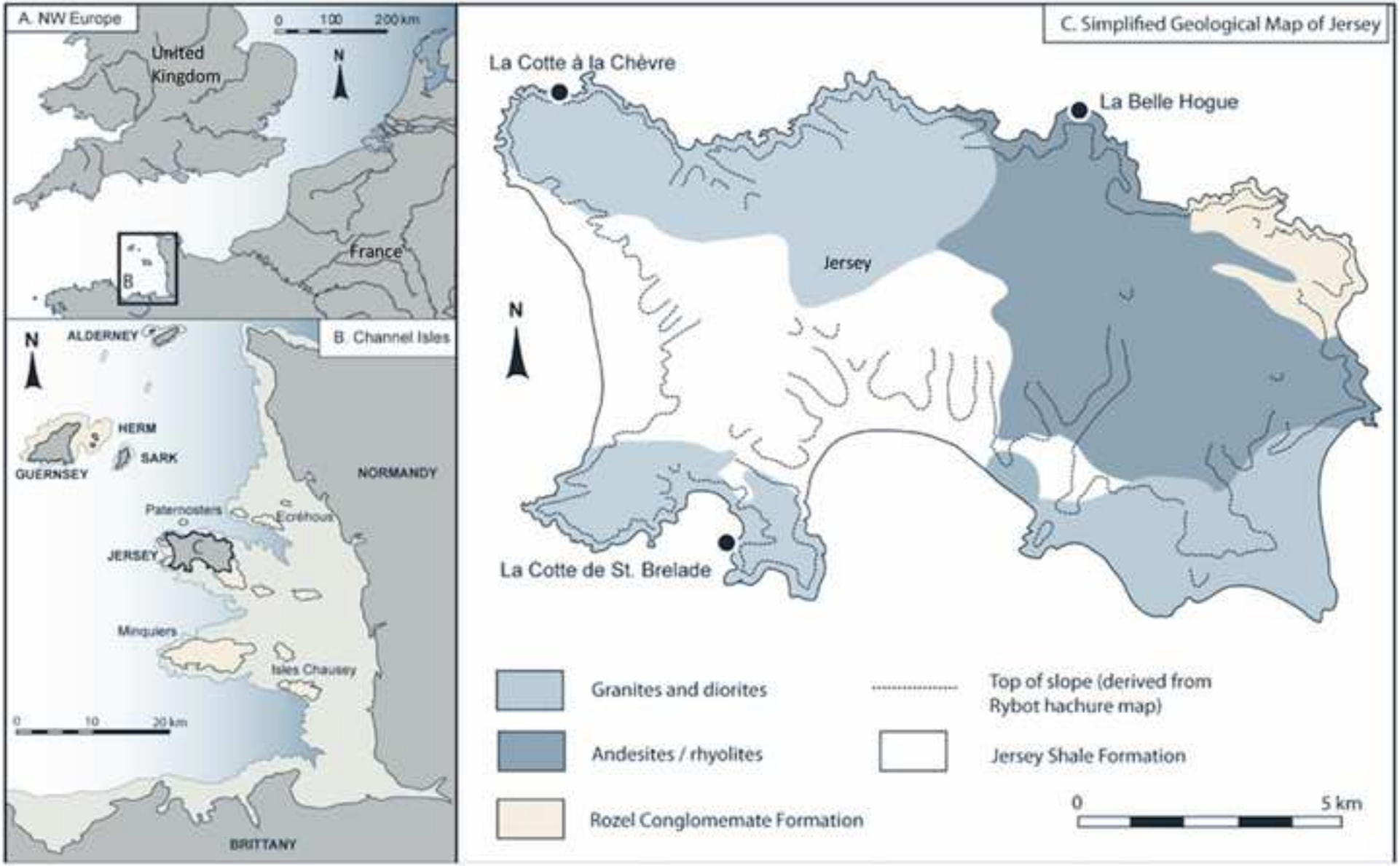

Figure

Click here to access/download;Figure;Figure 3 E T Nicolle at La Cotte in 1910.jpeg

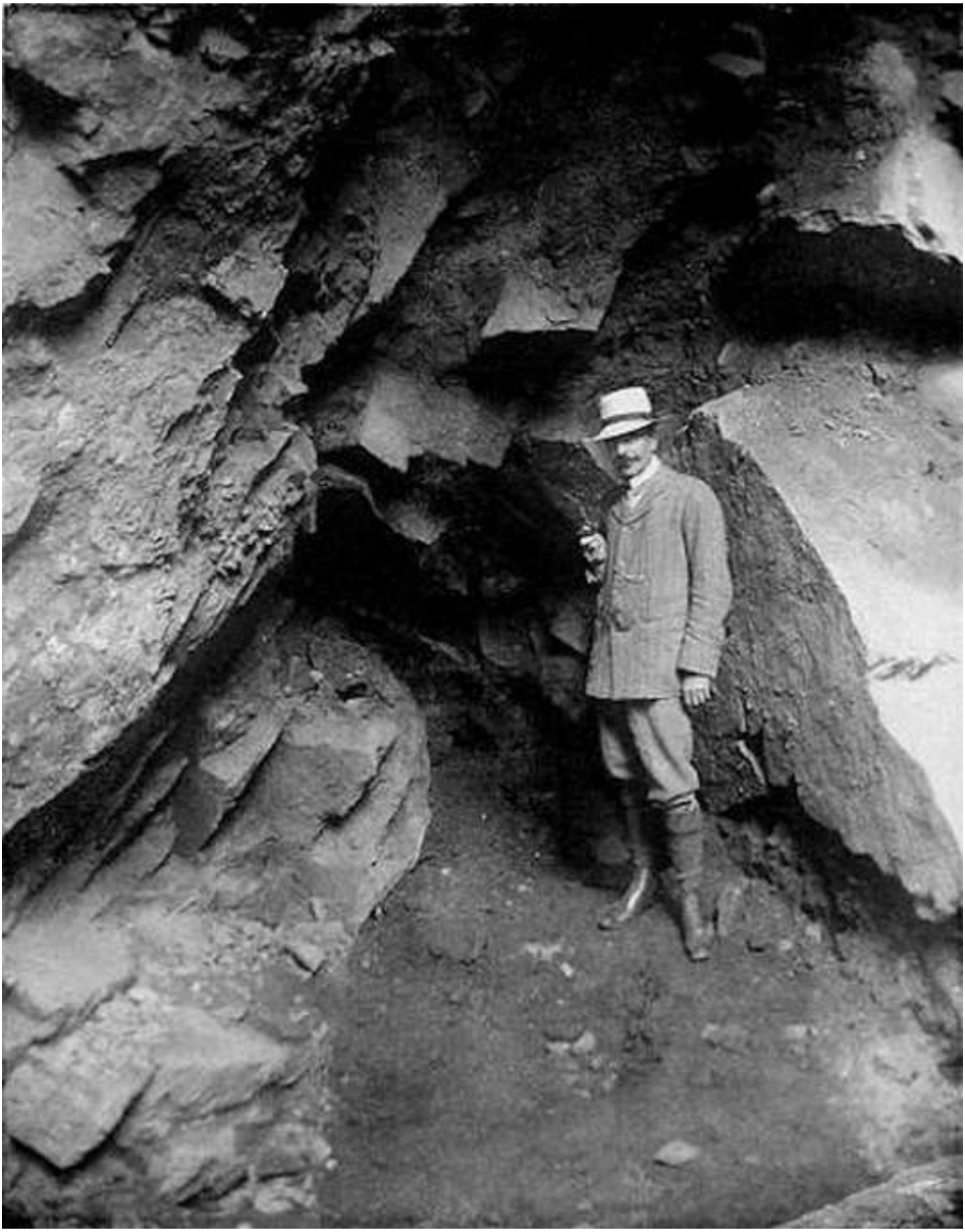

Figure

Click here to access/download;Figure;Figure 2 Site plan and cross section of La Cotte v2.jpg

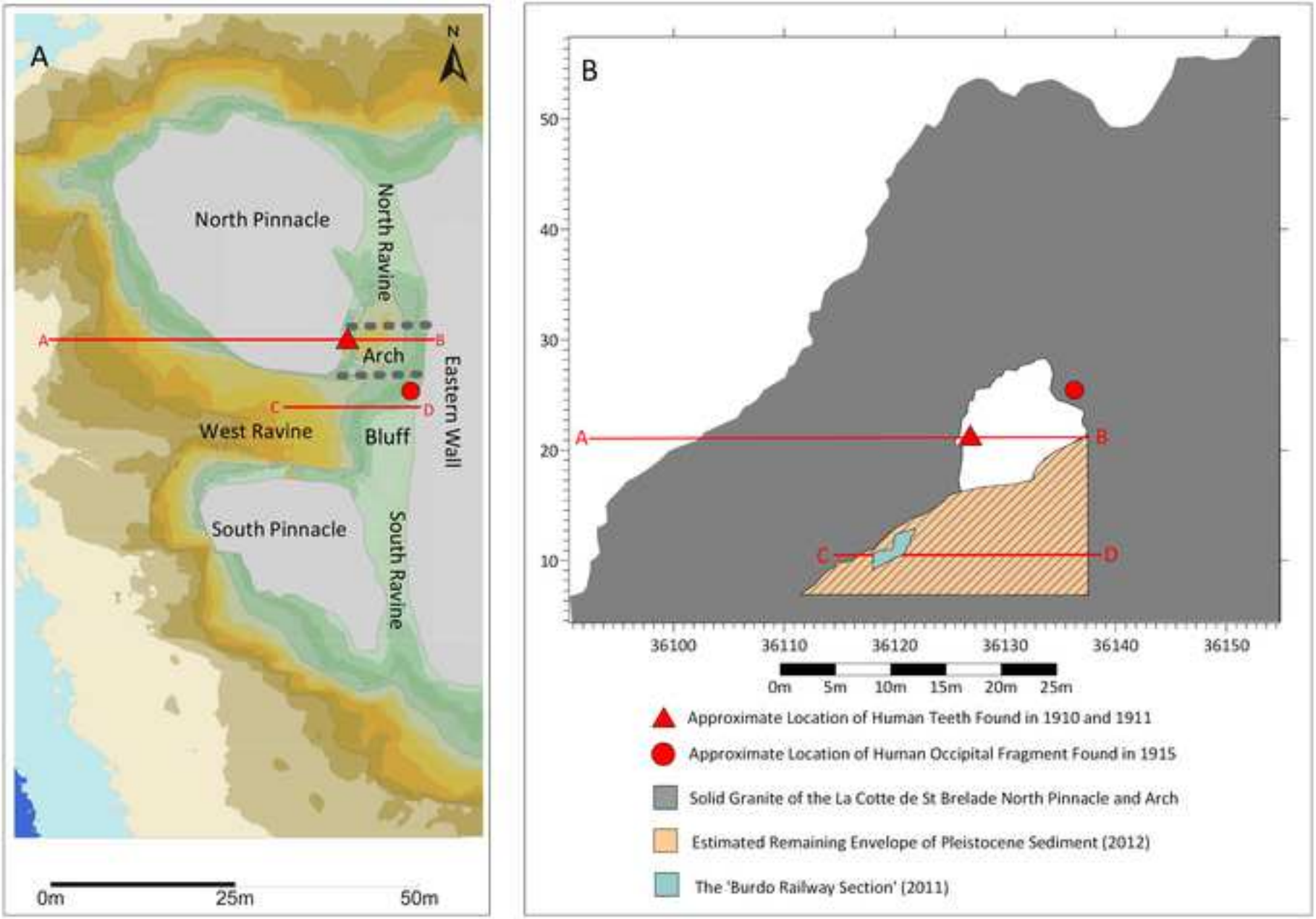

Figure

Click here to access/download;Figure;Figure 4 SJMJ2463 lower LC1.jpg

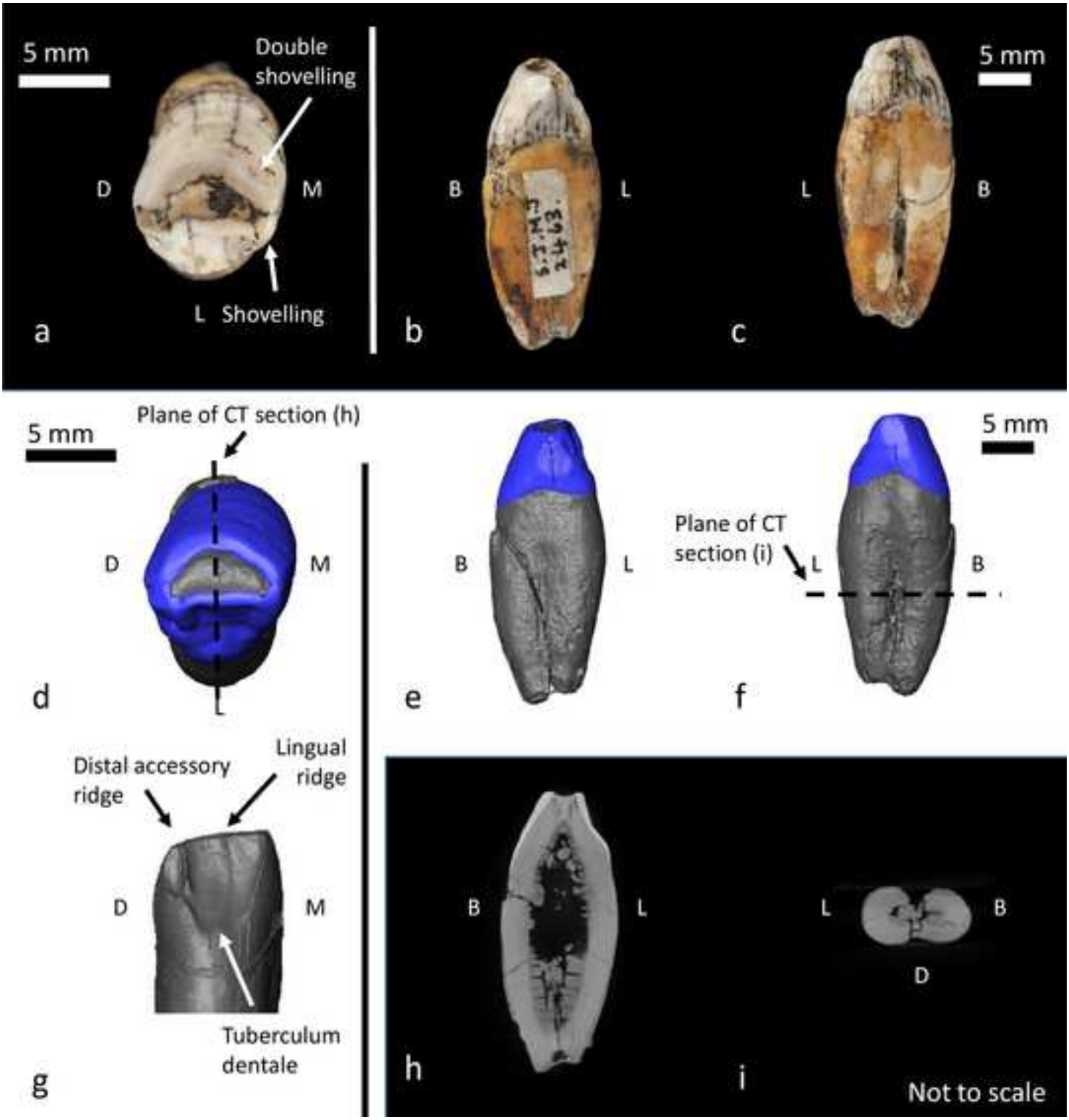

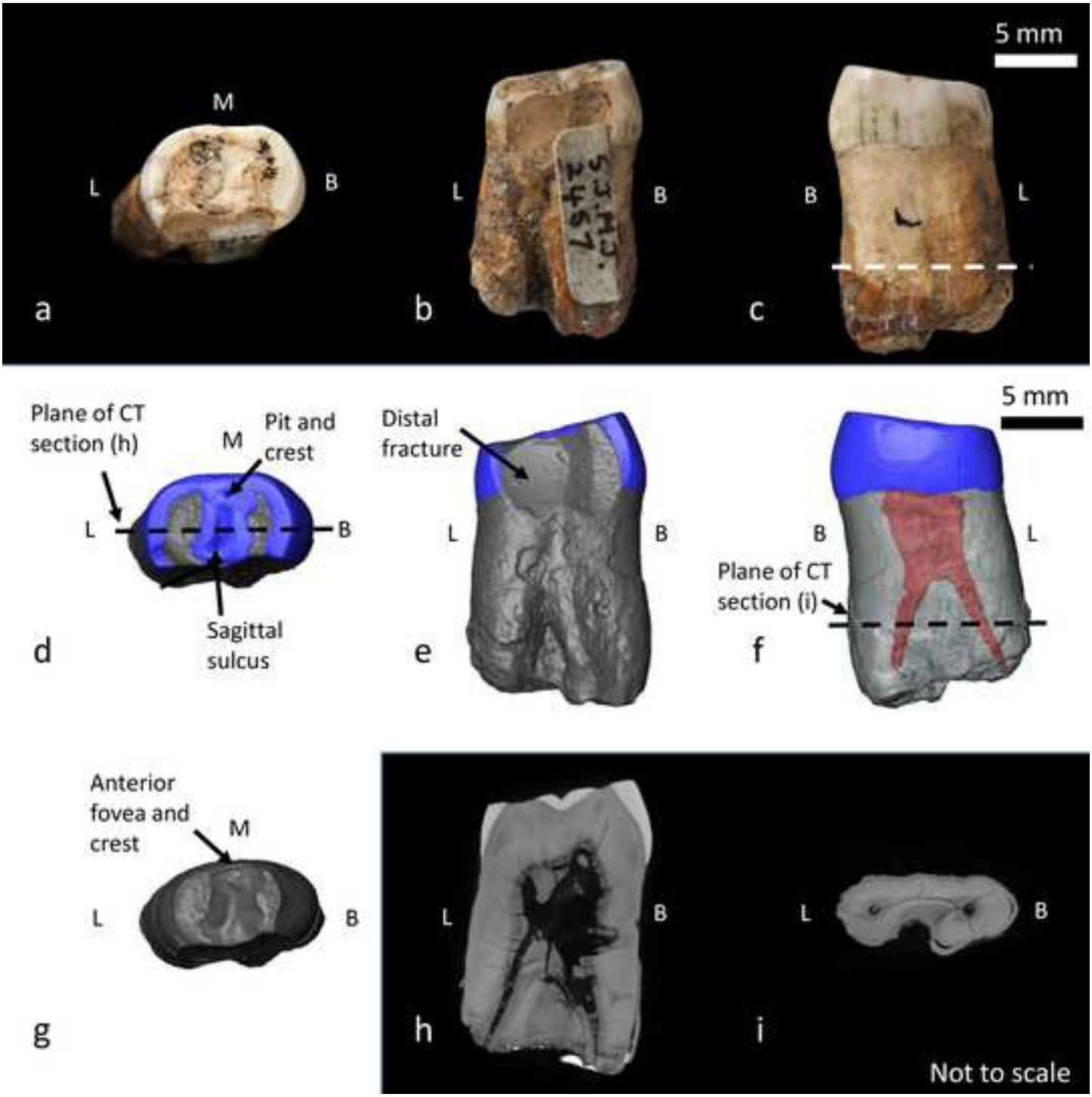

Figure

Click here to access/download;Figure;Figure 6 SJMJ2464 lower LP3.jpg

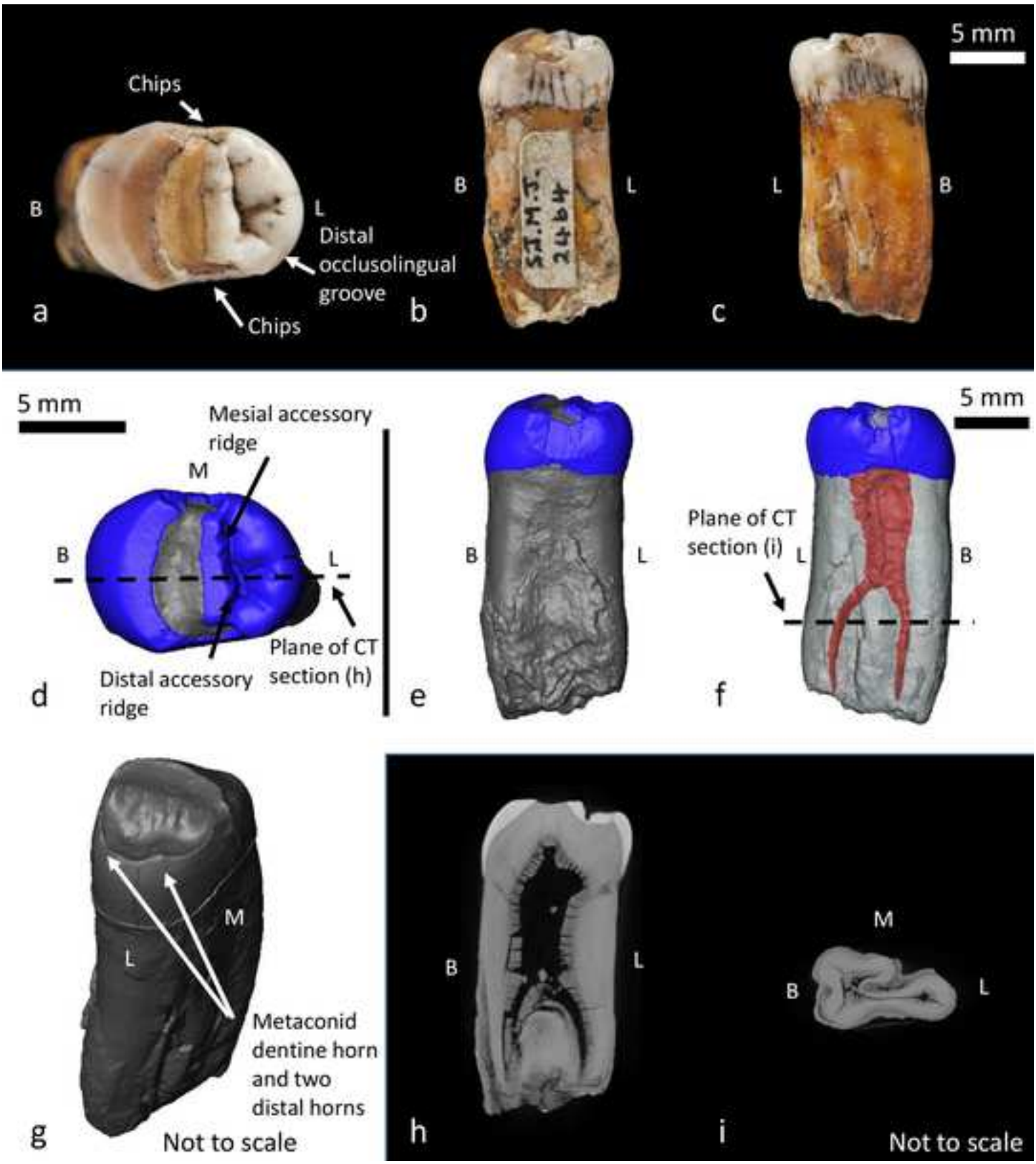

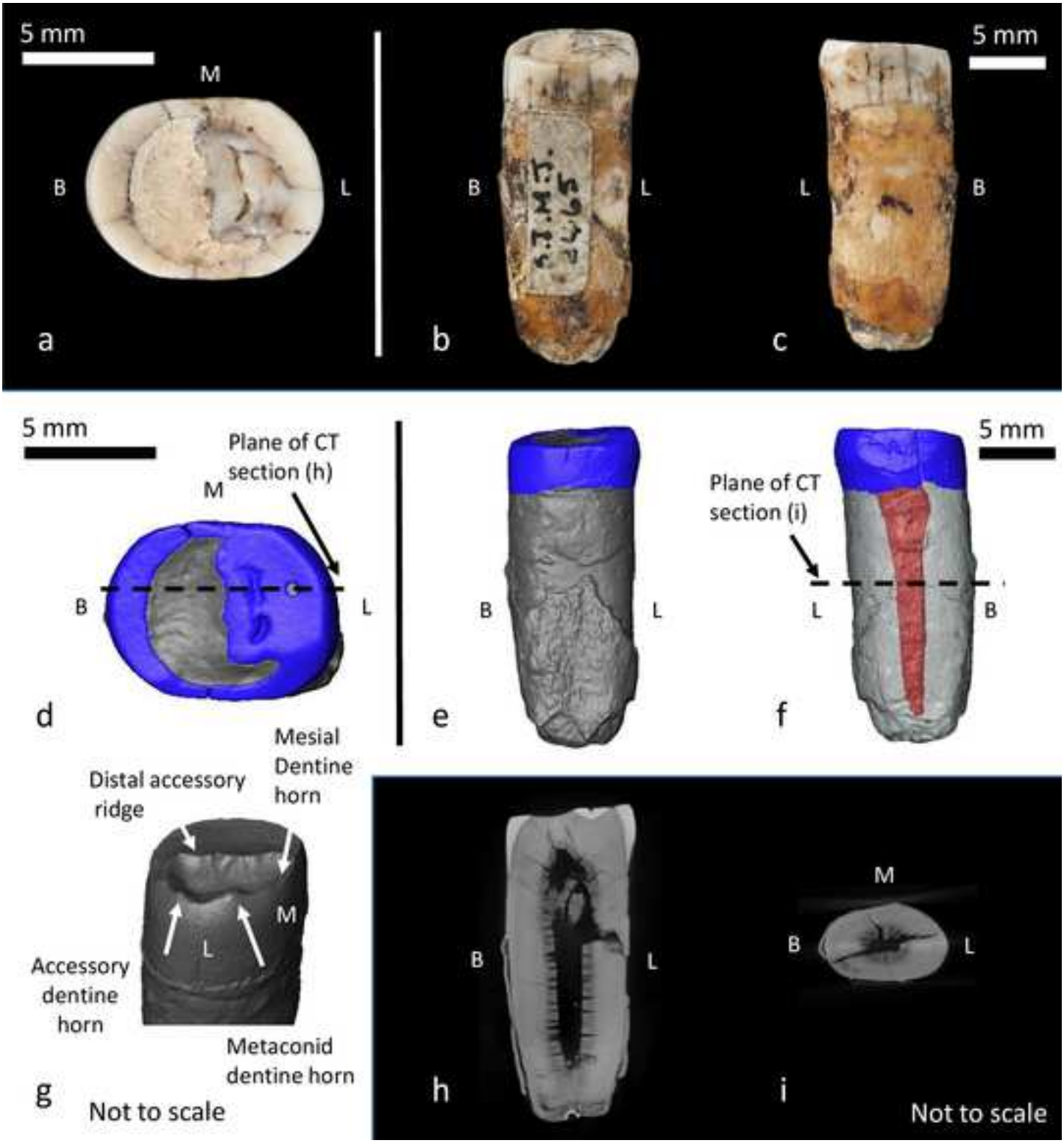

Figure

Click here to access/download;Figure;Figure 8 SJMJ2456 upper RM1.jpg

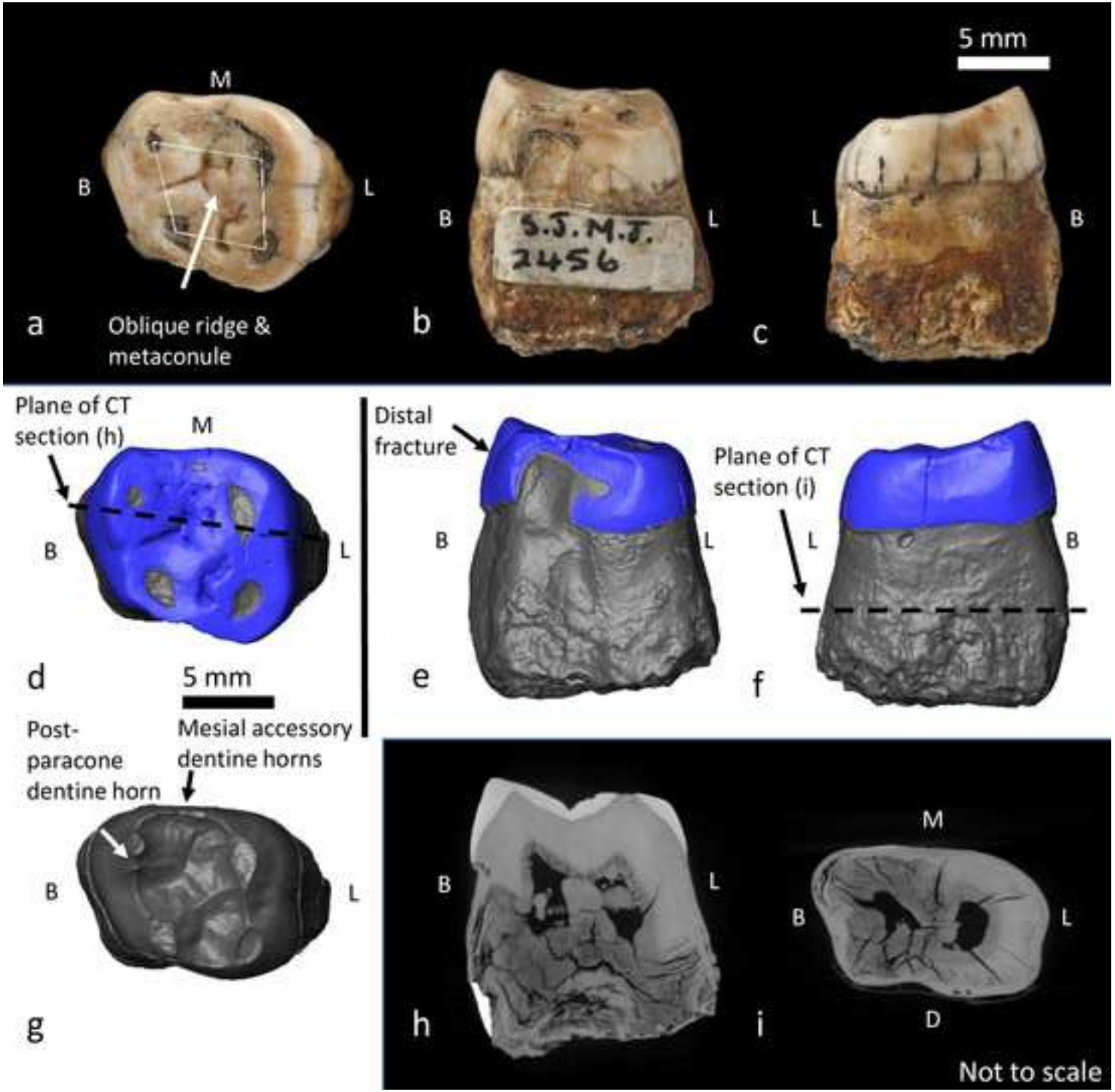

Figure

Click here to access/download;Figure;Figure 9 SJMJ2458 upper LM2.jpg

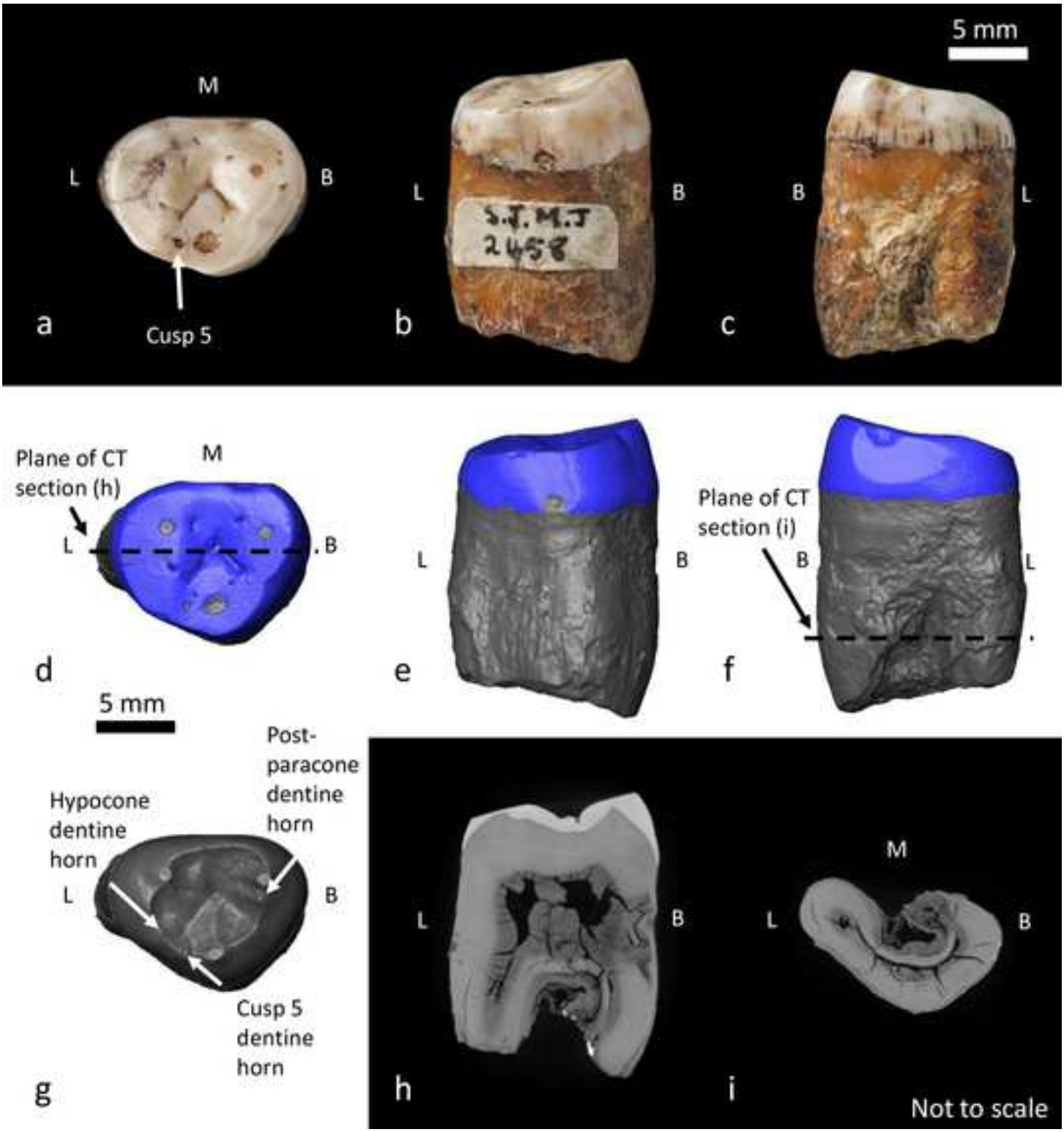

Figure

Click here to access/download;Figure;Figure 10 SJMJ2459 upper RM3.jpg

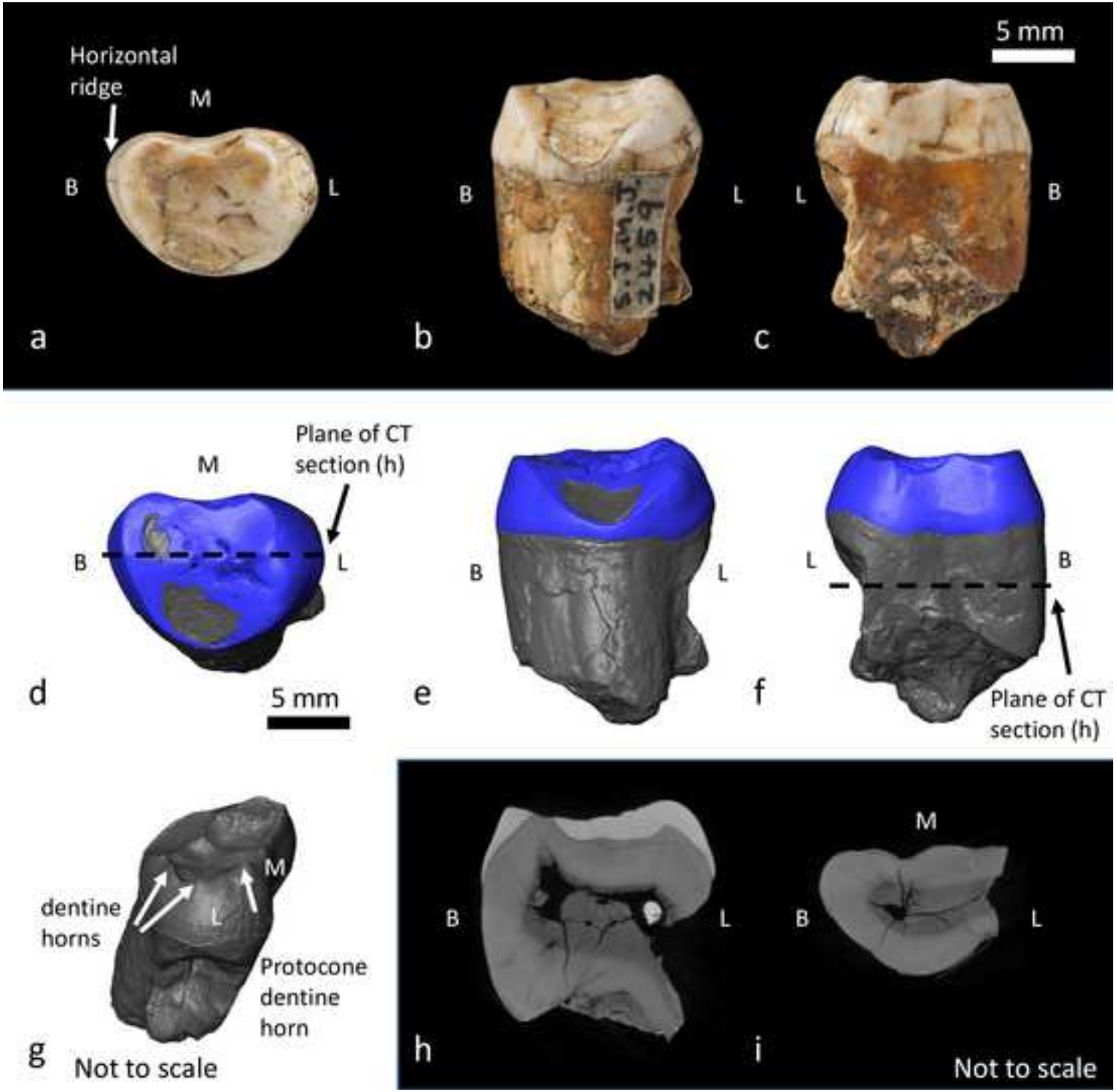

Figure

Click here to access/download;Figure;Figure 11 Cast of SJMJ2467 upper LM3.jpg

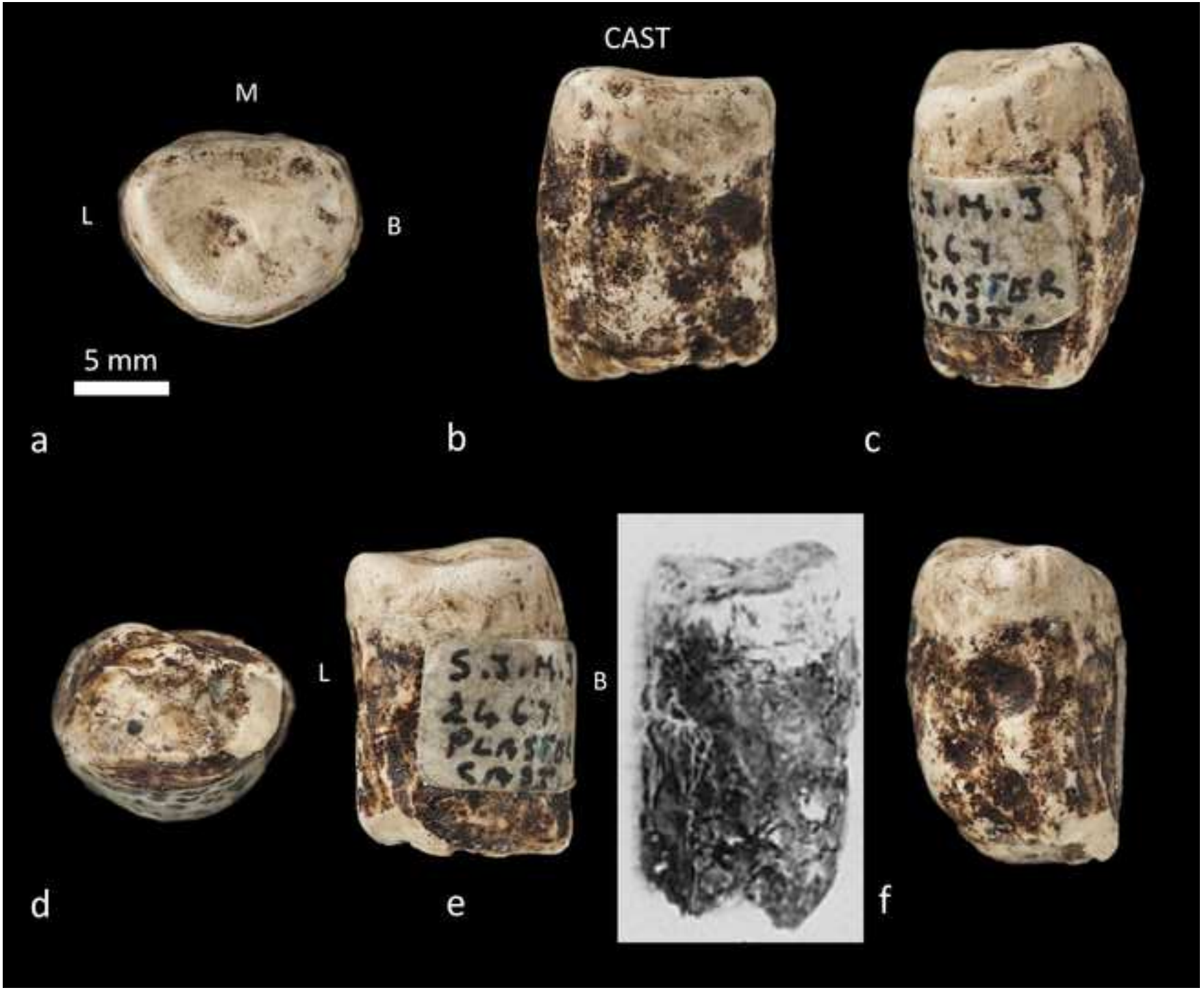

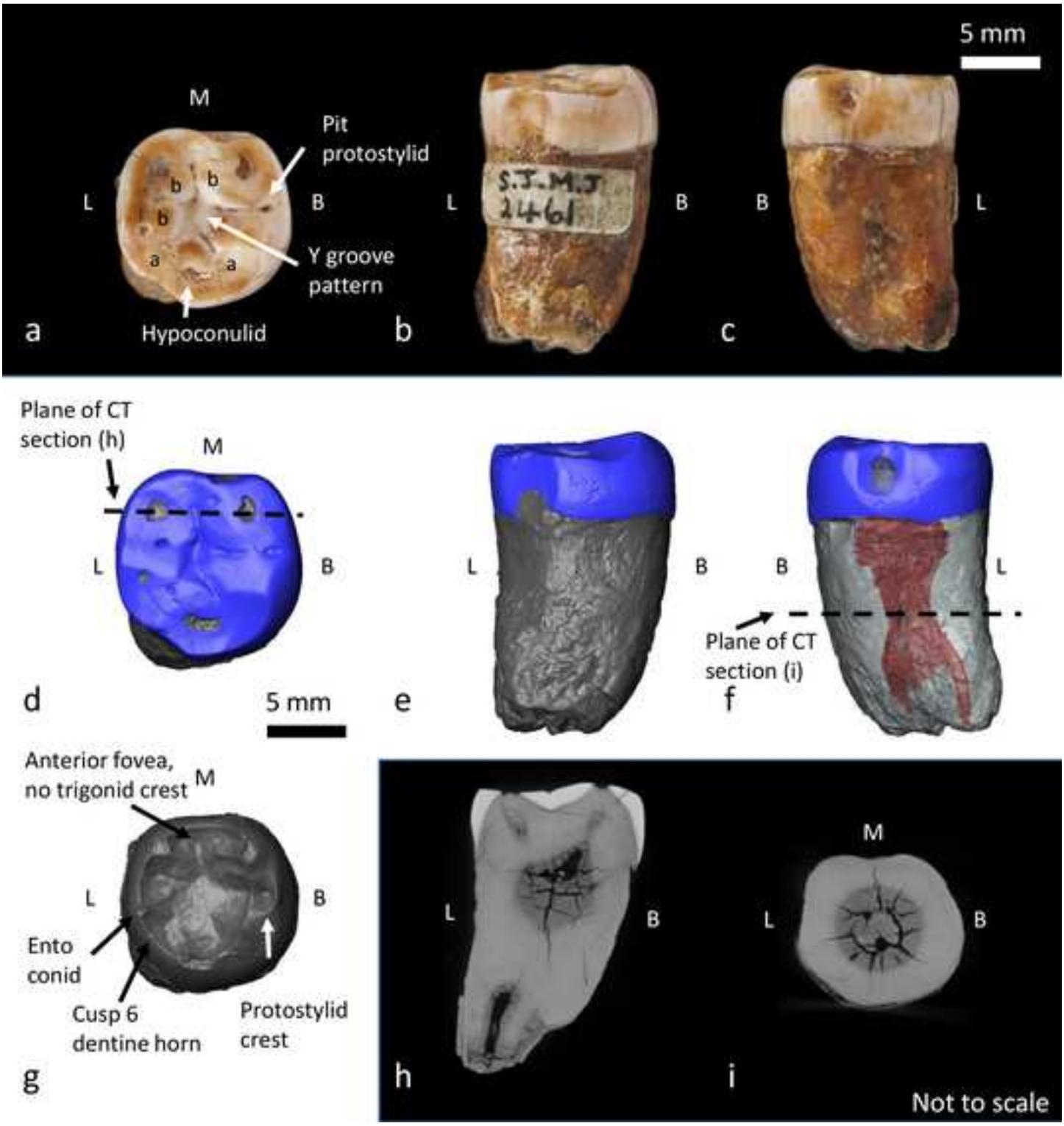

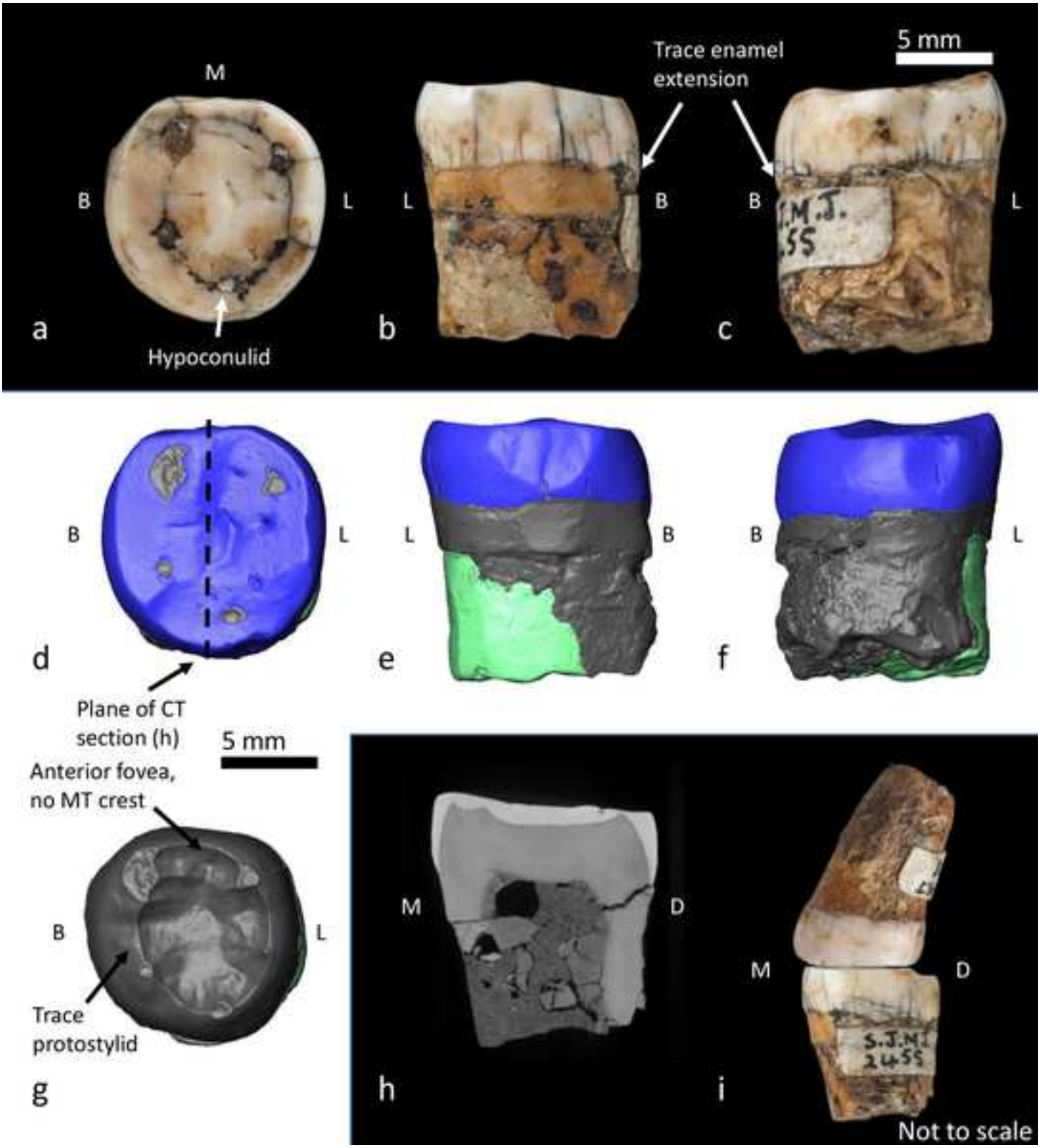

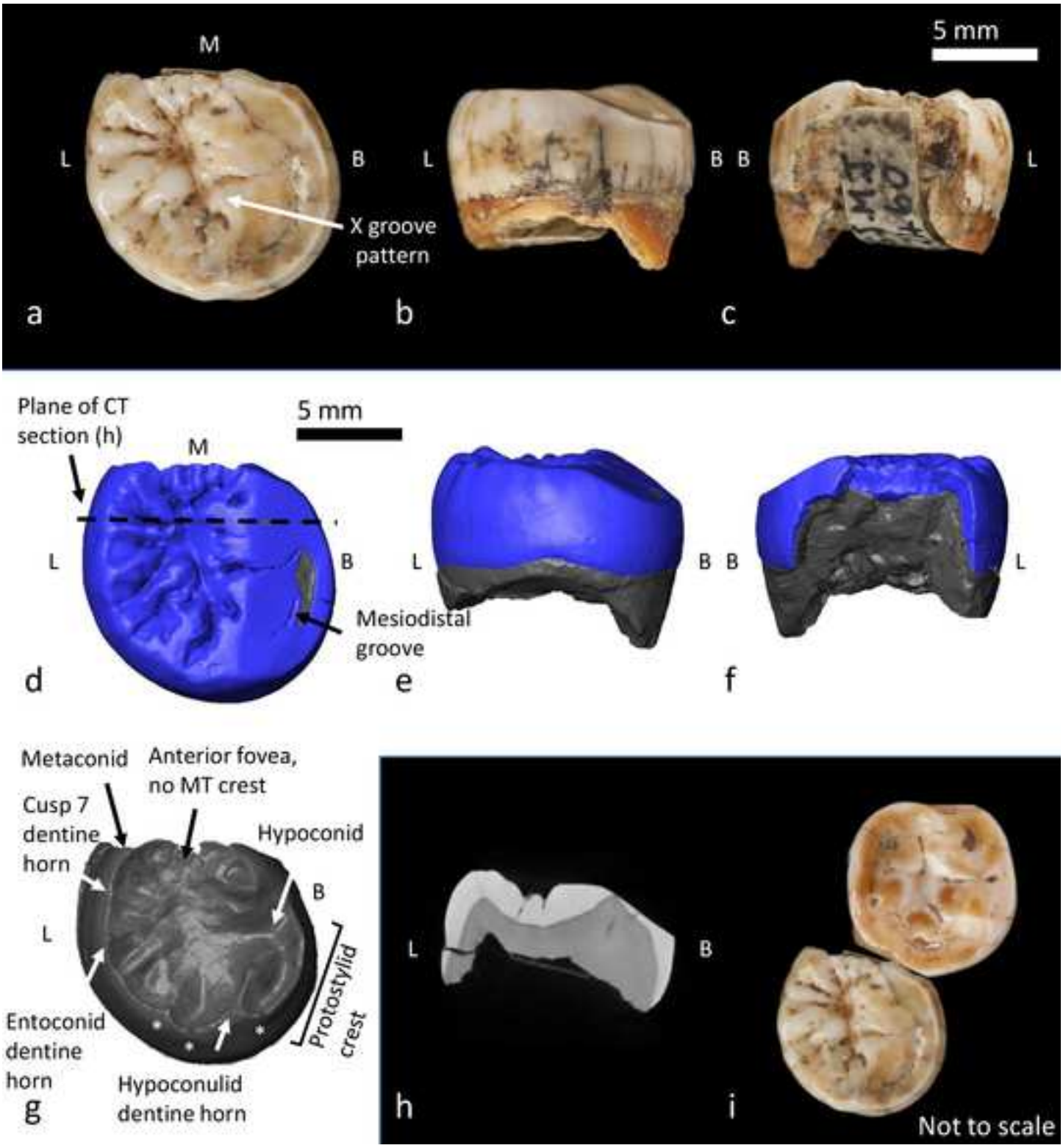

Figure

Click here to access/download;Figure;Figure 15 La Cotte SJMJ2452 occipital fragment.jpg

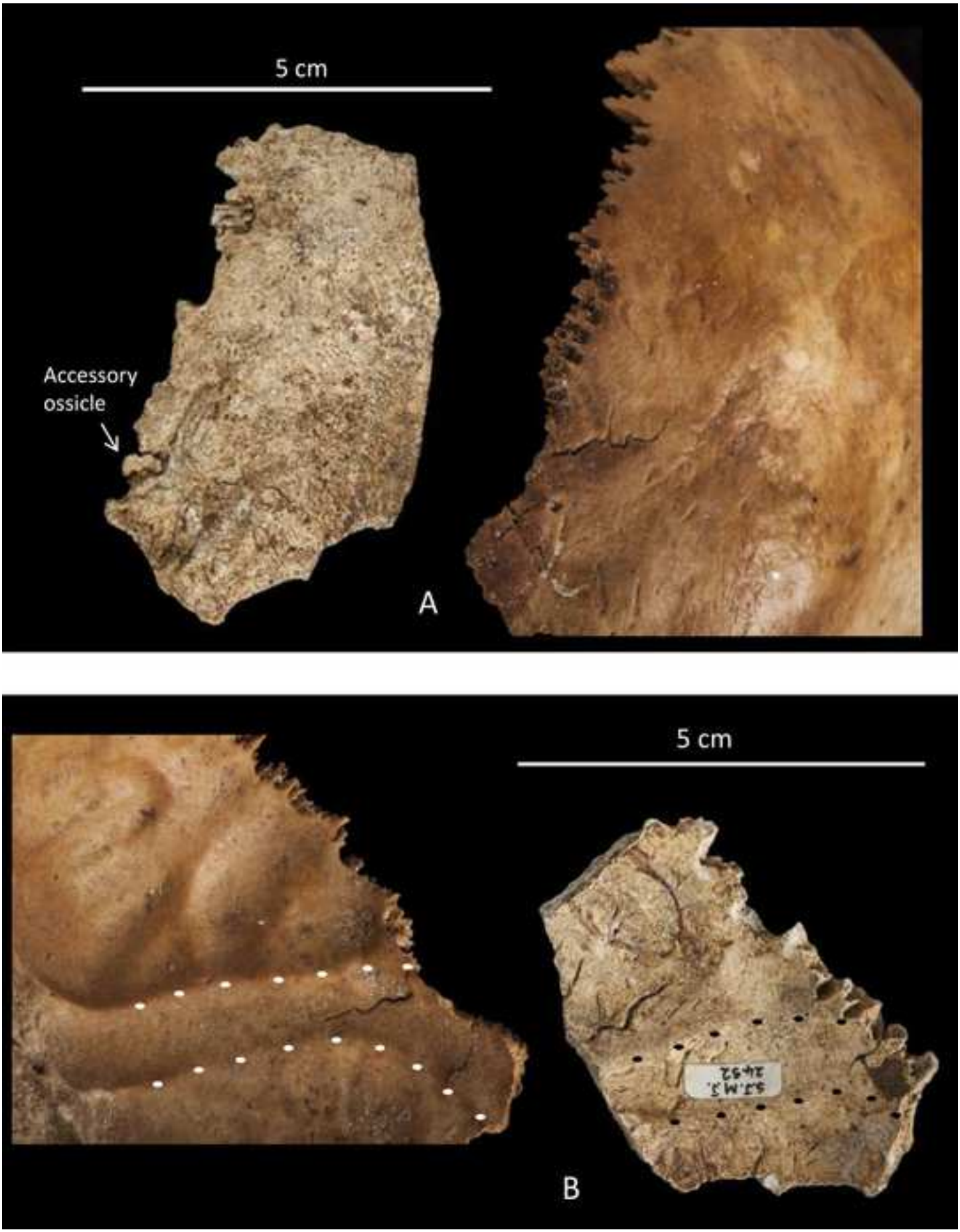

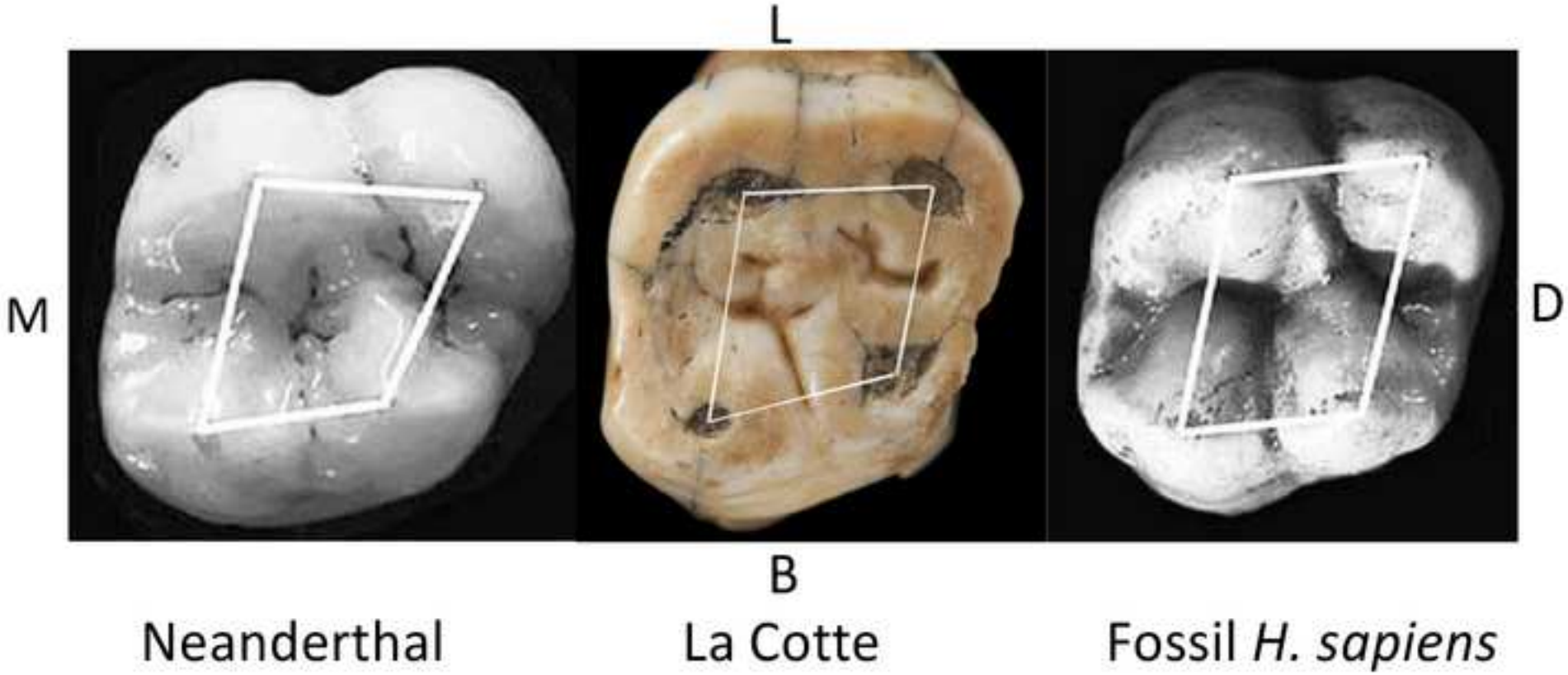

Figure

Click here to access/download;Figure;Figure 17 PCA plots and wireframes of cervix shape in UP4.jpg

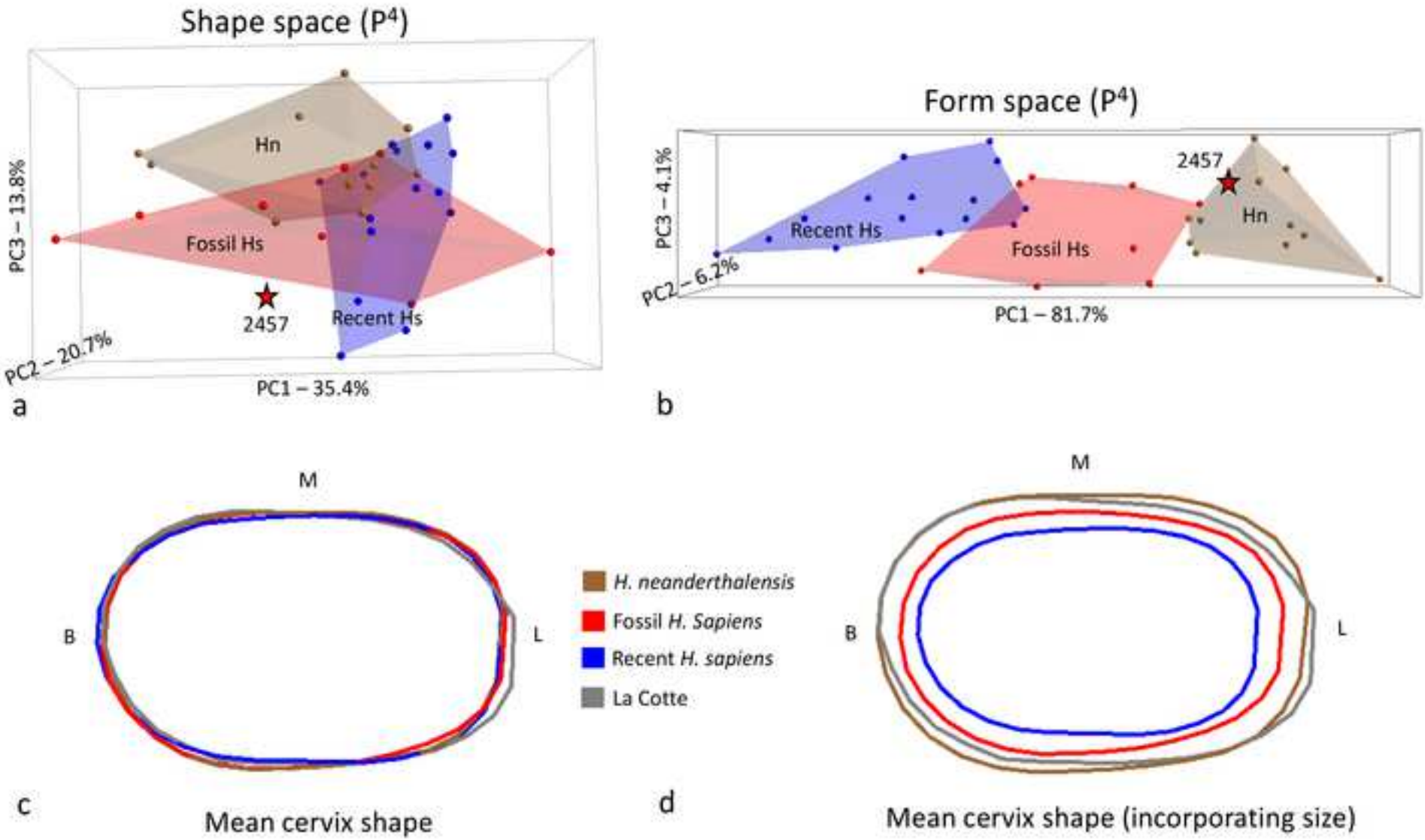

Figure

Click here to access/download;Figure;Figure 18 PCA plots and wireframes of cervix shape in LP3.jpg

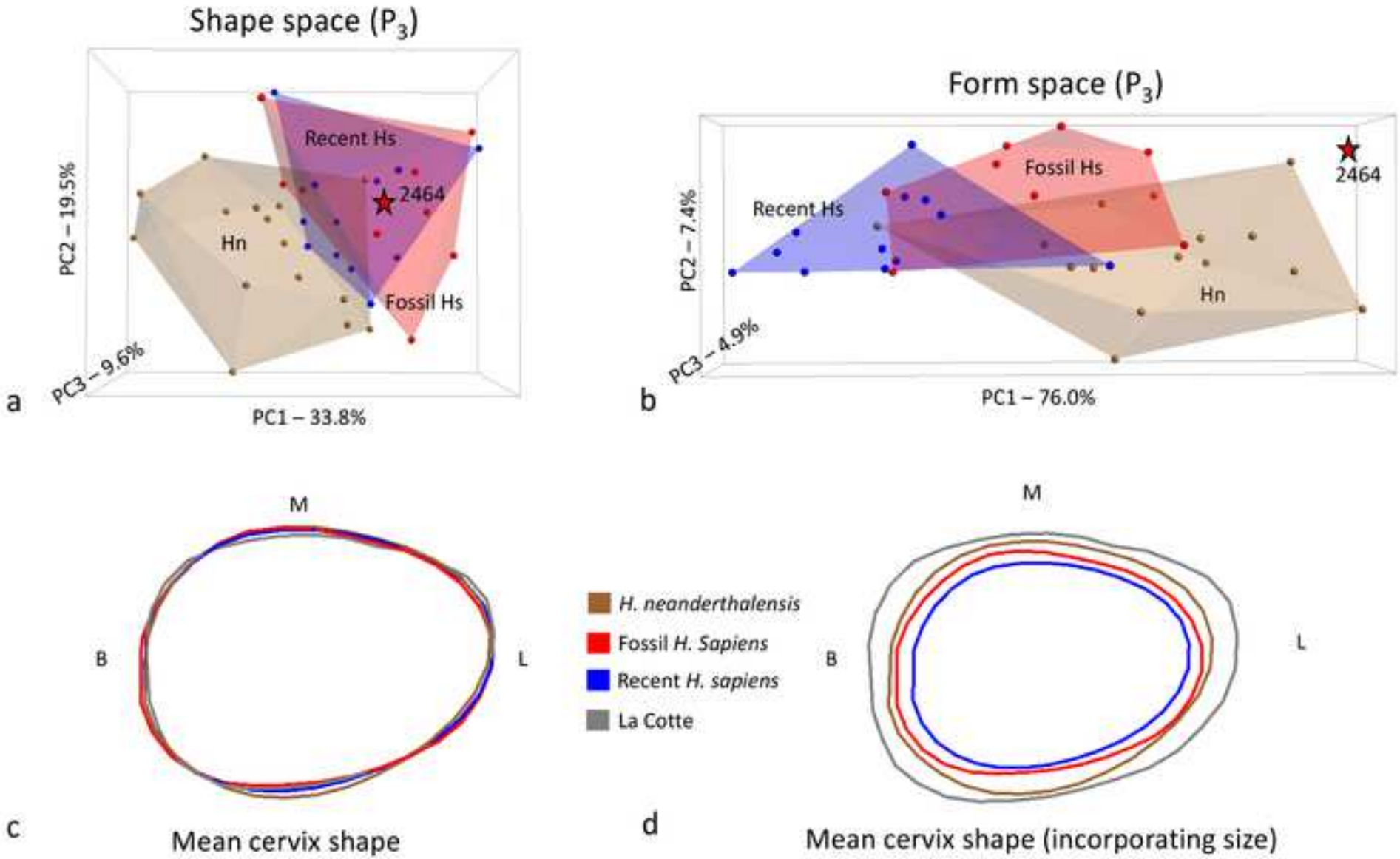

Figure

Click here to access/download;Figure;Figure 19 PCA plots and wireframes of cervix shape in LP4.jpg

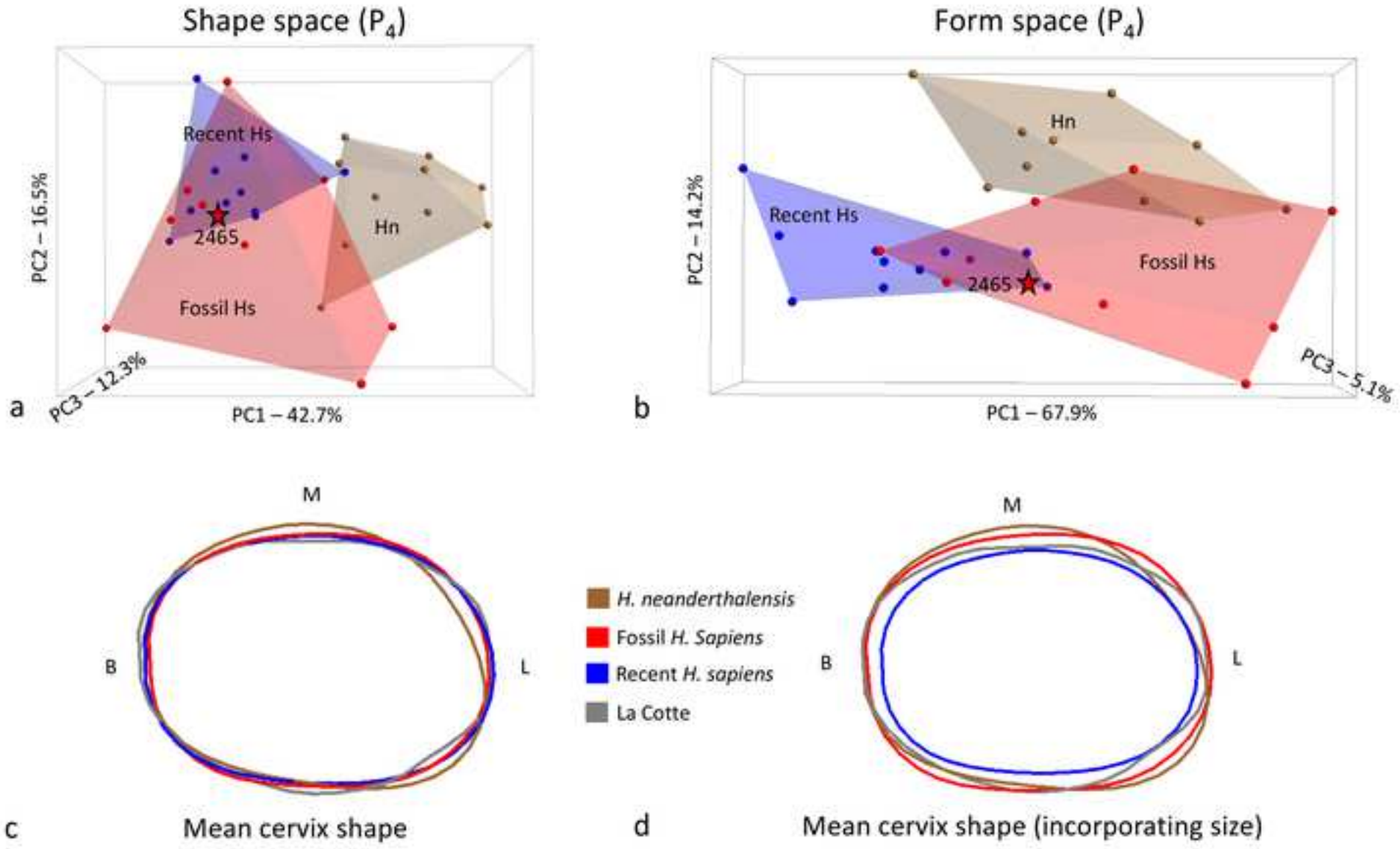

Figure

Click here to access/download;Figure;Figure 20 PCA plots and wireframes of cervix shape in UM1.jpg

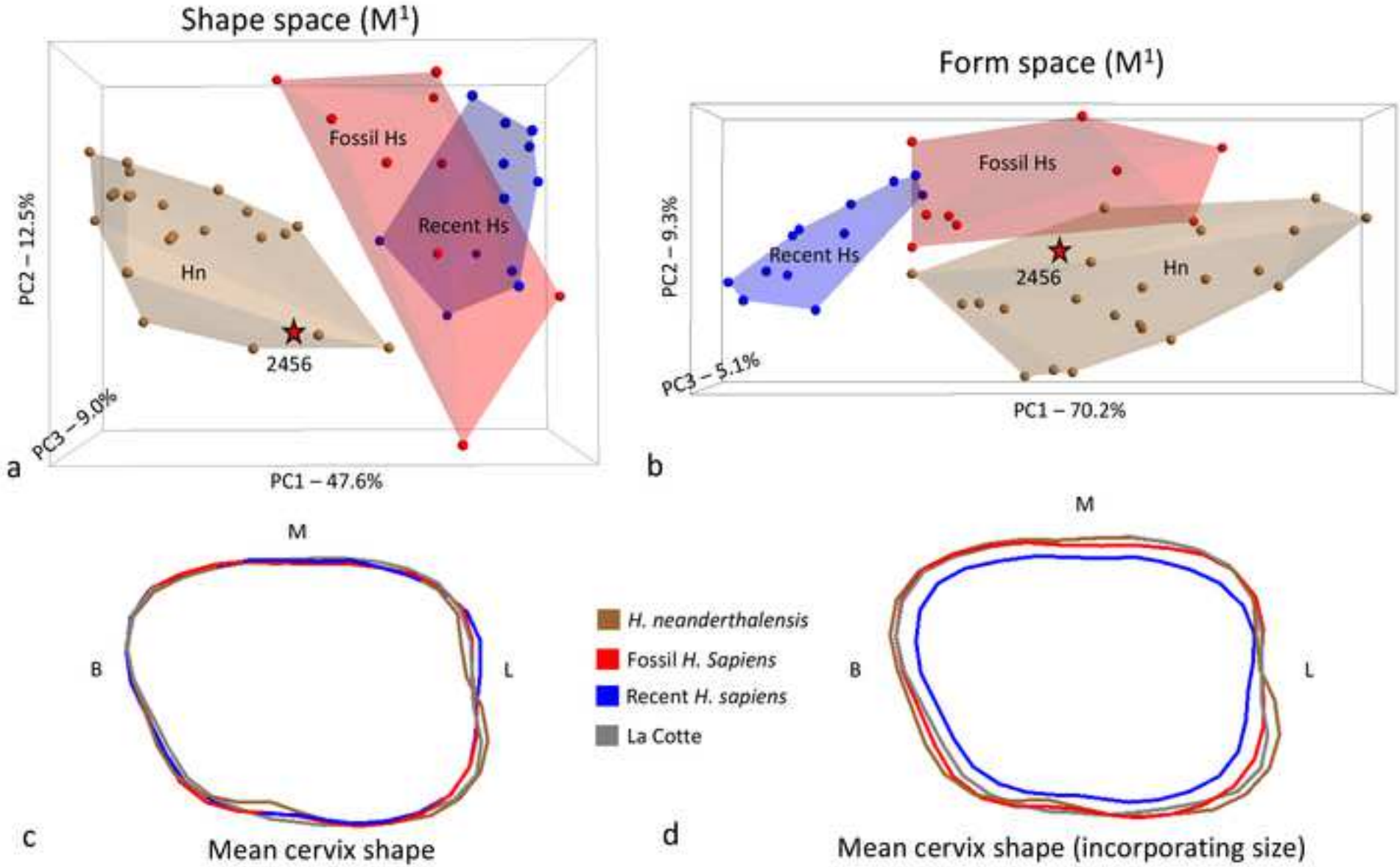

Figure

Click here to access/download;Figure;Figure 21 PCA plots and wireframes of cervix shape in UM2.jpg

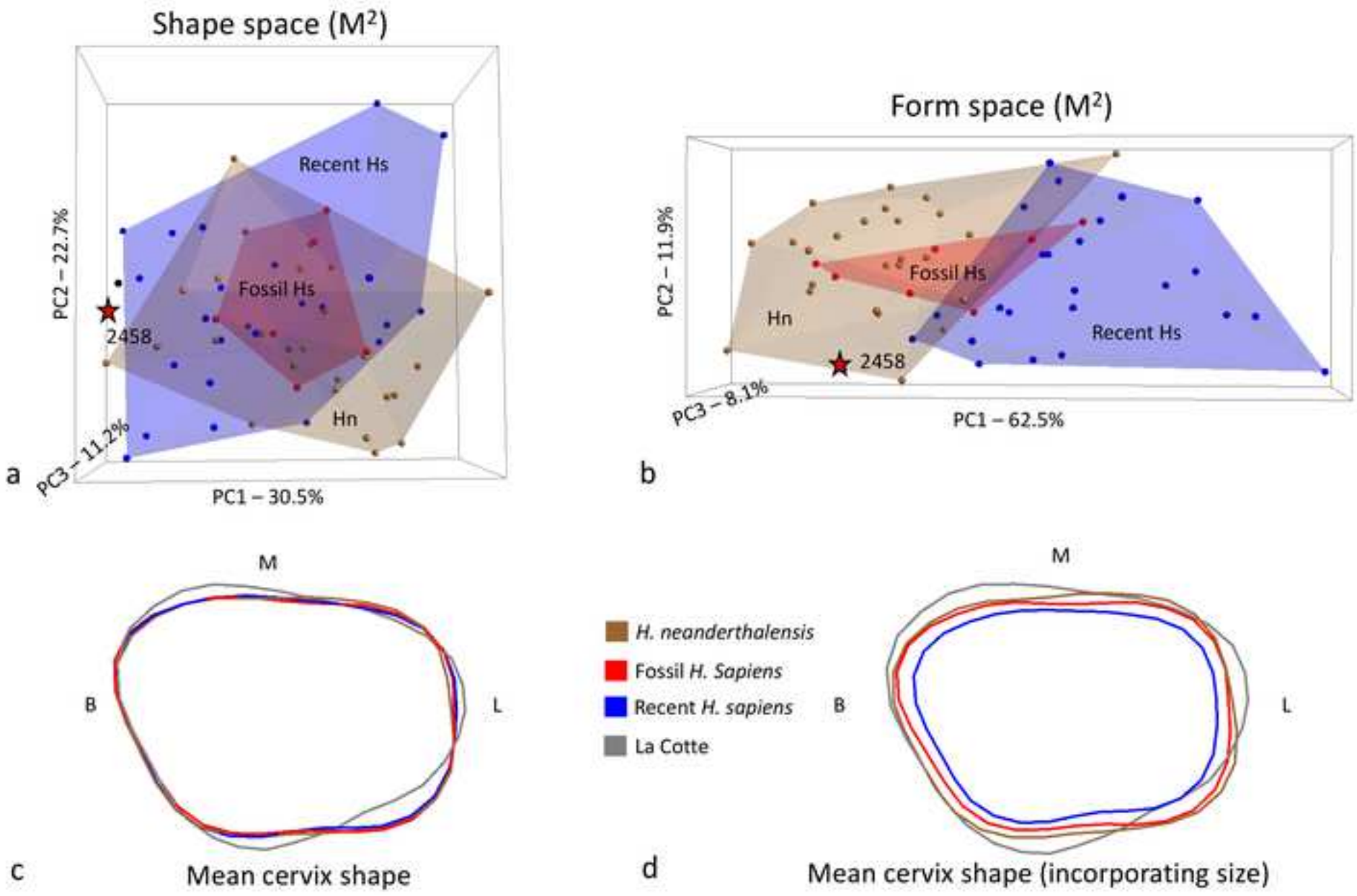

Figure

Click here to access/download;Figure;Figure 22 PCA plots and wireframes of cervix shape in UM3.jpg

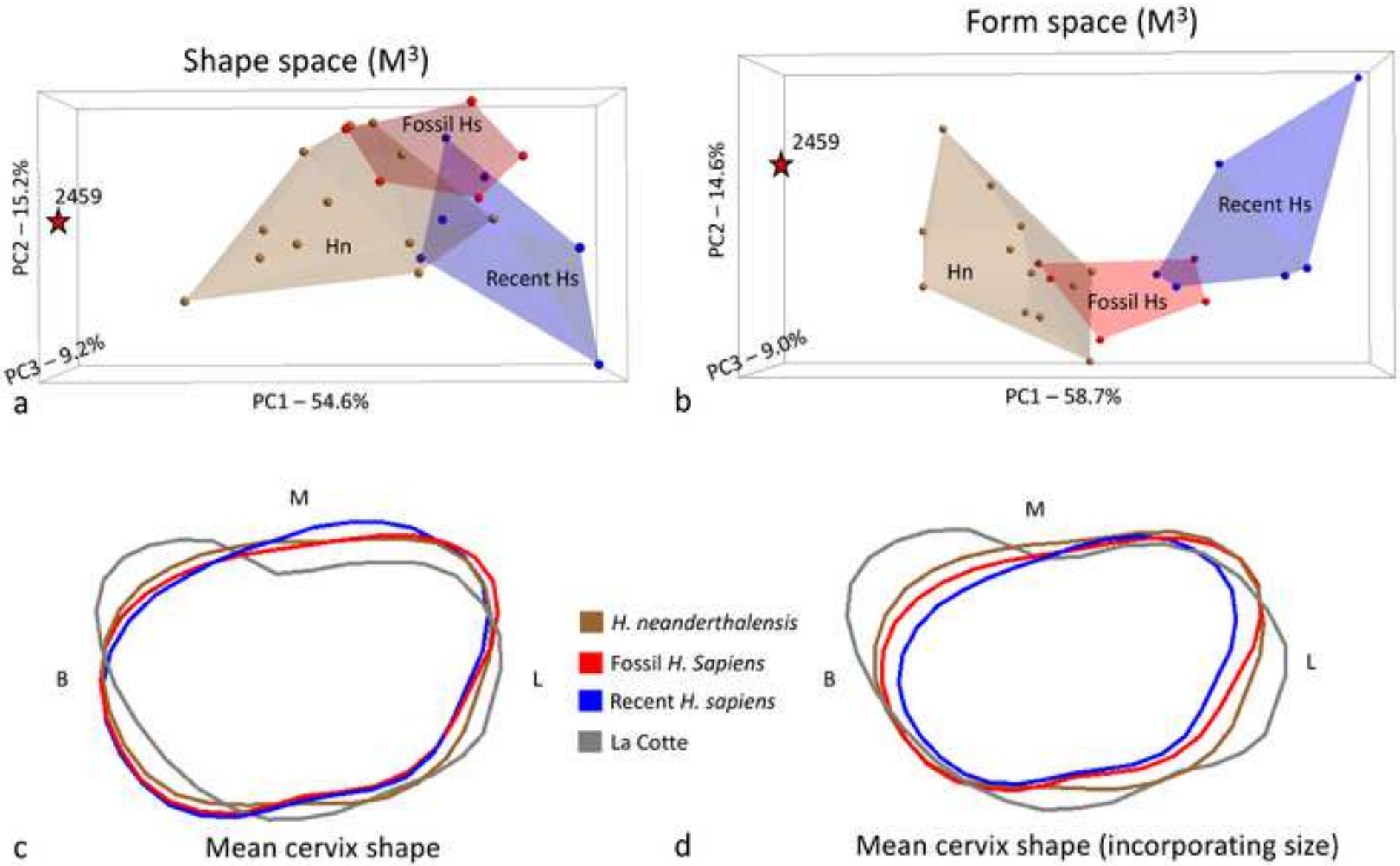

Figure

Click here to access/download;Figure;Figure 23 PCA plots and wireframes of cervix shape in LM2.jpg

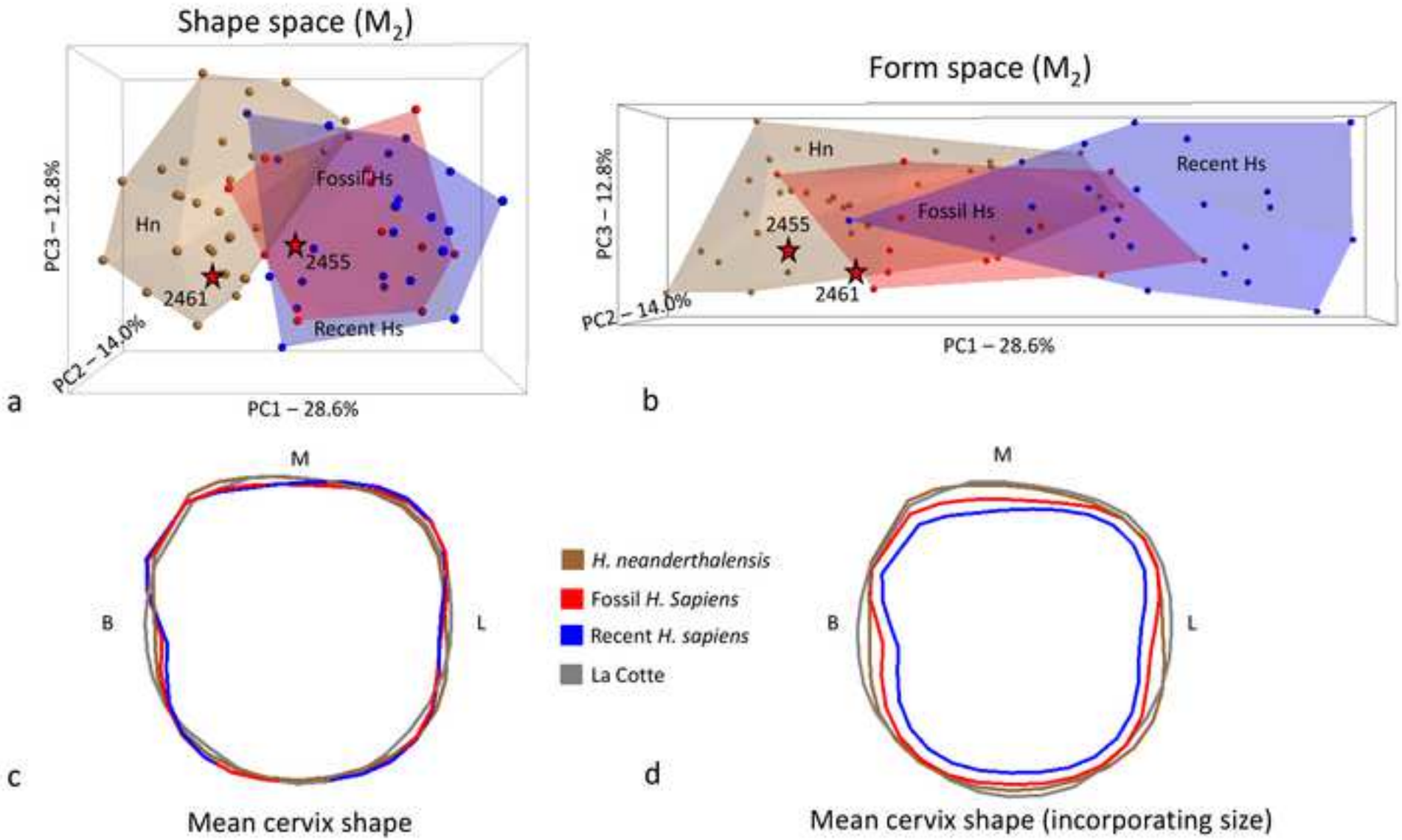

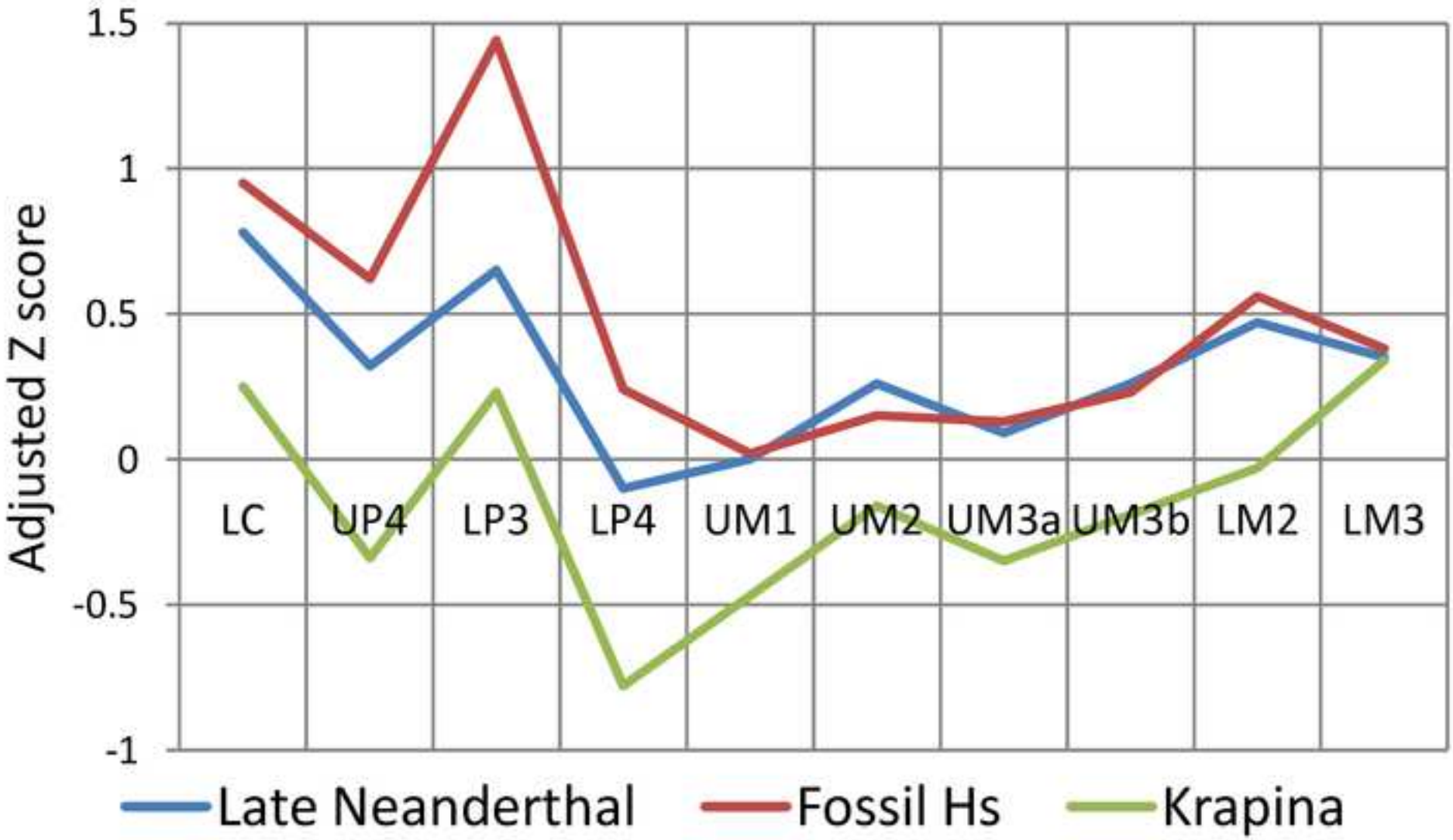

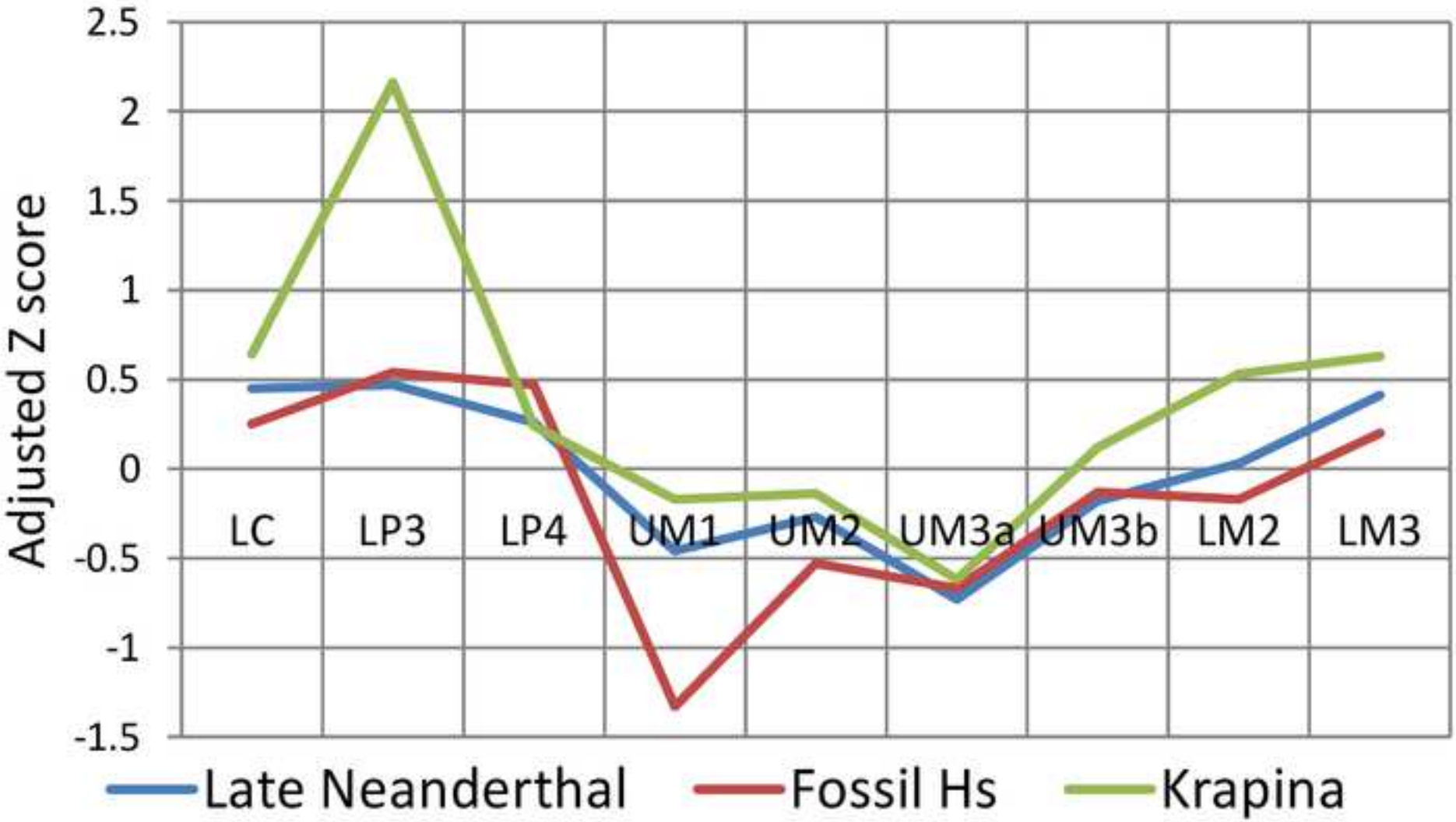

Table 1

La Cotte de St Brelade site stratigraphy.[a]

North ravine, central area (Zeuner, 1940; Callow, 1986c)		West ravine; north end (Burdo, 1960)		West ravine; railway section (Bates et al., 2013)		OSL	MIS
		A	Modern soil				
		B/C	Loess and loessic head				
		D	Fine gravel				
11	Loessic head	E–H	Loessic head[b]				
	Grey sand						
11	Pedogenisis						
11	Loessic deposit with anthropogenic material and Neanderthal teeth	1	Loessic head	Loessic head			
9.3	Ranker soil	2A	Humic granitic sand				
9.2	Granitic sand						
9.1	Ranker soil						
8.3	Fresh-water pond deposits	3B	White clay with rounded clasts				
				VII	Mid to dark brown clay-silt		
				VI	Grey brown sandy-silt	48.3 ± 3.0 ka	3
				XI	Dark brown to yellowish brown gravel	54.2 ± 9.9 ka	3
		5A	Coarse gritty sand	V	Mid brown to reddish brown sandy silt to silty sand	64.7 ± 7.7; 63.3 ± 11.2; 85.8 ± 12 ka	3/4 or 5A/5B
8.2		6	Peaty soil	IV	Very dark brown bedded clay-silt and sandy clay-silt	80.7 ± 6.5 ka	5A/5B

Abbreviations: MIS = marine isotope stage; OSL = optically stimulated luminescence dating.

[a] Numbers/letters before descriptions are context identifiers.

[b] Level at which occipital fragment discovered.

Table 2

La Cotte de St Brelade dental measurements (in mm).

SJMJ identity	Tooth type	Year found	Wear grade	Crown length MD[c]	Crown MD corrected	Crown breadth BL	Crown height	Pulp chamber height	Root trunk length	Total Root length	Cervix MD	Cervix BL[c]
2462[d]	RI_1	1910	4	5.75[a]		7.0[a]	>6.5[a]			>14.0[a]	5.0[a]	7.1
2463	LC_1	1910	4	8.1		10.0	>9.2			>17.6	6.7	10.1
2457	LP^4	1910	5	(6.0)	7.4	10.6	>6.2			>13.2	5.8	10.0
2464	LP_3	1910	4	7.8	8.1	10.2	>5.9			>16.3	6.5	9.3
2465	LP_4	1910	5	6.8	7.3	9.1	>4.5			>16.6	5.9	8.5
2456	RM^1	1910	4	(11.0)	11.6	11.6	>5.3	5.9	9.0	>10.5	8.9	11.5
2458	LM^2	1910	3	10.8	11.1	12.4	>5.0	6.1	8.0	>14.5	9.2	12.1
2459	RM^3	1911	5	10.0		12.3	>5.0	4.9	8.5	>11.6	8.5	—
2467	LM^3	1911	2/3	10.3		11.5	>5.0[a]	—	—	16.0[a]	—	—
2461	RM_2	1910	3	11.7	12.1	11.6	>5.1	5.5	7.0	>14.2	10.0	10.6
2455	LM_2	1910	3	11.9	12.3	11.7	>4.9	—	7.0[a]	>12.5[a]	10.0[a]	(11.0)
2460	RM_3	1911	3	(12.0)	12.0	11.7	6.0[b]	—	—	—	—	11.7

Abbreviations: BL = buccolingual; MD = mesiodistal; L = left; R = right.

[a] Measurements from Keith and Knowles (1912).

[b] Measured on lingual side of tooth.

[c] Parentheses indicate tooth damaged.

[d] SJMJ2462 considered to be non-hominin.

Table 3

Canine discrete morphological traits.[a]

Trait	La Cotte de St Brelade	Grade (0 = absent)	Comparative material: Early and late Neanderthal %	Early and late Neanderthal No.	Fossil *H. sapiens* %	Fossil *H. sapiens* No.	95% confidence intervals
Lower canine	SJMJ2463						
Tuberculum dentale	Small cuspule	>0	48	12/25	59	10/17	
Shoveling	2	>0	100	25/25	88	15/17	
Distal accessory ridge	4	>0	78	14/18	42	5/12	DF

Abbreviations: No. = number of specimens with trait in sample / sample size; DF = confidence interval for difference in frequencies does not include zero.

[a] Data source: Martinón-Torres et al. (2012).

Table 4

Premolar discrete morphological traits.

Trait	La Cotte de St Brelade[f]	Grade (0 = absent)	Comparative material: Early and late Neanderthal %	No.	Fossil *H. sapiens* %	No.	95% confidence intervals
Upper fourth premolar	SJMJ2457						
Buccal mesial accessory ridge	(0)	=0	83	10/12[e]	40	8/20[e]	DF
Buccal distal accessory ridge	(0)	=0	58	7/12[e]	40	8/20[e]	
Essential crest bifurcated	—	>0	67	10/15[b]	36	4/11[b]	
Transverse crest	0	>0	13	2/16[b]	18	2/11[b]	
Mesial/distal accessory cusps	(0 mesial)	>0	48	10/21[a]	33	1/3[a]	
Lower third premolar	SJMJ2464						
Buccal mesial accessory ridge	(1)	>0	24	4/17[a]	13	1/8[a]	
Buccal distal accessory ridge	(1)	>0	90	18/20[a]	100	9/9[a]	
Number of lingual cusps	3	>1	21	7/34[a]	7	1/14[a]	
Metaconid position mesial	Mesial	Mesial	6	2/32[a]	20	3/15[a]	
Transverse crest	0	=0	3	1/30[a]	19	3/16[a]	
Mesiolingual truncation (asymmetry)	0 (slight)	=0	6	1/18[a]	44	7/16[a]	DF
Mesial occlusolingual groove	0	>0	64	16/25[a]	50	7/14[a]	
Tomes' root	4	>3	12	2/17[c]	38	5/13[d]	
Taurodontism–BL widening	Present	>0	33	5/15[c]	71	5/7[d]	
Taurodontism–MD and BL	Present	>0	20	3/15[c]	14	1/7[d]	
Lower fourth premolar	SJMJ2465						
Buccal mesial accessory ridge	(0)	>0	13	2/16[a]	0	0/7[a]	

Buccal distal accessory ridge	(1)	>0	88	14/16[a]	25	2/8[a]	DF, SF
Number of lingual cusps	(3)	>1	94	29/31[a]	50	8/16[a]	DF, SF
Metaconid position mesial	Mesial	Mesial	97	31/32[a]	73	11/15[a]	DF
Transverse crest	0	=0	6	2/31[a]	76	13/17[a]	DF, SF
Mesiolingual truncation (asymmetry)	0 (very slight)	=0	6	2/31[a]	67	8/12[a]	DF, SF
Mesial occlusolingual groove	(0)	>0	8	2/25[a]	0	0/12[a]	
Tomes' root	0	>3	25	5/20[c]	23	3/13[d]	
Taurodontism–BL widening	Present	>0	50	8/16[c]	50	4/8[d]	
Taurodontism–MD and BL	Present	>0	19	3/16[c]	38	3/8[d]	

Abbreviations: BL = buccolingual; MD = mesiodistal; No. = number of specimens with trait in sample / sample size; DF = confidence interval for difference in frequencies does not include zero; SF = confidence intervals for sample frequencies do not overlap.

[a] Data source: Bailey (2006a).

[b] Data source: Martinón-Torres et al. (2012).

[c] Data source: Morphometrics comparative sample (SOM Table S1).

[d] Data source: Morphometrics comparative sample (SOM Table S3).

[e] Data source: Becam et al. (2019), sample under fossil *H. sapiens* is recent human.

[f] Parentheses denote interpretation at enamel dentine junction.

Table 5

Upper first molar occlusal polygons and relative cusp areas.[a]

	La Cotte SJMJ2456	Early and late Neanderthal	Fossil *H. sapiens*[b]
Occlusal polygon angles °		X (SD)	X (SD)
n		17	5
Protocone	100	106.1 (5.2)	106.3 (4.4)
Paracone	68	66.7 (6.7)	71.1 (2.7)
Metacone	116	118.0 (10.0)	110.3 (4.9)
Hypocone	76	69.0 (6.1)	73.3 (4.8)
Relative cusp areas (%)			
n		21	15
Protocone	33	29.9 (2.4)	31.8 (1.5)
Paracone	27	25.8 (2.1)	25.7 (2.3)
Metacone	21	20.6 (1.8)	22.4 (1.7)
Hypocone	19	23.7 (2.1)	20.1 (3.0)
Ratio of occlusal polygon area to crown base area (%)			
n		17	5
Value	24	26.7 (1.8)	32.7 (1.9)

Abbreviation: X = sample mean.

[a] Data sources: relative cusp areas from Quam et al. (2009), remainder from Bailey et al. (2008).

[b] European Late Pleistocene.

Table 6

Upper molar discrete morphological traits.

Trait	La Cotte de St Brelade[c]	Grade (0 = absent)	Comparative material: Early and late Neanderthal %	No.	Fossil *H. sapiens* %	No.	95% confidence intervals
Upper first molar	SJMJ 2456						
Cusp 5	(0)	>0	64	14/22[a]	53	9/17[a]	
Carabelli's trait	0	>2	68	17/25[a]	40	8/20[a]	
Mesial accessory cusps	(2)	>0	40	4/10[a]	22	2/9[a]	
Hypocone size (reduced)	5	<3	0	0/39[a]	0	0/25[a]	
Metacone size	5	>3	74	17/23[b]	74	14/19[b]	
Oblique ridge	2	>0	95	21/22[b]	84	16/19[b]	
Mesial transverse crest	(0)	>0	25	5/20[b]	31	4/13[b]	
Parastyle	0	>0	30	6/20[b]	0	0/15[b]	DF
Upper second molar	SJMJ 2458						
Cusp 5	2/3	>0	68	15/22[a]	39	7/18[a]	
Carabelli's trait	0	>2	50	11/22[a]	16	3/19[a]	DF
Mesial accessory cusps	(1)	>0	100	10/10[a]	13	1/8[a]	DF, SF
Hypocone size (reduced)	(1-2)	<3	6	2/33[a]	15	3/20[a]	
Metacone size	5	>3	48	10/21[b]	33	4/12[b]	
Oblique ridge	0	>0	71	15/21[b]	58	7/12[b]	
Mesial transverse crest	(0)	>0	24	4/17[b]	22	2/9[b]	
Parastyle	0	>0	0	0/19[b]	0	0/10[b]	

Upper third molar	SJMJ 2459	SJMJ 2467						
Cusp 5	—	0	>0	35	6/17[a]	29	4/14[a]	
Carabelli's trait	0	—	>2	14	2/14[a]	25	3/12[a]	
Mesial accessory cusps	(0)	—	>0	70	7/10[a]	28	3/11[a]	DF
Hypocone size (reduced)	(>2)	—	<3	68	13/19[a]	57	8/14[a]	
Metacone size	—	—	>3	17	3/18[b]	0	0/10[b]	
Oblique ridge	(0)	0	>0	29	5/17[b]	20	2/10[b]	
Mesial transverse crest	(0)	—	>0	7	1/14[b]	22	2/9[b]	
Parastyle	0	—	>0	13	2/16[b]	0	0/9[b]	

Abbreviations: No. = number of specimens with trait in sample / sample size; DF = confidence interval for difference in frequencies does not include zero; SF = confidence intervals for sample frequencies do not overlap.

[a] Data source: Bailey (2006a).

[b] Data source: Martinón-Torres et al. (2012).

[c] Parentheses denote interpretation at enamel dentine junction.

Table 7

Lower molar discrete morphological traits.

Trait	La Cotte de St Brelade[c]		Grade (0 = absent)	Comparative material: Early and late Neanderthal %	No.	Fossil *H. sapiens* %	No.	95% confidence intervals
Lower second molar	SJMJ 2455	SJMJ 2461						
Groove pattern	Y	Y	=Y	75	27/36[a]	44	12/27[a]	DF
Hypoconulid	5, D	5, D	>0	100	39/39[a]	65	13/20[a]	DF, SF
Deflecting wrinkle	(0)	(0)	>0	26	6/23[b]	22	5/23[b]	
Distal trigonid crest	(0)	0	>0	14	4/29[a]	0	0/24[a]	
Mid-trigonid crest	(0)	0	=0	4	1/26[a]	96	23/24[a]	DF, SF
Cusp 6	(0)	(1)	>0	50	11/22[a]	24	4/17[a]	
Cusp 7	(0)	(0)	>0	20	7/35[a]	8	2/24[a]	
Anterior fovea	(3/4)	(3/4)	>1	89	23/26[a]	50	10/20[a]	DF, SF
Protostylid	0	1(5)	>0	23	5/22[b]	14	3/22[b]	
Lower third molar	SJMJ 2460							
Groove pattern	X		=Y	41	7/17[a]	56	10/18[a]	
Hypoconulid	4, D		>0	100	23/23[a]	68	13/19[a]	DF, SF
Deflecting wrinkle	0		>0	7	1/15[b]	13	2/15[b]	
Distal trigonid crest	0		>0	11	2/19[a]	0	0/16[a]	
Mid-trigonid crest	0		=0	7	1/15[a]	100	16/16[a]	DF, SF
Cusp 6	1		>0	50	5/10[a]	41	7/17[a]	
Cusp 7	3		>0	40	6/15[a]	17	3/18[a]	

Anterior fovea	3	>1	93	13/14[a]	47	7/15[a]	DF
Protostylid	(6)	>0	39	5/13[b]	12	2/17[b]	

Abbreviations: D = distal; No. = number of specimens with trait in sample / sample size; DF = confidence interval for difference in frequencies does not include zero; SF = confidence intervals for sample frequencies do not overlap.

[a] Data source: Bailey (2006a).

[b] Data source: Martinón-Torres et al. (2012).

[c] Parentheses denote interpretation at enamel dentine junction.

Table 8

Comparative data for cervical dimensions (in mm).[a]

		Lower canine SJMJ2463			Upper fourth premolar SJMJ2457			Lower third premolar SJMJ2464			Lower fourth premolar SJMJ2465			Upper first molar SJMJ2456			Upper second molar SJMJ2458			Lower second molar SJMJ2461		
Sample		*n*	MD	BL	*n*	MD	BL	*n*	MD	BL	*n*	MD	BL	*n*	MD	BL	*n*	MD	BL	*n*	MD	BL
La Cotte de St Brelade			6.7	10.1		5.8	10.0		6.5	9.3		5.9	8.5		8.9	11.5		9.2	12.1		10.0	10.6
Neanderthal	X	16	5.8	8.9	9	5.3	9.0	12	5.5	7.8	16	5.8	8.2	7	8.7	11.2	7	8.8	11.5	9	10.3	9.8
	range		4.3–6.4	7.5–10.5		4.5–6.0	8.0–10.0		4.9–6.0	6.9–9.4		4.5–7.1	7.3–8.9		7.3–10.4	10.5–12.1		7.6–10.1	10.3–12.5		9.4–11.6	8.3–11.6
	SD		0.5	0.7		0.5	0.7		0.3	0.7		0.7	0.5		1.1	0.7		1.1	0.9		0.7	0.9
	Azs[b]		0.8	0.8		0.4	0.6		**1.5**	**1.0**		0.1	0.3		0.1	0.2		0.2	0.3		-0.2	0.4
Fossil *H. sapiens*	X	22	5.7	8.1	15	5.1	8.6	24	5.2	7.3	20	5.2	7.3	20	8.3	11.0	18	7.8	10.9	28	9.3	9.1
	range		4.8–6.6	6.7–9.7		4.6–5.9	7.9–10.4		4.6–6.0	5.8–8.4		4.2–6,6	6.4–9,7		7.9–9.4	9.9–12.6		6.6–9.1	8.8–13.2		8.0–10.7	7.6–11.0
	SD		0.5	0.8		0.4	0.7		0.4	0.6		0.5	0.7		0.4	0.6		0.6	1.0		0.6	0.8
	Azs[b]		**1.0**	**1.2**		0.8	0.9		**1.6**	**1.6**		0.7	0.8		0.7	0.4		**1.1**	0.6		0.6	0.9

Abbreviations: Azs = adjusted Z score; BL = buccolingual; MD = mesiodistal; X = sample mean.

[a] Data sources: Neanderthal C_1, Le Cabec (2013); Neanderthal remainder, see SOM Table S5; fossil *H. sapiens*, see SOM Table S3.

[b] Values in bold: adjusted Z score ≥ ±1.0.

Table 9

Summary of principal Neanderthal and modern human traits in La Cotte de St Brelade teeth.

Individual and group	SJMJ Identity	Tooth type	Neanderthal features	*H. sapiens* features	Attribution
A−1	2458	Left M^2	Mesial accessory cusp; cusp tips internally placed; roots taurodont; cervical measurements		N
	2461	Right M_2	Root shape; roots taurodont; cervix shape	Mid-trigonid crest absent	N/Hs
	2455	Left M_2	Root shape; roots taurodont; cervix shape	Mid-trigonid crest absent	N/Hs
	2460	Right M_3	Multiple cusps and accessory crests	Mid-trigonid crest absent; metaconid dentine horn tip not centrally placed	N/H s
A−2	2463	Left C_1	Large distal accessory ridge; root shape and robusticity; root canal form; crown area; cervical measurements		N
	2464	Left P_3	Buccal cusp form; buccal cingulum at EDJ; root robusticity; root taurodont; crown area; cervical measurements	Transverse crest absent; mesiolingual truncation (asymmetry) absent; cervix shape	N/Hs
A−3	2456	Right M^1	Cusp tips internally placed; distobuccal truncation; relative size and shape of occlusal polygon; roots	Relatively small hypocone and large hypocone angle	N/Hs

			taurodont; cervix shape; crown index		
A−4	2467	Left M^3	Roots taurodont; root length		N
B−1	2457	Left P^4	Inclination of buccal surface; root robust and two-rooted; root taurodont	Cervix shape	N/Hs
	2465	Left P_4	Three lingual cusps; root taurodont	Transverse crest absent; mesiolingual truncation (asymmetry) absent; cervix shape	N/Hs
B−2	2459	Right M^3	Inferred presence multiple distal cusps; roots taurodont; cervix shape		N

Abbreviations: Hs = *H. sapiens*; N = Neanderthal.